ROBUST CORRELATION BETWEEN NORTHERN HEMISPHERE JET RESPONSE AND ARCTIC-MINUS-SUBTROPICAL WARMING ACROSS CMIP5 MODELS

by

Nicholas Clay Golden

A thesis submitted to the faculty of
The University of North Carolina at Charlotte
in partial fulfillment of the requirements
for the degree of Master of Science in
Earth Science

Charlotte

2020

Approved by:

_____
Dr. Jacob Scheff

_____
Dr. Matthew Eastin

_____
Dr. Brian Magi

ABSTRACT

NICHOLAS CLAY GOLDEN. Robust correlation between Northern Hemisphere jet response and Arctic-minus-subtropical warming across CMIP5 models. (Under the direction of DR. JACOB SCHEFF)

The response of the atmospheric circulation to global warming is still not well known. A specific area of interest is the westerlies of the Northern Hemisphere, most notably the strengthening or weakening of the westerlies, which could change mid-latitude weather patterns. Previous studies have termed the phrase tug-of-war idea, which is the interaction between the warming of the tropics and the warming of the Arctic, with opposite jet response to each. This study focused on the difference between specific areas of the tropics and Arctic for two different time periods. The first was the future using 30-year RCP8.5 (2070-2099) minus 30-year historical (1975-2004) climate model run outputs for temperature change and zonal wind change. The second was the satellite era (1979-2018) using concatenated historical and RCP8.5, halved into two 20-year periods, Past (1979-1998) and Present (1999-2018), and taking the difference between those two periods for the same climate model outputs. For the future period, using 41 climate models from CMIP5, a robust correlation was found between the strengthening (weakening) of the westerlies and warming of the tropics (Arctic). Specifically, for every degree of difference in warming between the Arctic troposphere (60-90°N, 850-300 mb) and subtropical troposphere (20-40°N, 850-200 mb) the mid-latitude zonal wind response (30-70°N, 1000-200 mb) decreased by -0.5 ms^{-1} (r = -0.9245). A strong correlation was also found for the satellite era, using 91 ensemble

members from 42 climate models, using the same parameters for the atmosphere from the future period above that showed a decrease in mid-latitude zonal wind response of -0.47 ms^{-1} (r = -0.7643) per degree of warming difference. This strong correlation in the satellite era will allow future studies to be performed using observations from reanalysis and/or microwave satellite data to determine which models are expected to be more accurate.

ACKNOWLEDGEMENTS

I would like to say a well-deserved thank you to Dr. Jack Scheff for this great opportunity to work as a Research Assistant on this study at UNC Charlotte, for being an amazing advisor, and giving me the motivation and support I needed over the past two and half years to complete this study. I would also like to thank my committee members Dr. Matthew Eastin and Dr. Brian Magi for working with my schedule and their guidance on this study. I would like to thank all the professors from our department that taught me over the past two years. I would like to thank my fellow graduate students for being such a supportive group, both in and out of the office. I would like to say thank you to my family and friends for their support and encouraging words when I needed them most. Finally, we would like to acknowledge the World Climate Research Program's Working Group on Coupled Modeling, which is responsible for CMIP, and we thank the climate modeling groups (Table 1) for producing and making available their model output. For CMIP the U.S. Department of Energy's Program for Climate Model Diagnosis and Intercomparison provides coordinating support and led development of software infrastructure in partnership with the Global Organization for Earth System Science Portals.

TABLE OF CONTENTS

LIST OF TABLES

LIST OF FIGURES

CHAPTER ONE: INTRODUCTION

For the last few decades climate scientists have been trying to determine, using climate models, how the atmosphere is going to respond to the warming being caused by anthropogenic greenhouse gas emissions. The most recent consensus from climate models on what is predicted to occur over the next 80 years was published in the IPCC Fifth Assessment Report (Collins et al. 2013). In this publication an averaged plot of all the climate models indicated that a strong warming for the entire troposphere and a cooling for the stratosphere is to occur. For the troposphere it indicated a noticeably stronger warming aloft of the tropics than the Arctic. In this scenario it is theorized that there will be an expansion of the Hadley cell resulting in a poleward shift of the northern jet stream and mid-latitude storms (Collins et al. 2013; Lu et al. 2007; Staten 2018). A recent study focusing on observed radiosonde temperature and wind data from 1979-2012 determined that warming of the tropics did not occur as much in the troposphere as the climate models showed but was still considerable and there was a noticeable strengthening of the subtropical jet (Sherwood and Nishant 2015). While this is the consensus there have been studies based on reanalysis of the past 30 years that indicate that the opposite may be occurring (Graversen et al. 2008; Feldstein and Lee 2014; Francis and Vavrus 2015). There is also indication from microwave sounding observation trends that the opposite is occurring as well (Santer et al. 2013, 2018). That instead of the tropics warming more aloft the Arctic is warming more at the surface. In this scenario the reverse would occur with an equatorward movement of the northern jet stream. These two scenarios are what is known as the tug-of-war idea (Held 1993; Butler

et al. 2010; Deser et al. 2015; Yim et al. 2016b; Shaw et al. 2016; Francis 2017; Screen et al. 2018). This is the idea that whichever part of the atmosphere, Arctic at the surface or the tropics aloft, warms the most will win the tug-of-war. If the Arctic warms more at the surface there is a decrease in zonal wind speed and an equatorward movement of the northern jet stream is expected. This would also be known as a negative North Atlantic Oscillation (NAO)/ Arctic Oscillation (AO) response (Feldstein and Lee 2014; Barnes and Polvani 2015). If the Tropics warms more aloft there is an increase in zonal wind speed and a poleward movement of the northern jet stream is expected. This would also be known as a positive NAO/AO response (Feldstein and Lee 2014).

This study uses the tug-of-war idea to explain the differences between the different CMIP5 model zonal wind responses. Using CMIP5 Historical and RCP8.5 climate model outputs this study has determined there is a strong correlation between the difference in tropical warming aloft and Arctic warming at the surface and the increase or decrease in zonal winds of the mid-latitude jet stream. This will allow for future work to see if by combining CMIP5 climate model data, observational data, and reanalyses will allow a better insight on what the future holds for the atmospheric circulation and the mid-latitude jet.

CHAPTER TWO: BACKGROUND

Our understanding of the atmospheric circulation in a warming world is not complete. As the warming occurs there is still not a consensus if zonal wind will increase in speed and cause a poleward shift of the mid-latitude jet or decrease in speed and cause an equatorward shift of the mid-latitude due to the tug-of-war between the warming of the tropics aloft and the warming of the Arctic at the surface.

The mid-latitude jet is a pivotal part in the Northern Hemisphere (NH) climate and weather pattern. The mid-latitude jet directs the much-needed synoptic weather systems for precipitation for most of the mid-latitudes but can also be the cause of extreme weather events such as flooding, droughts, severe weather outbreaks, heat waves and cold snaps (Francis and Vavrus 2015; Francis 2017). Therefore, it is vital to understand the effects warming of the atmosphere will have on the atmospheric circulation, especially the mid-latitude jet, in the coming future. This is the case not only from a weather and climate point of view but also from an agricultural and hydro-climatological one as well.

Some key aspects that have been determined in climate model driven studies are that warming aloft in the tropical troposphere drives modeled mid-latitude jet circulation poleward along with storm tracks as well (Butler et al. 2010; Ceppi and Hartmann 2016; Deser et al. 2015; Yim et al. 2016a; Yim et al. 2016b; Shaw and Tan 2018; Peings et al. 2018) and that cooler lower-stratospheric Arctic temperatures also result in a poleward movement of the mid-latitude storm tracks (Butler et al. 2010; Deser et al. 2015; Yim et al. 2016a; Yim et al. 2016b; Shaw and Tan 2018; Peings et al.

2018). However, Shaw and Tan (2018) found that subtropical warming aloft is possibly the real driver for the strengthening and poleward movement of the mid-latitude jet, not tropical warming aloft. This was determined by manipulating carbon dioxide in the subtropics and tropics in the climate models. Warming of the Arctic at the surface, in contrast, results in equatorward motion of mid-latitude storm tracks and an equatorward shift in the mid-latitude jet (Butler et al. 2010; Barnes and Polvani 2015; Deser et al. 2015; Ceppi and Hartmann 2016; Yim et al. 2016b; Shaw and Tan 2018; Peings et al. 2018). This is consistent with the tug-of-war framework.

Ceppi & Hartmann (2016) examined the effects clouds have on atmospheric circulation from shortwave and longwave radiation. This study was able to predict what effect each type of radiation had on atmospheric circulation using the tug-of-war framework that was discussed in the previous paragraph. For example, by increasing carbon dioxide, shortwave cloud radiation effects increased temperatures aloft over the tropics and decreased temperatures at the Arctic surface. This resulted in the tropics winning the tug-of-war; stronger temperature gradient between the tropics aloft and Arctic surface resulting in a strengthening of the westerlies and causing the mid-latitude jet to shift poleward. One drawback to this study is it only used one climate model, the GFDL AM2.1, to perform these runs and gain these results.

Arctic Amplification (AA) is the warming that occurs over the Arctic at the surface, in the lower troposphere, and has warmed more than double the global average (Cohen et al. 2014). AA is caused by sea ice loss and increased greenhouse gas emissions (Cohen et al. 2014). By 2100, AA occurs in almost all the CMIP5 climate models (Barnes

and Polvani 2015). Correlations between mid-latitude jet movement and AA have been shown but AA is not the sole or primary reason for the future change in the mid-latitude jet in the models (Barnes and Polvani 2015). However, the Deser et al. (2015) study determined a different response from the CCSM4 CMIP5 climate model. Deser et al. (2015) used two different runs from the climate model, one with ice coupling and one without. In these run outputs Deser et al. (2015) shows that Arctic sea ice loss is the primary reason for AA and that AA leads to the weakening of the westerlies and an equatorward shift of the mid-latitude jet. These results align with the tug-of-war framework.

In contrast to the other climate model studies, Barnes & Polvani (2015) also indicated that climate models are not conclusive enough and there is too much variation between models to indicate what the mid-latitude jet response will be in the future, but the models are a good starting point.

Other studies that used reanalysis instead of climate models show there is evidence indicating the mid-latitude jet's poleward motion is controlled by greenhouse gas emission warming of the tropics from the 1960s through 1990s (Feldstein and Lee 2014). Since that time though there has been a reversal, in re-analysis, indicating an equatorward shift (Feldstein and Lee 2014). The possible explanation of this is due to Arctic sea ice loss which enhances AA and is also caused by greenhouse gas emission warming (Feldstein and Lee 2014; Francis and Vavrus 2015). Another study that used re-analysis instead of climate models showed that the warming of the Arctic at the surface (and aloft) was larger than the warming of the tropics aloft (Graversen et al. 2008). This

study is considered controversial because the reanalysis used, ERA-40, is not necessarily applicable for climate reanalysis (Thorne 2008). In Santer et al. (2013, 2018) there is microwave sounding unit data that also shows the Arctic is warming more aloft and at the surface compared to the tropics which is not warming as much throughout the atmosphere. In these studies, the results indicate that the Arctic is winning the tug-of-war, the mid-latitude jet should be weakening and moving equatorward, which is opposite of the current consensus.

From the climate model analysis, the consensus is that the tropics will warm the most and win the tug-of-war. From an observational analysis, the Arctic is warming the most and winning the tug-of-war. This is what has motivated us to determine which part of the atmosphere will warm the most, leading us to examine each model independently. By using the tug-of-war idea, we are able to show the differences that occur between climate models. This allows us to show how if the tropics or Arctic warms the most, there is an effect on the zonal wind and mid-latitude jet.

Barnes & Polvani (2015) was the first study to closely examine differences in the tug-of-war idea between different climate models. Barnes & Polvani (2015) gave us a starting point on how to define Arctic temperature change. Their definition is the difference in temperature from the CMIP5 RCP8.5 2076-2099 and Historical 1980-2004 output vertically averaged over the latitude range of 70°N-90°N and between the pressure levels of 925-700 hPa. This Arctic temperature change is then divided by the global mean temperature change from the same periods and defined as Arctic Amplification (AA). This was then compared to the averaged zonal wind at the 500 hPa

level for a latitude box from 30°-70°N, 130°-10°W. Barnes & Polvani (2015) determined there was a wintertime (JFM) correlation of -0.64 between AA and zonal wind speed. This negative correlation is consistent with the tug-of-war framework. Compared to JFM, the correlation was even stronger for the months of May, June, July, and August with June having the highest, which was close to -1.

Another study that looked at climate model to model differences was Yim et al. (2016b). This study focused on 34 CMIP5 RCP4.5 pathway climate model and ensemble runs to show that not all climate models agree on a poleward shift of the mid-latitude jet as the multi-model mean of the climate models shows (Collins et al. 2013). This study showed the difference between each model run's zonal-mean wind response and a visualization of the movement of the mid-latitude jet. The most significant finding was the change in the mid-latitude jet in the models with stronger warming at the Arctic surface led to an equatorward shift and in contrast a poleward shift was associated with stronger Arctic lower stratospheric cooling. This further confirms the tug-of-war idea in climate models.

The most methodical climate model study to compare the difference between climate models was Peings et al. (2018). This study focused on the atmospheric circulation using two ensembles with the first consisting of 36 CMIP5 Historical and RCP8.5 climate model runs and the second being the Community Earth System Model Large Ensemble (CESM-LENS) which consisted of 40 ensemble members. This study took a more dynamical approach to understanding the changes in the mid-latitude jet while focusing on the North Atlantic between the months of October thru March. This study

determined that there was a narrowing of the mid-latitude jet due to the warming of the Arctic surface and warming of the tropics aloft, again supporting the tug-of-war idea. This study's most significant finding for our work is the strong statistical correlation of 0.84 that was found between the zonal index (ZON) and the "ratio between upper-troposphere tropical and Arctic warming (RUTAW)" (Peings et al. 2018). The zonal index is used to indicate the strength, by geostrophic balance, of the mid-latitude jet and is defined as the difference of height between the latitudes 60-90°N and 20-50°N. The RUTAW is the zonal mean temperature change between 20°S-20°N from 400-150 hPa divided by the zonal mean temperature change between 60°N-90°N from 1000-700 hPa. The ZON vs. RUTAW correlation results allows the tug-of-war idea to be used to quantitatively predict the movement of the mid-latitude jet.

This study's method, which will be discussed later, is different but similar in determining the difference between the Historical and RCP8.5 zonal wind and temperature changes that occur in each CMIP5 model run. The correlation between ZON and RUTAW that was determined in Peings et al. (2018) using a standard linear regression method discussed in their Appendix section is comparable to this study's findings but not as strong. The results of this study will be discussed more in detail in the results section.

These studies have led us to ask many questions. Which part of the atmosphere is warming the most and is currently winning the tug-of-war? Is it the tropics, the subtropics, the Arctic, or a combination? What does each CMIP5 climate model individually produce compared to the averaged plot of all the climate models for

temperature change and zonal wind change? How does the warming of each model affect the atmospheric circulation, more precisely the mid-latitude jet? Is there a correlation between the Arctic and tropical/subtropical temperature change difference compared to the zonal wind change? Can we predict how the real-world mid-latitude jet will respond using the tug-of-war idea?

CHAPTER THREE: DATASET

a) Future Era – RCP8.5 minus Historical CMIP5

The first part of this study utilized the output from 41 Coupled Model Intercomparison Project Phase 5 (CMIP5) climate models (Taylor et al. 2012; Table 1) for temperature and zonal wind from Future and Historical runs (previous studies did not use as many climate models). The Historical time used a 30-year period from 1975-2004 and the Future time used a 30-year period from 2070-2099. The Future period used the Representative Concentration Pathway (RCP) 8.5 (Riahi et al. 2011). This RCP was chosen since current greenhouse gas emission is on course to warm the atmosphere this much in the future, which is comparable to raising the level of radiative forcing by 8.5 Wm^{-2} (Riahi et al. 2011). By using the RCP8.5 difference between the Future and Historical period, for both temperature and zonal wind, there will be a higher signal to noise ratio than the lower RCPs. This is the main reason this study is using RCP8.5.

b) Satellite Era – Present minus Past CMIP5

The second part of this study again utilized the output from CMIP5 climate models for temperature and zonal wind from RCP8.5 and Historical runs. The satellite era used 91 ensemble members from 42 CMIP5 climate models for the years 1979-2018. The 42nd climate model is the CESM1-WACCM. This climate model was not implemented in the statistical analysis for the RCP8.5 minus Historical part of the study due to the model not having an ensemble member 1. All the ensemble members are being applied because there is an expected bigger difference between them, due to the small signal to noise ratio that is expected to be found. This is in contrast with the RCP8.5 ensemble

members. Those members had a much lower difference between them and the original members, showing minute changes in difference when compared to the ensemble member 1. This dataset used the CMIP5 Historical (1979-2005) and the RCP8.5 (2006-2018) climate model run outputs for both zonal wind and temperature. The CMIP5 RCP8.5 is being used for these years because it represents the closest to what occurred in the real world, for 2006-2018, compared to the other RCP products (Riahi et al. 2011; Schwalm et al. 2020). The Historical and the RCP8.5 datasets were first concatenated together. Then the combined dataset was halved into two twenty-year sections, Past (1979-1998) and Present (1999-2018).

Table 1: This is a list of the 41 CMIP5 climate models being used for this study. The numbers identify the climate models on the correlation scatter plots for the future era (Figure 15 – 17) and satellite era (Figure 28 – 30). *Model 42 is only being used in the satellite era.

Number	Model	Number	Model
1	ACCESS1-0	22	GFDL-ESM2M
2	ACCESS1-3	23	GISS-E2-H
3	CMCC-CESM	24	GISS-E2-R
4	CMCC-CM	25	HadGEM2-AO
5	CMCC-CMS	26	HadGEM2-CC
6	CNRM-CM5	27	HadGEM2-ES
7	CSIRO-Mk3-6-0	28	IPSL-CM5A-LR
8	GFDL-CM3	29	IPSL-CM5A-MR
9	MIROC-ESM-CHEM	30	IPSL-CM5B-LR
10	bcc-csm1-1	31	MIROC5
11	bcc-csm1-1-m	32	MIROC-ESM
12	BNU-ESM	33	MPI-ESM-LR
13	CanESM2	34	MPI-ESM-MR
14	CCSM4	35	MRI-CGCM3
15	CESM1-BGC	36	MRI-ESM1
16	CESM1-CAM5	37	GISS-E2-H-CC
17	FGOALS-g2	38	GISS-E2-R-CC
18	FGOALS-s2	39	inmcm4
19	EC-EARTH	40	NorESM1-M
20	FIO-ESM	41	NorESM1-ME
21	GFDL-ESM2G	42*	CESM1-WACCM

CHAPTER FOUR: METHODS

The first part of this study took the difference between the Future (RCP8.5 2070-2099) versus the Historical (1975-2004) climate model outputs for temperature(K) and zonal wind(ms^{-1}). The difference was then plotted for the zonal-mean temperature and zonal mean wind for each model and the ensemble members of each model on a separate latitude-pressure plot. Each model and ensemble member have two plots: one for temperature difference and one for zonal wind difference. Figures 1-10 have the latitude-pressure plots for ensemble member 1 for each model, odd being temperature difference and even being zonal wind difference. Figures A1-A28 have the latitude-pressure plots for each climate model with more than one ensemble member, which are nearly identical. Therefore, this analysis will only be using the latitude-pressure plots for the ensemble member 1 for each model for the next part of this study.

This procedure is comparable to Yim et al. (2016b) with a few key differences. Namely, this analysis is using 41 RCP8.5 CMIP5 climate model runs for a 30-year climate period for all seasons instead of 34 RCP4.5 CMIP5 climate model runs for a 40-year period for December through February.

For the second part of this study, vertical boxes were defined from one latitude to another and from one pressure level in the atmosphere to another and then the average of the zonal wind and temperature was taken over the set vertical boxes. Zonal wind used a few different latitude ranges from 50°N to 70°N, 40°N to 70°N, 30°N to 60°N, and 30°N to 70°N to determine the best area associated with the Northern mid-latitude jet. The pressure levels for these boxes went from the surface (1000mb) to

400mb, surface to 300mb, and surface to 200mb. This area for zonal wind is where, in most of the latitude-pressure plots, the mid-latitude jet is defined and shows an increase or decrease in wind speed giving the indication of a strengthening or weakening of the mid-latitude jet.

For temperature two different vertical boxes were defined, one for the tropics and one for the Arctic. The Arctic vertical box was defined from 60°N to 90°N in latitude. For the pressure levels of the Arctic vertical box, we tried many different intervals from the lower troposphere (ex. 850mb) to the lower stratosphere (ex. 100mb). For the tropics we used a few different latitude ranges from 20°S to 20°N, 30°S to 30°N, Equator to 30°N, Equator to 20°N, 10°N to 40°N, 10°N to 30°N, 20°N to 30°N, and 20°N to 40°N. This analysis used both tropical and subtropical latitudes to determine the area of the atmosphere that is highly correlated with the strengthening or weakening of the mid-latitude jet. Subtropical latitudes are being used due to the Shaw and Tan (2018) study which determined that subtropical latitudes from 20°N to 40°N had the most significant mid-latitude jet response when higher amounts of carbon dioxide where introduced. For the pressure levels of the tropical or subtropical vertical box, many different intervals were experimented with, from the lower troposphere (ex. 925mb) to the upper troposphere (ex. 200mb), similar to the Arctic box. The Arctic and Tropical/Subtropical pressure levels were chosen due to two studies giving us starting points as well as the visualization, from latitude-pressure plots, showing the tropical warming bullseye aloft and the Arctic surface warming or Arctic Amplification. Those studies were Barnes and Polvani (2015) which used 925-700 hPa for Arctic Amplification and Peings et al. (2018)

which used 400-150 hPa for the tropical warming aloft and 1000-700 hPa for the Arctic surface warming.

Once the temperature was averaged over the vertical boxes, the Arctic vertical box was subtracted from a tropical or subtropical vertical box to determine the difference in temperature response between these two vertical boxes for each of the 41 CMIP5 models. These temperature response differences are then compared to each of the zonal wind change vertical box averages of each corresponding CMIP5 model output. The correlation was then determined across models between the change in zonal-mean wind speed and the average temperature change differences between the Arctic and tropical/subtropical vertical boxes. By using a correlation analysis this may allow us to predict the zonal wind response by using the tug-of-war framework.

The third part of this study was focused on the satellite era (1979-2018). The temperature and zonal wind difference were then taken between the Present (1999-2018) and the Past (1979-1998). This difference was then used to make the latitude pressure plots for all the climate models and ensemble members for the satellite era as was done for the RCP8.5 minus Historical part. As with the RCP8.5 minus Historical part each climate model and ensemble member have two plots: one for temperature difference and one for zonal wind difference. Figures 11-20 has the latitude-pressure plots for ensemble member 1 for each model, odd being temperature difference and even being zonal wind difference. Figures B1-B34 has the latitude-pressure plots for each climate model with more than one ensemble member.

The fourth part of this study is the statistical analysis for the satellite era. The vertical box method that was implemented for the RCP8.5 minus Historical part will again be applied for the satellite era. This again is using the warming difference in temperature and change in zonal wind speed between the Arctic and tropics to determine a correlation between the two. This part of this study is trying to determine if a strong correlation will be found between all the climate models and ensemble members for the satellite era as compared to the RCP8.5 minus Historical part of the study. The focus will be on the vertical boxes that were found to have a strong correlation in the RCP8.5 minus Historical part of the study. We are eager that the outcome of this study will lead to a future study, by using the satellite era defined vertical boxes along with observations and reanalysis. Combing these three datasets may allow a future study to be able to predict the strength of the mid-latitude jet in the future by determining which part of the atmosphere warms the most.

CHAPTER FIVE: RESULTS – FUTURE ERA

a) RCP8.5 minus Historical Latitude-Pressure Plots

When comparing the change in warming for the 41 CMIP5 climate model outputs between the average Historical (1970-2009) and the average RCP8.5 (2074-2099) latitude-pressure plots there was a warming for the tropical troposphere aloft and the Arctic surface for every model (Figures 1-9, odd). Another notable trend is the cooling of the lower stratosphere that occurs from the mid-latitudes to the Arctic for every climate model. The most notable difference between the climate models is how different the expected warming is supposed to be for each part of the atmosphere especially compared to the overall consensus (Collins et al. 2013). For example, the CNRM-CM5 (Figure 1) shows a significant amount of warming occurring at the surface of the Arctic compared to the tropics aloft. While the IPSL-CM5A-LR (Figure 7) and the IPSL-CM5A-MR (Figure 7) both show the tropics aloft warming (≥9 K) more than the surface of the Arctic (≤8 K). These results show that many climate models differed on which area of the atmosphere warmed the most. The objective for these warming difference plots was to determine qualitatively which part of the atmosphere, the tropics or Arctic, warmed the most compared to one another to align with the tug-of-war idea.

This study then compared the change in zonal wind speed for the 41 CMIP5 climate models using the same procedures for temperature change (Figures 2-10, even). Each plot is overlaid with a historical zonal wind average to show if there is any change in the strength or latitudinal shift of the westerlies. The noticeable similarity between these zonal wind change plots is the strengthening and poleward migration of the

Southern Jet. This is consistently evident for each zonal wind change plot. The reason this is so consistent is the warming aloft of the tropics has won the tug-of-war in the Southern Hemisphere and is warming more than the Antarctic surface (Armour et al. 2016) leading to a strengthening of the Southern jet and a poleward shift. The noticeable differences with the zonal wind plots are the location and strength of the northern mid-latitude jet. There is a noticeable shift in the location of the northern mid-latitude jet depending on the strengthening or weakening of the westerlies. For example, the CNRM-CM5 (Figure 2), CanESM2 (Figure 4), EC-EARTH (Figure 6), MRI-CGCM1 (Figure 8), and INM-CM4 (Figure 10) plots all show a weakening of the westerlies and equatorward movement of the Northern mid-latitude jet. While the GFDL-CM3 (Figure 2), FGOALS-s2 (Figure 4), GISS-E2-R (Figure 6), IPSL-CM5B-LR (Figure 8) and GISS-E2-R-CC (Figure 10) plots all show a strengthening of the westerlies and a poleward movement of the Northern mid-latitude jet. The objective for these change in zonal wind plots was to determine qualitatively the strengthening or weakening of the westerlies and if a latitudinal shift of the Northern mid-latitude jet occurred.

This study then compared each CMIP5 climate model temperature change plot to the associated zonal wind change plot to determine if the tug-of-war idea held merit. There were strong indicators showing that temperature change plots showed the tropics (Arctic) warming the most corresponded to zonal wind change plots that increased (decreased) westerly wind speed and strengthened (weakened) the mid-latitude jet as what occurred in the IPSL-CM5A-LR and IPSL-CM5A-MR (CNRM-CM5). These findings aligned with the tug-of-war idea along with the results of other studies indicating that

the tug-of-war idea can be used in climate models. However, the change in latitude or poleward/equatorward shift does not follow the tug-of-war idea consistently in the zonal wind latitude-pressure plots. Most of the models show a poleward shift in the mid-latitude jet even if the Arctic surface warms more. Therefore, this study will only focus on the strength of the zonal wind and not the position of the mid-latitude jet.

b) RCP8.5 minus Historical Correlation Scatter Plots

The correlation analysis for this study consisted of comparing the change in zonal wind speed (ΔU) and the warming difference between the Arctic (ΔT-Ar) and the tropical (ΔT-Tr) vertical boxes across models. The following vertical box correlations were the first preliminary results that were discarded later due to finding more powerful predictive vertical boxes. The first ΔU vertical boxes ranged from 50°N-70°N and 40°N-70°N, from the surface (1000mb) to 400mb, 300mb, or 200mb (Figure 11). The first ΔT-Ar vertical boxes ranged from 60°N to 90°N, from the surface to 300mb, 400mb, 600mb, or 850mb (Figure 12). The first ΔT-Tr vertical boxes ranged from 20°S to 20°N, from the surface to 200mb, 300mb, 600mb, or 850mb (Figure 12). Each CMIP5 climate model is represented by a number on the scatter plot (Table 1). Our correlation results between the 50°N-70°N ΔU and the ΔT-Ar and ΔT-Tr vertical box difference ranged from -0.25 (ΔU 200mb, ΔT-Ar 850mb, ΔT-Tr 850mb) to -0.43 (ΔU 300mb & 400mb, ΔT-Ar 850mb, ΔT-Tr 850mb) (Table 2). While our correlation results between the 40°N-70°N ΔU and the ΔT-Ar and ΔT-Tr vertical box difference ranged from -0.45 (ΔU 200mb, ΔT-Ar 850mb, ΔT-Tr 850mb) to -0.64 (ΔU 300mb, ΔT-Ar 600mb, ΔT-Tr 200mb) (Table 3). Most of these correlations were

significant at 95% apart from the 50°N-70°N ΔU 200-400mb, ΔT-Ar 850mb, ΔT-Tr 850mb vertical boxes (Table 2).

The above procedure and results allowed us to hone our vertical box metrics after a considerable amount of trial and error (Table 4 & 5). The vertical box metric Tables 4 and 5 show each change in latitude and pressure that was implemented for each vertical box and the resulting correlation value. Here is a step by step process on how the strongest correlation was found for the future era.

The latitude of the ΔU vertical box was resized to 30°N to 60°N and then expanded to 30°N to 70°N (Figure 13) while the pressure levels remained the same. The latitude of the ΔT-Ar was kept the same (60°N to 90°N) and ΔT-Tr was tested through many different ranges and was finally settled on the 20°N to 40°N (Table 5, Figure 14). This latitude range was determined in Shaw and Tan (2018) as having the most effect on the zonal wind strength and poleward movement in climate models. The pressure levels for ΔT-Ar vertical box were from 850-300mb and ΔT-Tr vertical box were from 850-200mb. With the above ΔT-Ar and ΔT-Tr vertical boxes and the ΔU 200mb vertical box, this resulted in the best correlation value of -0.9245 (Figure 15). Specifically, for every degree of difference in warming between the Arctic troposphere (60-90°N, 850-300 mb) and subtropical troposphere (20-40°N, 850-200 mb) the mid-latitude zonal wind response (30-70°N, 1000-200 mb) decreased by -0.5 ms^{-1} (r = -0.9245). The pressure levels of 850-200mb for the ΔT-Tr vertical box correlated the best because the warming aloft of the tropics/subtropics were expected to have a significantly higher correlated response compared to the surface even though this pressure level is closer to the

surface compared to other studies (Butler et al. 2010; Barnes and Polvani 2015; Deser et al. 2015; Ceppi and Hartmann 2016; Shaw et al. 2016; Yim et al. 2016; Francis 2017; Peings et al. 2018; Screen et al. 2018; Shaw and Tan 2018). The pressure levels of 850-300mb for the ΔT-Ar vertical box were surprising results. From previous studies we expected the surface (1000mb) would be involved but did not expect the warming to extend into the troposphere as much as it did, other studies indicated that the surface of the Arctic would be key (Butler et al. 2010; Deser et al. 2015; Ceppi and Hartmann 2016; Yim et al. 2016b; Shaw and Tan 2018; Peings et al. 2018). There were also other vertical boxes that gave strong correlation values around -.92 with only slightly different ΔT-Ar and ΔT-Tr vertical box metrics (Table 5, Figure 16-17). The same vertical box parameters were ΔU 200mb 30°N to 70°N and latitudes for the ΔT-Tr vertical box. The differences were the change in pressure levels for ΔT-Ar and ΔT-Tr (Table 5, Figure 16-17).

There are four factors to why there are better correlations with these more optimal vertical boxes compared to the less optimal original vertical boxes. The first, which is the most significant, is the expansion of the zonal wind field latitudes to 30°N to 70°N (Table 4). This caused a significant jump of -.1666 (ΔU 200mb), -.1843 (ΔU 300mb), and -.1893 (ΔU 400mb) in the correlation value compared to the highest 40°N to 70°N vertical box correlations values (Table 3 & 4). This suggest that the ΔU vertical box 40°N to 70°N latitudes were presumably missing part of the mid-latitude jet. The latitude-pressure plot vertical box example for the ΔU (Figure 13) gives a good visualization of the expansion from 40°N to 70°N to 30°N to 70°N. This shows how much more of the mid-latitude jet was captured in this vertical box metric for each climate model member. The

next was the expansion of the ΔT-Ar from the lower (1000 mb) and middle troposphere (600 mb) to the complete troposphere (1000-200 mb) in the Arctic (Table 4). This increased the correlation by -0.0642 for ΔU 200mb but decreased the correlation for ΔU 300mb by 0.0204 and ΔU 400mb by 0.0281. The third was the 20°N to 40°N for the ΔT-Tr vertical box, again as determined in Shaw and Tan (2018). This latitude range had the highest increase in the correlation value compared to any other latitude range that was tested (30°S-30°N, 20°S-20°N, 0°-20°N, 0°-30°N, 0°-40°N, 10°-40°N, and 10°-30°N) for the ΔT-Tr vertical box (Table 4 & 5). The final was the slight changes in pressure levels for both the ΔT-Ar and ΔT-Tr vertical boxes. The pressure levels were changed from the surface for the ΔT-Ar (1000 mb to 850 mb) and towards the surface for ΔT-Tr (600 mb to 850 mb). This led to the most robust correlations overall (Table 5, Figure 15-17). These results indicate that the mid troposphere for both the ΔT-Ar and ΔT-Tr warming difference is more correlated to the strength of the mid-latitude jet than the Arctic surface or the tropical upper troposphere.

With these correlation results this allows us to potentially predict the future response of the mid-latitude jet strength. Our correlation results were stronger than that of Barnes and Polvani (2015) of -0.64. This is likely because Barnes and Polvani (2015) focused on the warming for the global mean at the surface and winter (JFM) while we focused on the warming for the tropics/subtropics aloft for all seasons. Our correlation was also stronger than that of Peings et al. (2018) of 0.84. This is likely because Peings et

al. (2018) focused on the warming for the tropics (20°S-20°N) from October-March while this study focused on the warming of the subtropics (20-40°N) for the whole year.

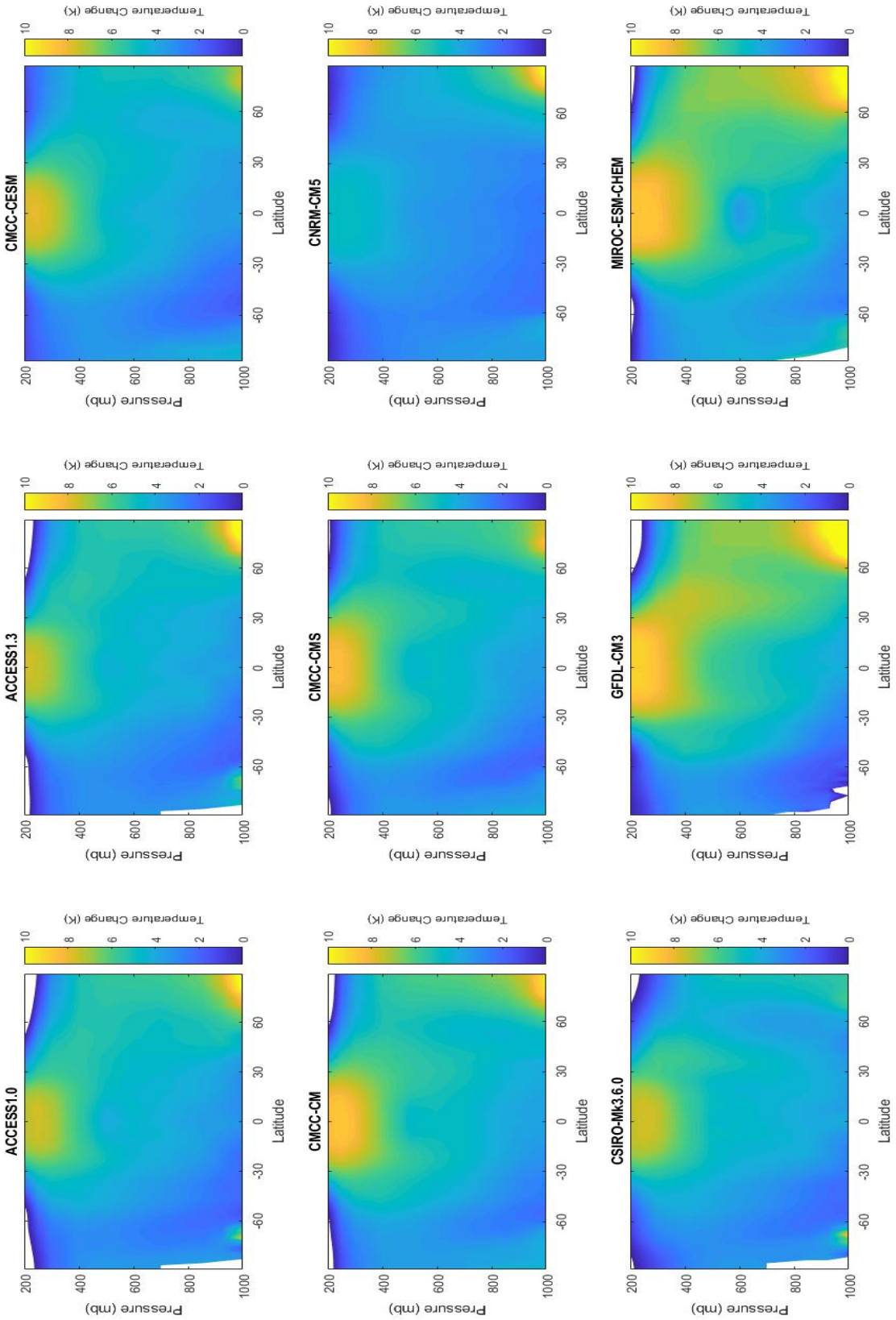

Figure 1: Warming between the RCP8.5 (2070-2099) and Historical (1975-2004) climate model r1 output for models 1-9 of 41.

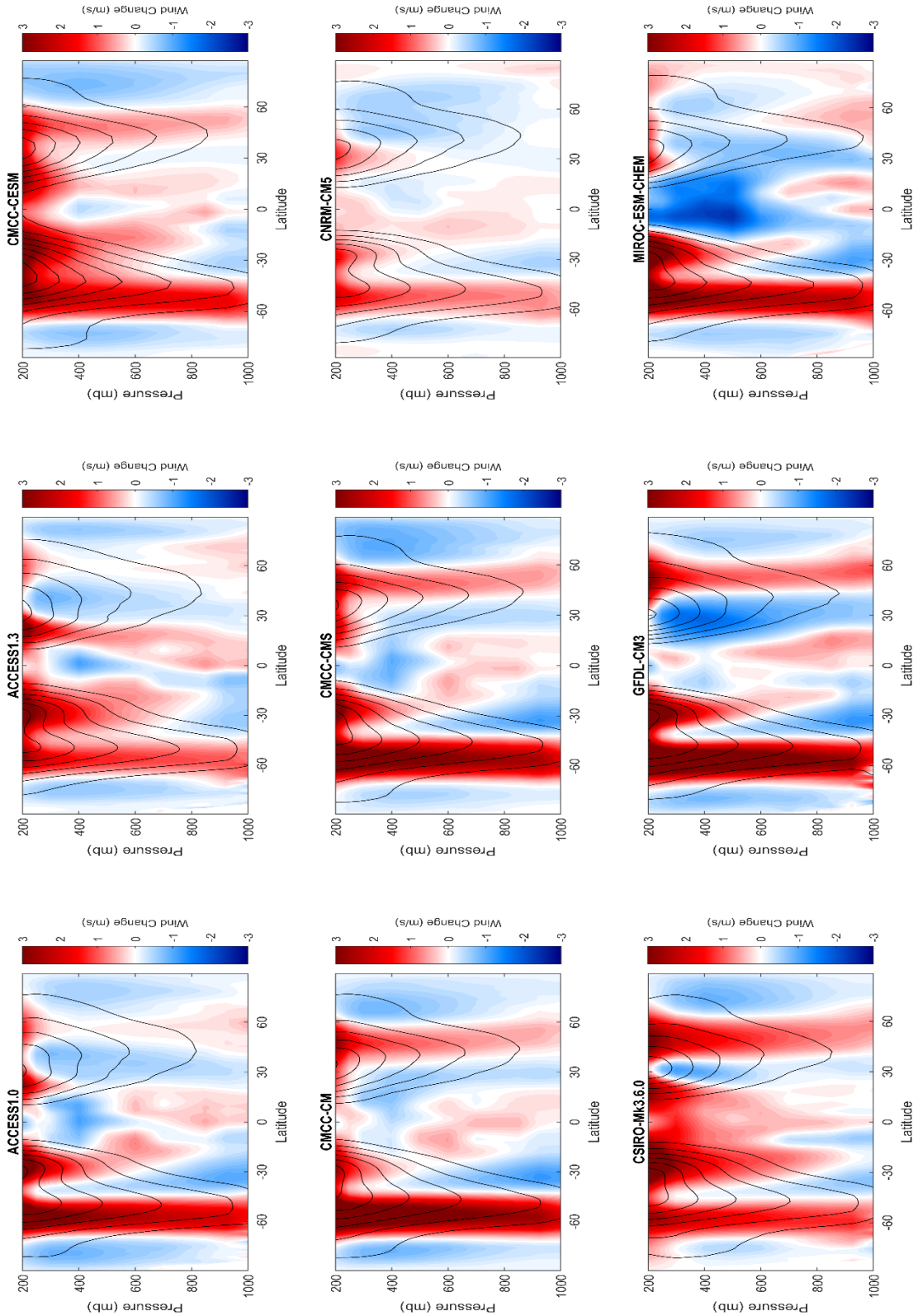

Figure 2: Zonal wind change between the RCP8.5 (2070-2099) and Historical (1975-2004) climate model r1 output for models 1-9 of 41.The black contours are the Historical zonal wind mean and are in increments of 5 ms-1.

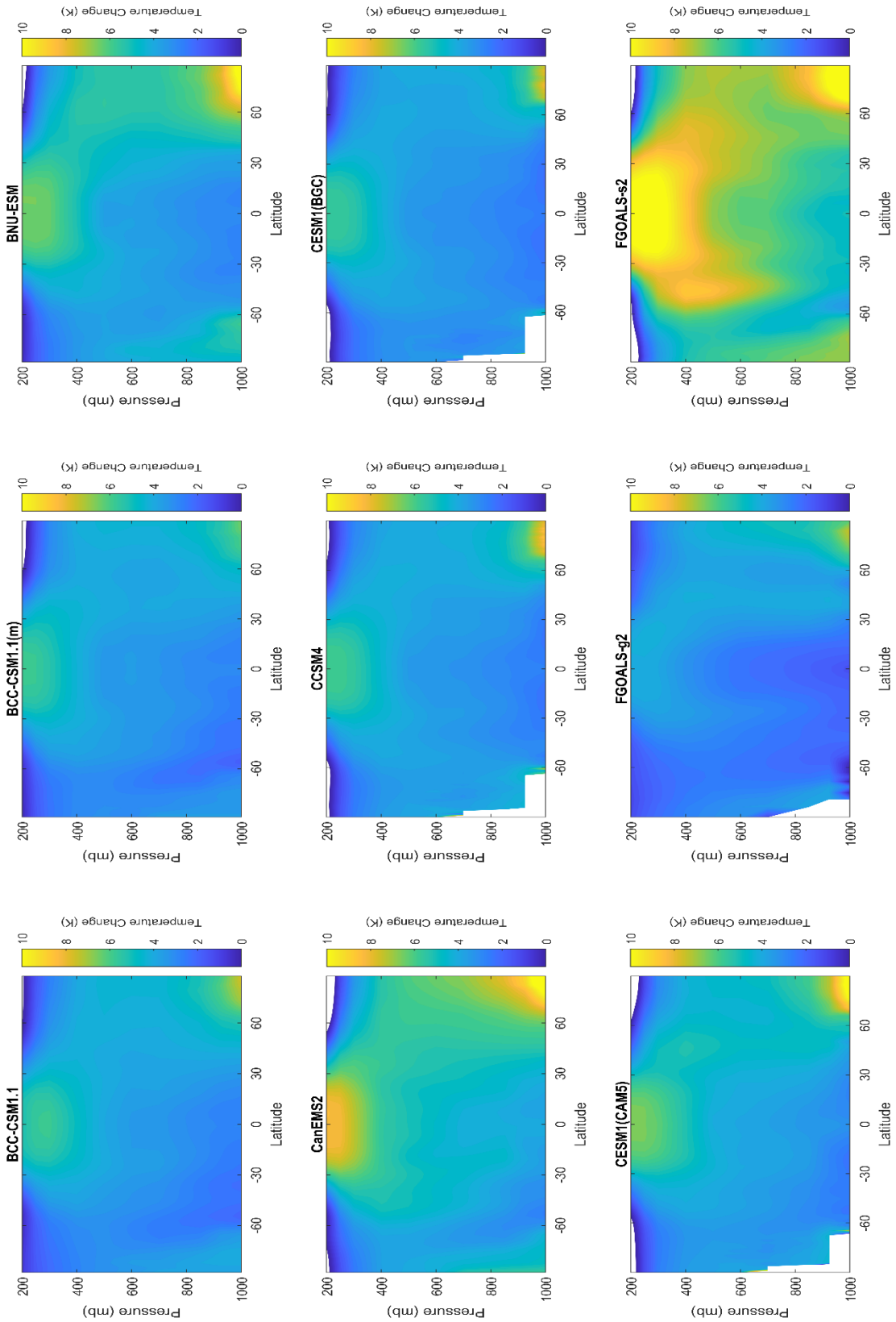

Figure 3: As in Figure 1 but for models 10 through 18 of 41.

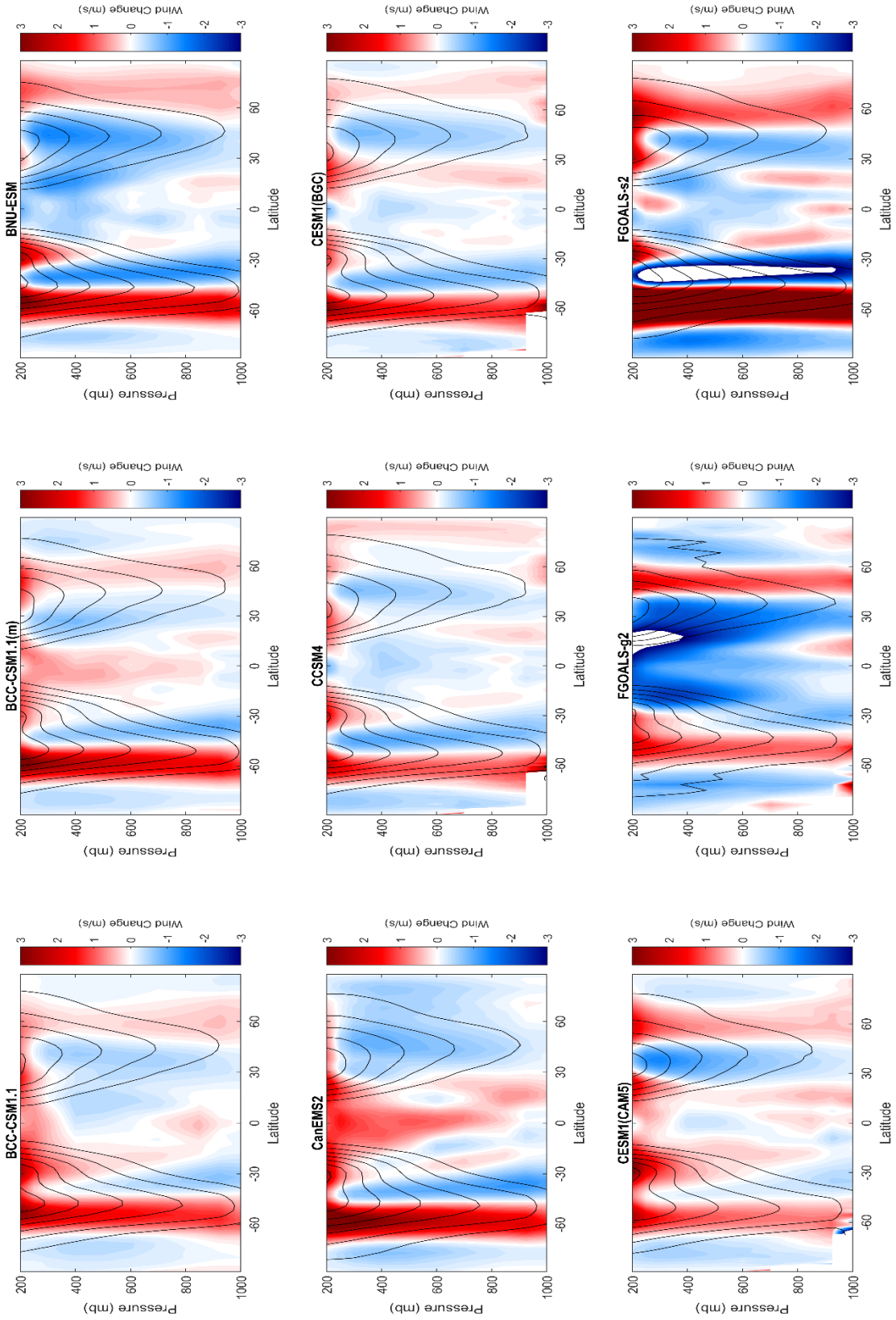

Figure 4: As in Figure 2 but for models 10 through 18 of 41.

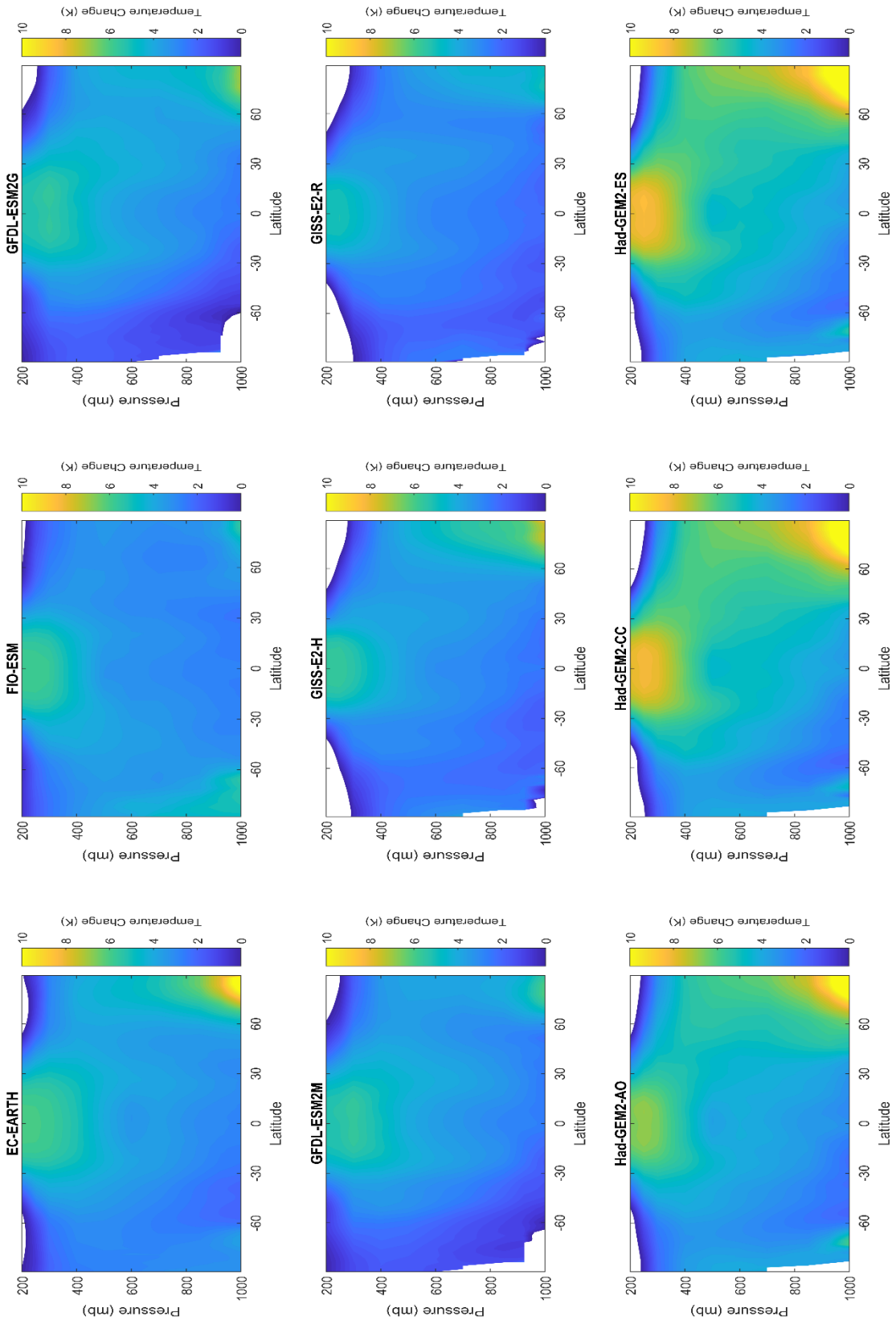

Figure 5: As in Figure 1 but for models 19 through 27 of 41.

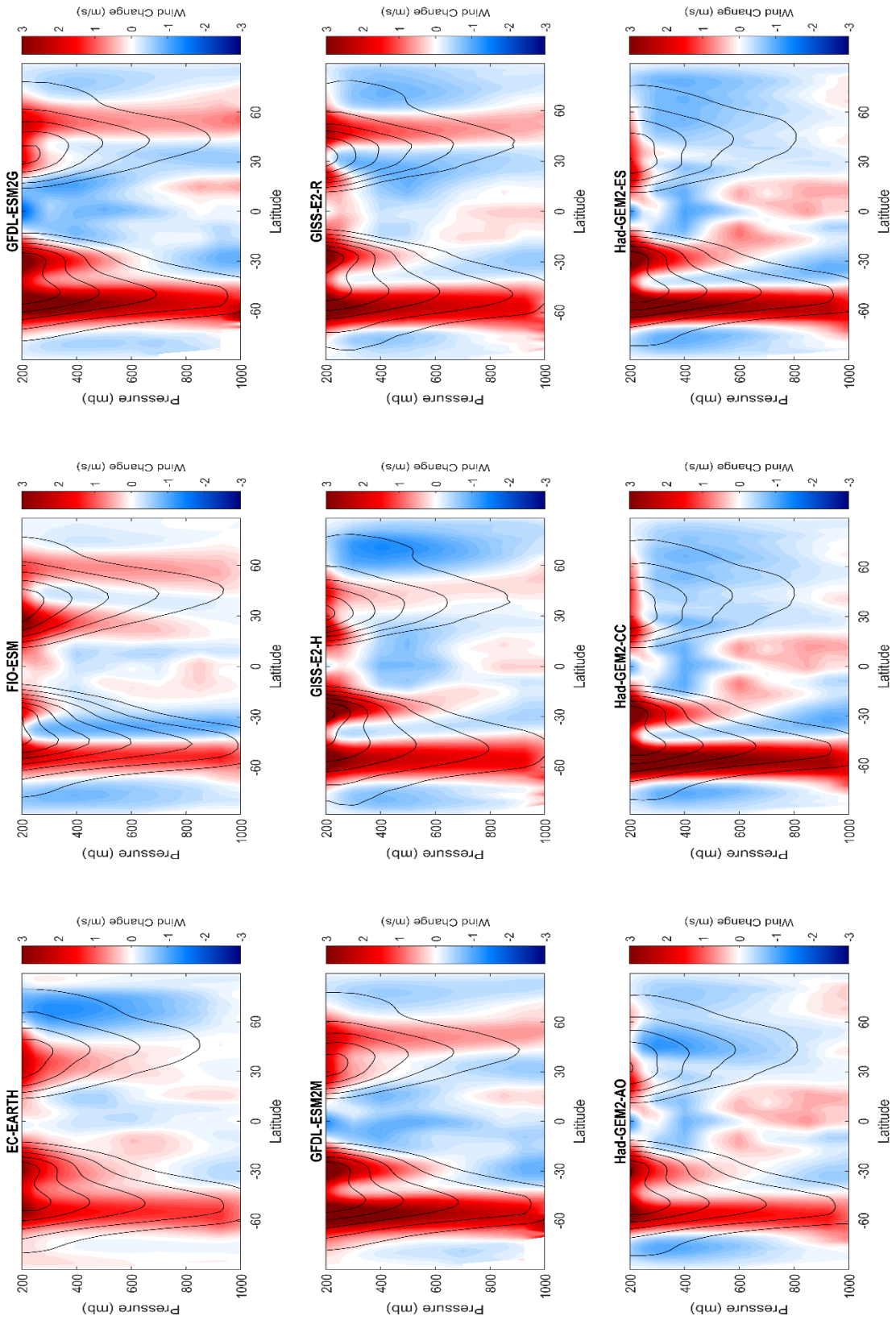

Figure 6: As in Figure 2 but for models 19 through 27 of 41.

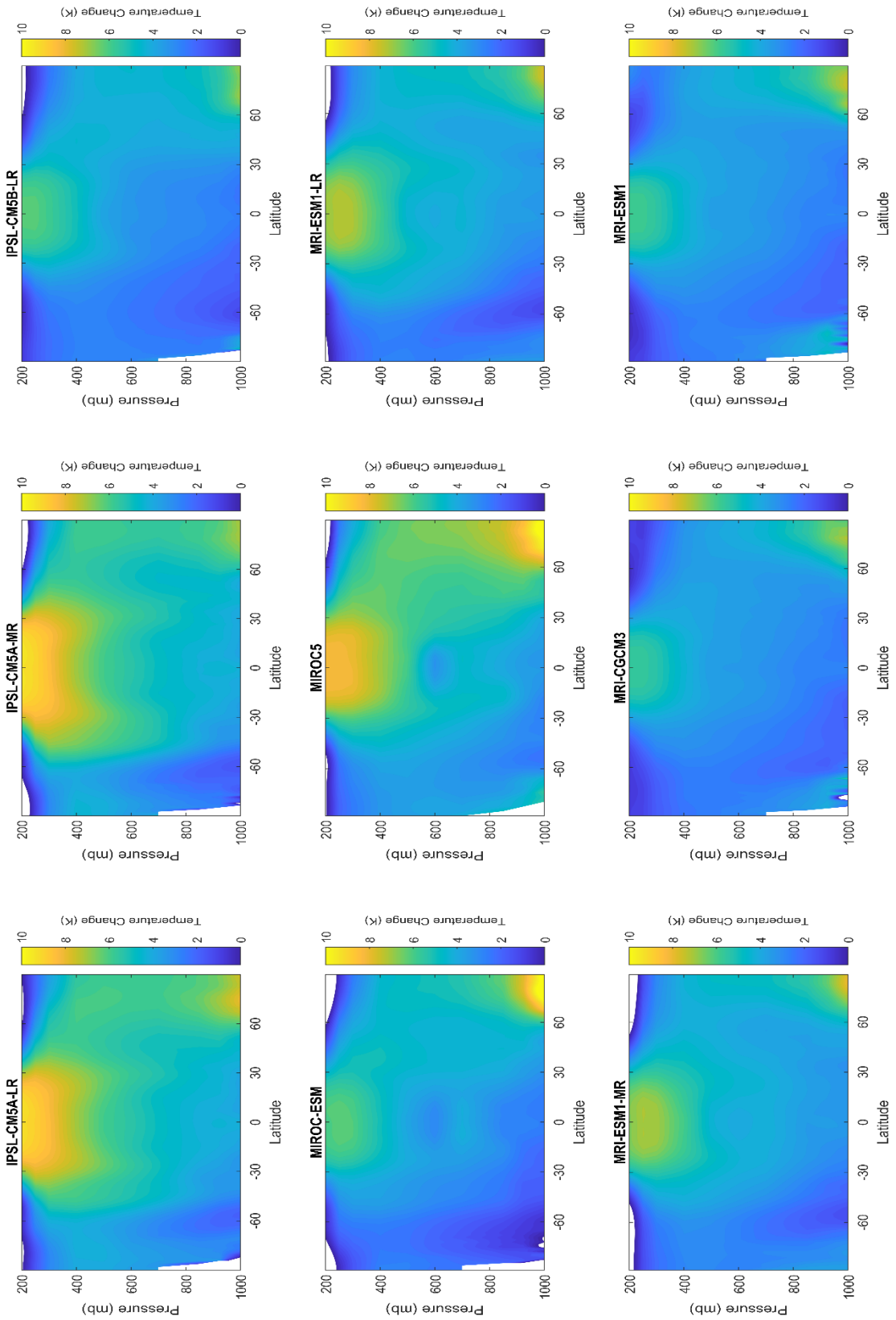

Figure 7: As in Figure 1 but for models 28 through 36 of 41.

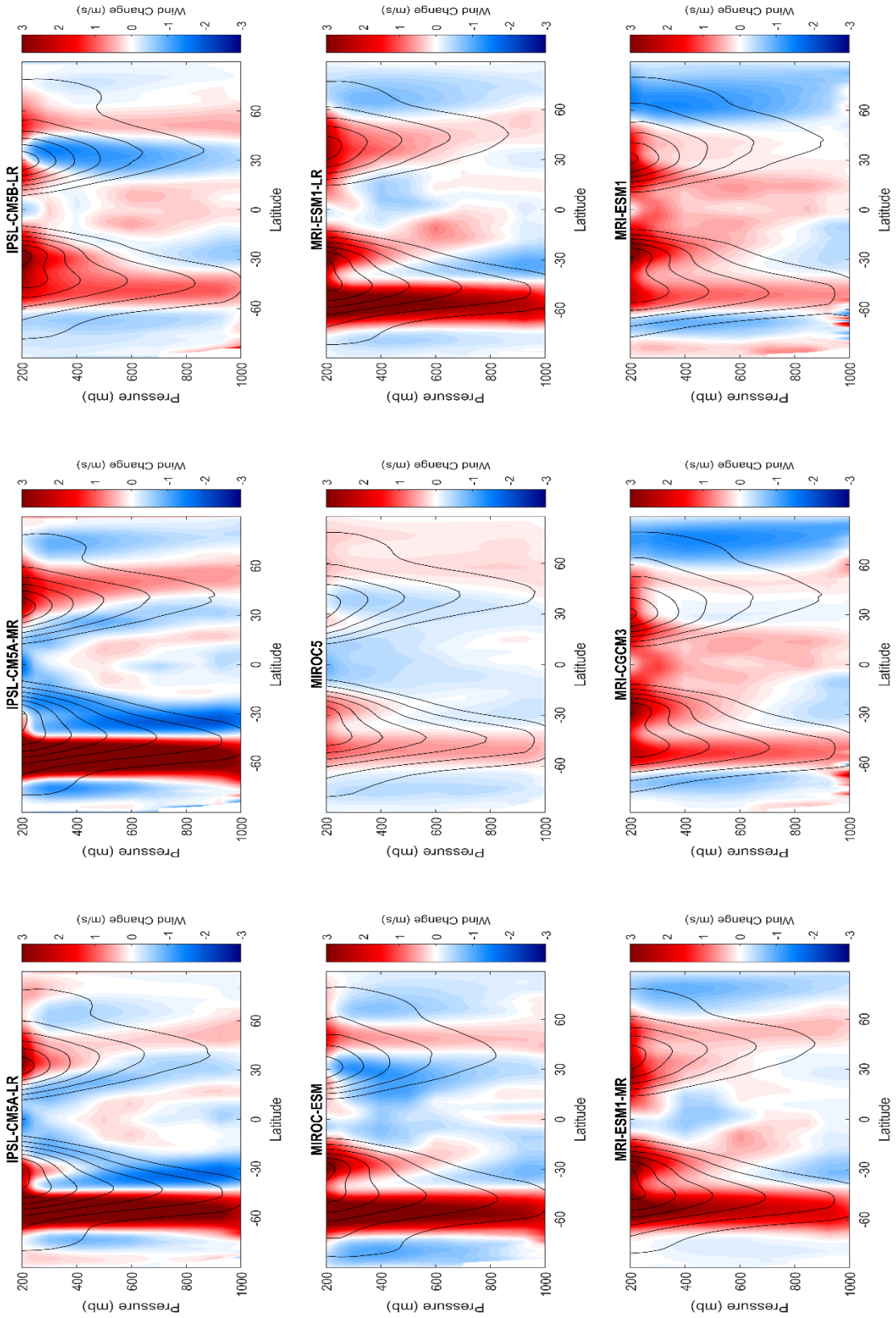

Figure 8: As in Figure 2 but for models 28 through 36 of 41.

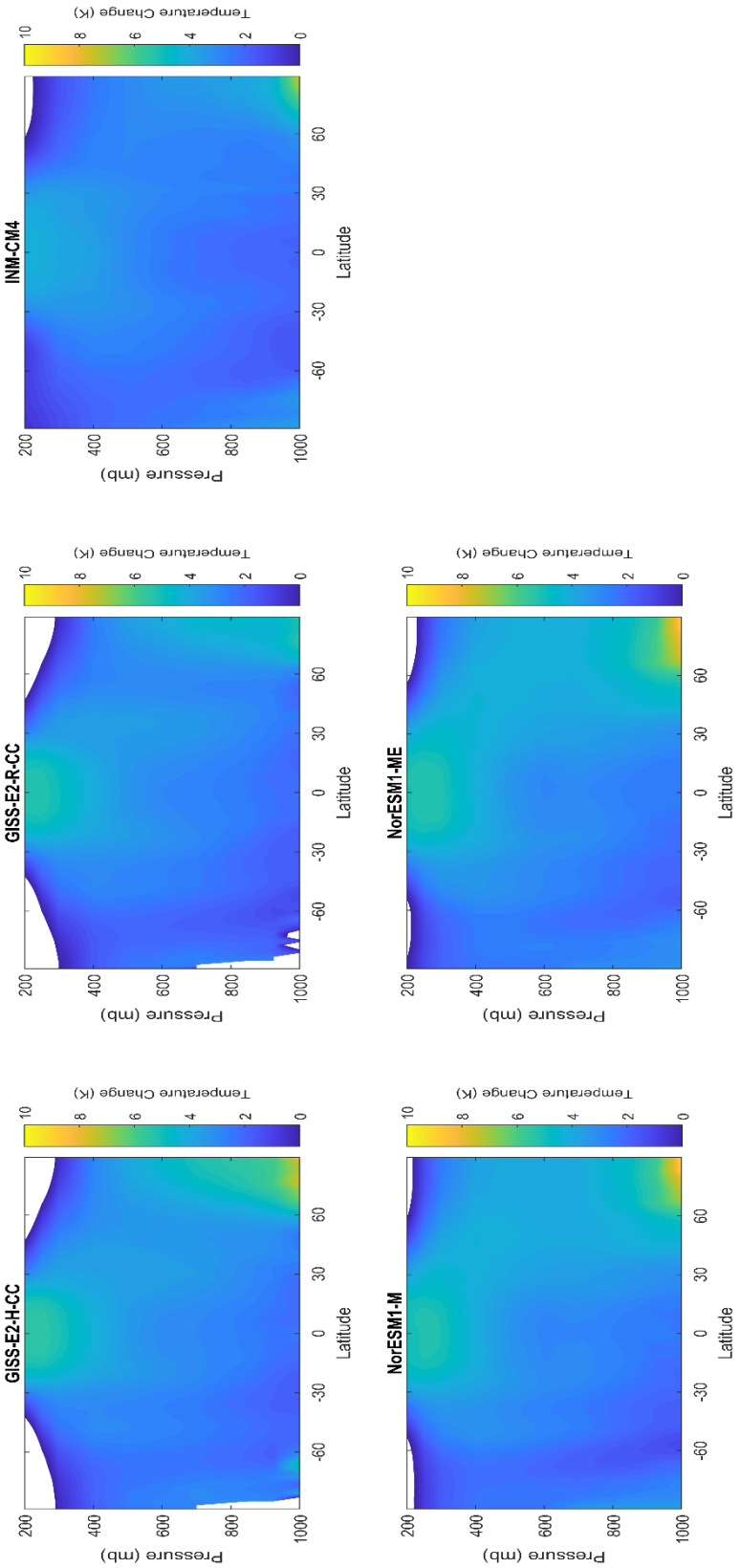

Figure 9: As in Figure 1 but for models 36 through 41 of 41.

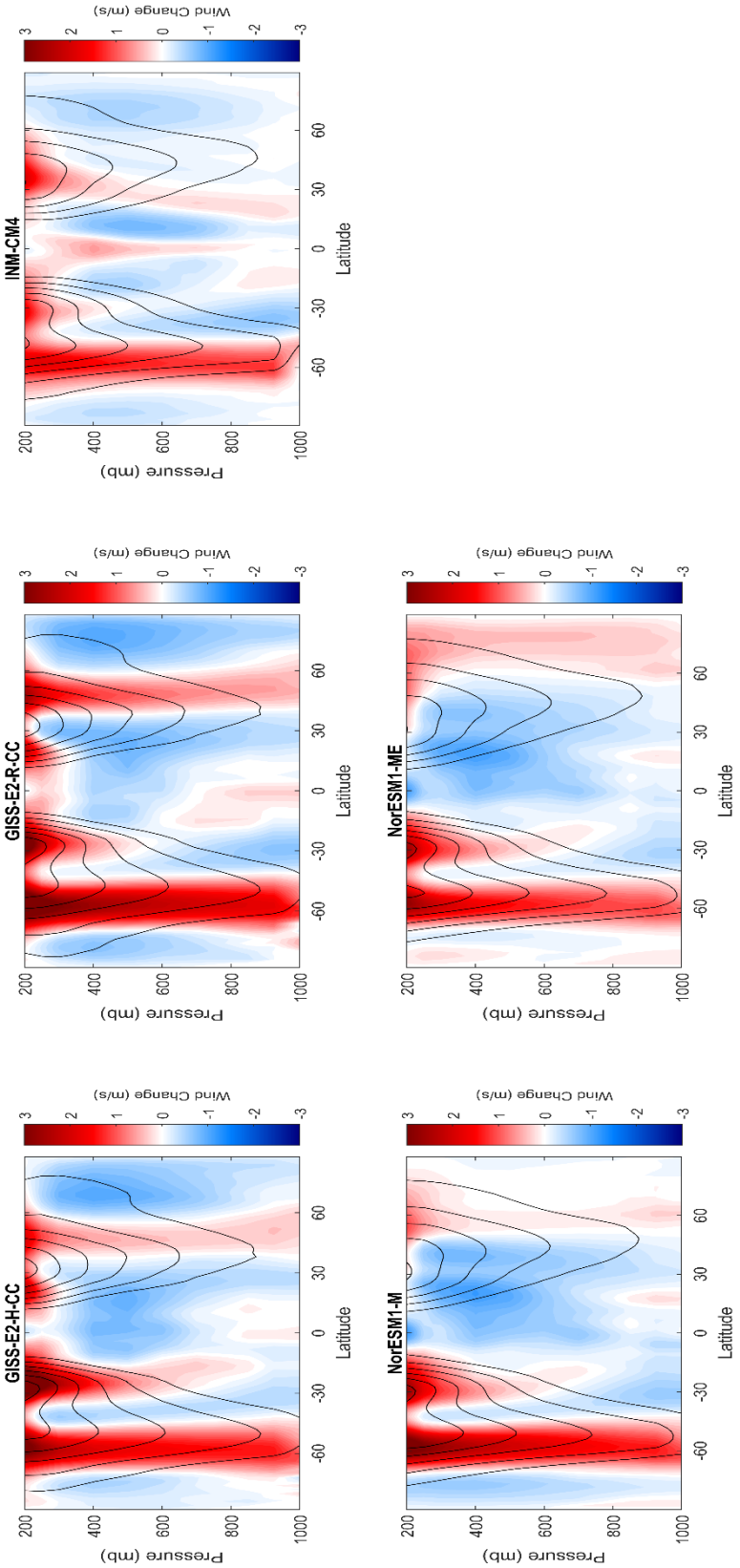

Figure 10: As in Figure 2 but for models 36 through 41 of 41.

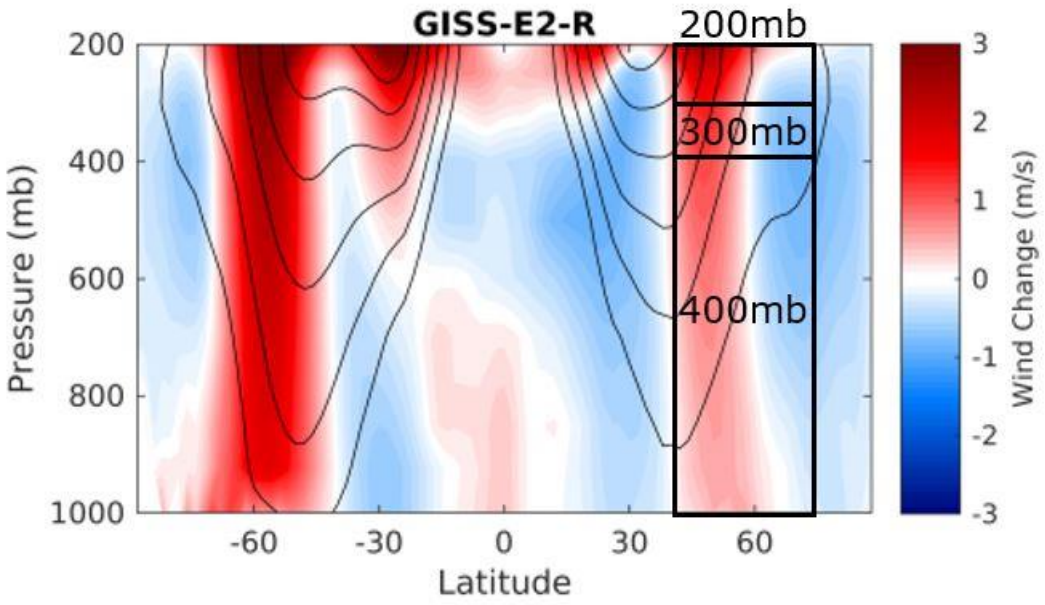

Figure 11: Visual example of vertical box areas of interest in the zonal wind change latitude-pressure plot between CMIP5 RCP8.5 (2070-2099) and Historical (1975-2004). 40-70°N from the surface to 200mb, 300mb, and 400mb.

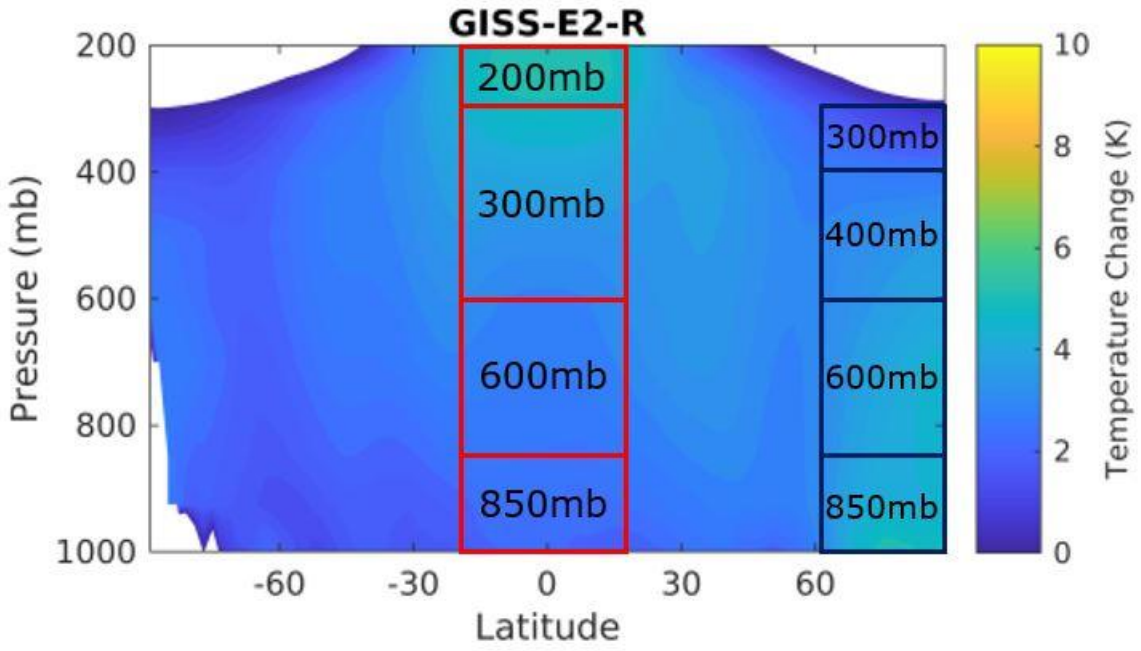

Figure 12: Visual example of vertical box areas of interest in the warming difference latitude-pressure plot between CMIP5 RCP8.5 (2070-2099) and Historical (1975-2004). 20°S to 20°N from the surface to 200mb, 300mb, 600mb, and 850mb for the tropics and 60-90°N from the surface to 300mb, 400mb, 600mb, and 850mb for the Arctic.

Table 2: Preliminary correlation analysis results for comparing the change in zonal wind speed (ΔU) for the latitude range of 50°N to 70°N and the warming between the given Arctic (ΔT-Ar) and the tropical (ΔT-Tr) vertical boxes. Each box goes from the surface (1000 mb) to the indicated pressure level.

50N to 70N	Correlation	P-value
Ua 200mb Arctic 400mb - Tropics 200mb	-0.39	0.012
Ua 200mb Arctic 600mb - Tropics 200mb	-0.42	0.0066
Ua 200mb Arctic 850mb - Tropics 300mb	-0.39	0.012
Ua 200mb Arctic 850mb - Tropics 850mb	-0.25	0.11
Ua 300mb Arctic 400mb - Tropics 200mb	-0.4	0.0094
Ua 300mb Arctic 600mb - Tropics 200mb	-0.43	0.0045
Ua 300mb Arctic 850mb - Tropics 300mb	-0.4	0.0094
Ua 300mb Arctic 850mb - Tropics 850mb	-0.29	0.064
Ua 400mb Arctic 400mb - Tropics 200mb	-0.4	0.01
Ua 400mb Arctic 600mb - Tropics 200mb	-0.43	0.0047
Ua 400mb Arctic 850mb - Tropics 300mb	-0.4	0.01
Ua 400mb Arctic 850mb - Tropics 850mb	-0.28	0.072

Table 3: Same as Table 2 with change in zonal wind speed (ΔU) for the latitude range of 40°N to 70°N vertical box.

40N to 70N	Correlation	P-value
Ua 200mb Arctic 400mb - Tropics 200mb	-0.62	1.80E-05
Ua 200mb Arctic 600mb - Tropics 200mb	-0.63	9.90E-06
Ua 200mb Arctic 850mb - Tropics 300mb	-0.62	1.80E-05
Ua 200mb Arctic 850mb - Tropics 850mb	-0.45	3.50E-03
Ua 300mb Arctic 400mb - Tropics 200mb	-0.62	1.50E-05
Ua 300mb Arctic 600mb - Tropics 200mb	-0.64	5.60E-06
Ua 300mb Arctic 850mb - Tropics 300mb	-0.62	1.50E-05
Ua 300mb Arctic 850mb - Tropics 850mb	-0.49	1.00E-03
Ua 400mb Arctic 400mb - Tropics 200mb	-0.61	2.60E-05
Ua 400mb Arctic 600mb - Tropics 200mb	-0.63	9.10E-06
Ua 400mb Arctic 850mb - Tropics 300mb	-0.61	2.60E-05
Ua 400mb Arctic 850mb - Tropics 850mb	-0.48	1.40E-03

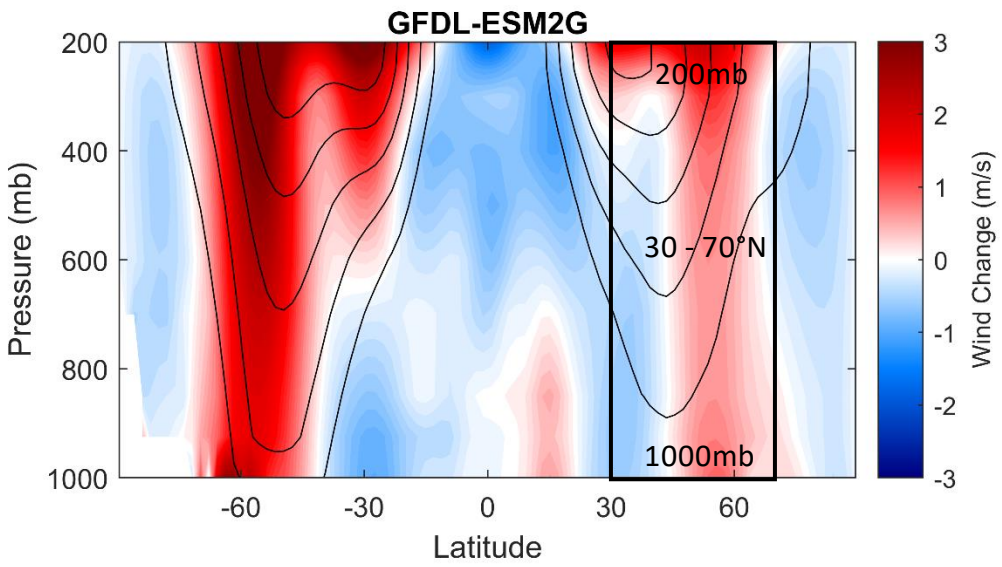

Figure 13: Most correlated vertical box area of interest in the zonal wind change latitude-pressure plot between CMIP5 RCP8.5 (2070-2099) and Historical (1975-2004). Latitudes of 30-70°N and from the surface (1000mb) to 200mb.

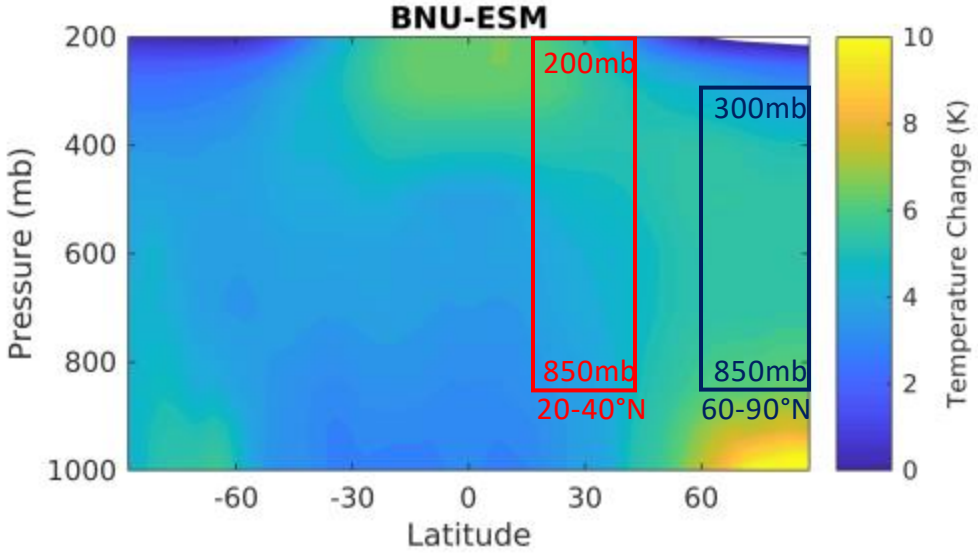

Figure 14: Most correlated vertical box area of interest in warming difference latitude-pressure plot between CMIP5 RCP8.5 (2070-2099) and Historical (1975-2004). Latitudes of 20-40°N and pressure levels from 850-200mb for the subtropics and latitudes of 60-90°N and pressure levels from 850-300mb for the Arctic.

Table 4: Future Era list of vertical box metrics for change in zonal wind speed (ΔU), the warming difference of the Arctic (ΔT-Ar) and the tropics/subtropics (ΔT-Tr), and the resulting correlation between the ΔU vertical box and the difference between ΔT-Ar and the ΔT-Tr vertical box. Red indicates metric that was changed compared to the vertical box before.

ΔU (M/S)			ΔT-Ar (K)				ΔT-Tr (K)				STATS	
1st Lat (°)	2nd Lat (°)	Press. (mb)	1st Lat (°)	2nd Lat (°)	1st Press. (mb)	2nd Press. (mb)	1st Lat (°)	2nd Lat (°)	1st Press. (mb)	2nd Press. (mb)	Correlation	P-value
40	70	200	60	90	1000	600	-20	20	1000	200	-0.6300	9.90E-06
40	70	300	60	90	1000	600	-20	20	1000	200	-0.6400	5.60E-06
40	70	400	60	90	1000	600	-20	20	1000	200	-0.6300	9.10E-06
30	60	200	60	90	1000	600	-20	20	1000	200	-0.7710	3.67E-09
30	60	300	60	90	1000	600	-20	20	1000	200	-0.7883	9.46E-10
30	60	400	60	90	1000	600	-20	20	1000	200	-0.7785	2.08E-09
30	70	200	60	90	1000	600	-20	20	1000	200	-0.7966	4.70E-10
30	70	300	60	90	1000	600	-20	20	1000	200	-0.8243	3.54E-11
30	70	400	60	90	1000	600	-20	20	1000	200	-0.8139	9.81E-11
30	70	200	60	90	1000	600	0	20	1000	200	-0.8002	3.42E-10
30	70	300	60	90	1000	600	0	20	1000	200	-0.8274	2.56E-11
30	70	400	60	90	1000	600	0	20	1000	200	-0.8170	7.28E-11
30	70	200	60	90	1000	600	-30	30	1000	200	-0.7977	4.26E-10
30	70	300	60	90	1000	600	-30	30	1000	200	-0.8285	2.30E-11
30	70	400	60	90	1000	600	-30	30	1000	200	-0.8179	6.67E-11
30	70	200	60	90	1000	600	0	30	1000	200	-0.8115	1.23E-10
30	70	300	60	90	1000	600	0	30	1000	200	-0.8414	5.65E-12
30	70	400	60	90	1000	600	0	30	1000	200	-0.8311	1.75E-11
30	70	200	60	90	1000	600	0	40	1000	200	-0.8114	1.24E-10
30	70	300	60	90	1000	600	0	40	1000	200	-0.8481	2.60E-12
30	70	400	60	90	1000	600	0	40	1000	200	-0.8393	7.16E-12
30	70	200	60	90	1000	500	0	40	1000	200	-0.8173	7.07E-11
30	70	300	60	90	1000	500	0	40	1000	200	-0.8503	1.99E-12
30	70	400	60	90	1000	500	0	40	1000	200	-0.8399	6.69E-12
30	70	200	60	90	1000	400	0	40	1000	200	-0.8249	3.30E-11
30	70	300	60	90	1000	400	0	40	1000	200	-0.8539	1.28E-12
30	70	400	60	90	1000	400	0	40	1000	200	-0.8417	5.45E-12
30	70	200	60	90	1000	300	0	40	1000	200	-0.8542	1.22E-12
30	70	300	60	90	1000	300	0	40	1000	200	-0.8696	1.62E-13
30	70	400	60	90	1000	300	0	40	1000	200	-0.8548	1.14E-12
30	70	200	60	90	1000	200	0	40	1000	200	-0.8815	2.81E-14
30	70	300	60	90	1000	200	0	40	1000	200	-0.8277	2.49E-11
30	70	400	60	90	1000	200	0	40	1000	200	-0.8112	1.26E-10
30	70	200	60	90	1000	200	10	40	1000	200	-0.9010	1.01E-15
30	70	300	60	90	1000	200	10	40	1000	200	-0.8491	2.31E-12
30	70	400	60	90	1000	200	10	40	1000	200	-0.8330	1.42E-11
30	70	200	60	90	1000	200	10	30	1000	200	-0.8821	2.54E-14
30	70	300	60	90	1000	200	10	30	1000	200	-0.8225	4.24E-11
30	70	400	60	90	1000	200	10	30	1000	200	-0.8041	2.43E-10

Table 5: Same as Table 4 with the change in zonal wind speed (ΔU) vertical box latitudes set to 30°N and 70°N and the strongest correlations.

ΔU (M/S)	ΔT-Ar (K)				ΔT-Tr (K)				STATISTICS	
Press. (mb)	1st Lat (°)	2nd Lat (°)	1st Press. (mb)	2nd Press. (mb)	1st Lat (°)	2nd Lat (°)	1st Press. (mb)	2nd Press. (mb)	Correlation	P-value
200	60	90	1000	200	20	40	1000	200	-0.9150	5.82E-17
300	60	90	1000	200	20	40	1000	200	-0.8700	1.52E-13
400	60	90	1000	200	20	40	1000	200	-0.8555	1.05E-12
200	60	90	925	200	20	40	1000	200	-0.8643	3.33E-13
300	60	90	925	200	20	40	1000	200	-0.7862	1.12E-09
400	60	90	925	200	20	40	1000	200	-0.7699	4.00E-09
200	60	90	925	300	20	40	1000	200	-0.8997	1.27E-15
300	60	90	925	300	20	40	1000	200	-0.9112	1.34E-16
400	60	90	925	300	20	40	1000	200	-0.8953	2.84E-15
200	60	90	925	400	20	40	1000	200	-0.8518	1.66E-12
300	60	90	925	400	20	40	1000	200	-0.8811	2.96E-14
400	60	90	925	400	20	40	1000	200	-0.8686	1.84E-13
200	60	90	925	300	20	40	925	200	-0.9143	6.79E-17
300	60	90	925	300	20	40	925	200	-0.9140	7.28E-17
400	60	90	925	300	20	40	925	200	-0.8972	2.02E-15
200	60	90	925	300	20	40	850	200	-0.9201	1.82E-17
300	60	90	925	300	20	40	850	200	-0.9080	2.54E-16
400	60	90	925	300	20	40	850	200	-0.8900	7.09E-15
200	60	90	925	300	20	40	700	200	-0.9193	2.22E-17
300	60	90	925	300	20	40	700	200	-0.8938	3.70E-15
400	60	90	925	300	20	40	700	200	-0.8745	7.99E-14
200	60	90	925	300	20	40	600	200	-0.9009	1.03E-15
300	60	90	925	300	20	40	600	200	-0.8672	2.26E-13
400	60	90	925	300	20	40	600	200	-0.8478	2.69E-12
200	60	90	850	300	20	40	850	200	-0.9245	6.36E-18
300	60	90	850	300	20	40	850	200	-0.8926	4.56E-15
400	60	90	850	300	20	40	850	200	-0.8706	1.40E-13
200	60	90	700	300	20	40	850	200	-0.9225	1.03E-17
300	60	90	700	300	20	40	850	200	-0.8693	1.68E-13
400	60	90	700	300	20	40	850	200	-0.8430	4.71E-12
200	60	90	600	300	20	40	850	200	-0.9128	9.42E-17
300	60	90	600	300	20	40	850	200	-0.8471	2.92E-12
400	60	90	600	300	20	40	850	200	-0.8175	6.94E-11

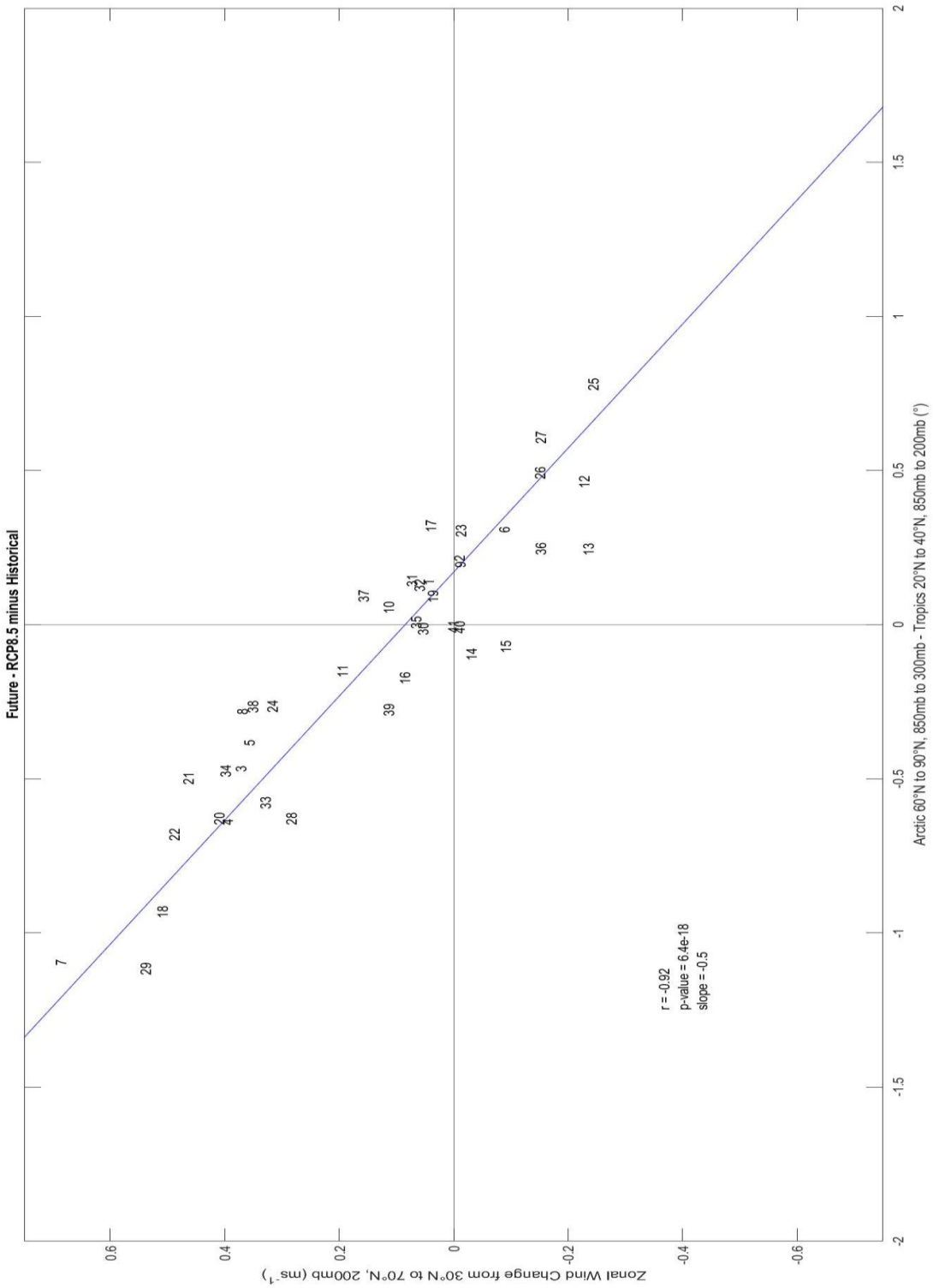

Figure 15: Future era scatter plot for zonal wind (30-70°N, surface to 200mb) versus the warming difference between the given Arctic (60-90°N, 850-300mb) and subtropics (20-40°N, 850-200mb) vertical box. Each number is one climate model (see Table 1).

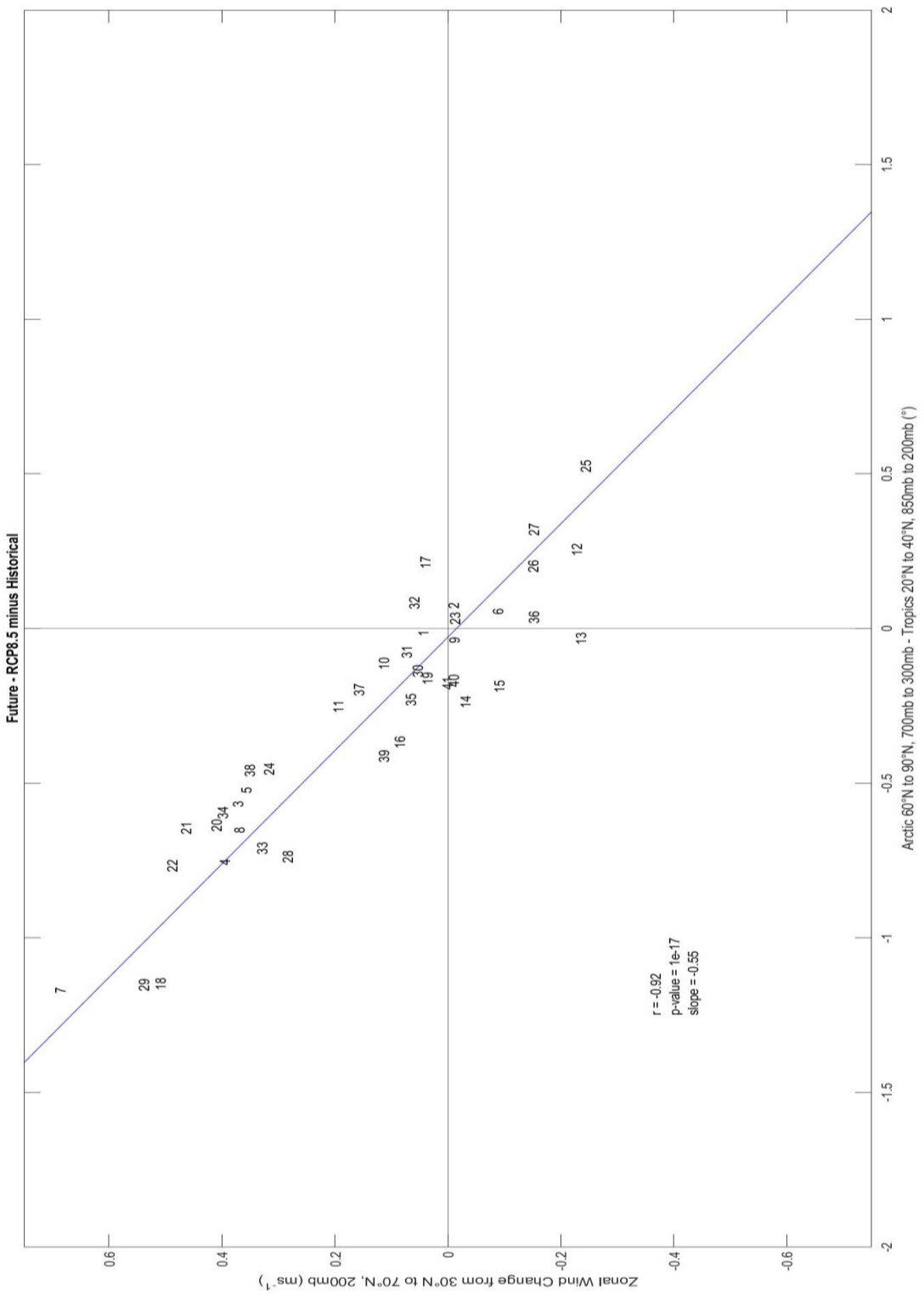

Figure 16: Future era scatter plot for zonal wind (30-70°N, surface to 200mb) versus the warming difference between the given Arctic (60-90°N, 700-300mb) and subtropics (20-40°N, 850-200mb) vertical box. Each number is one climate model (see Table 1).

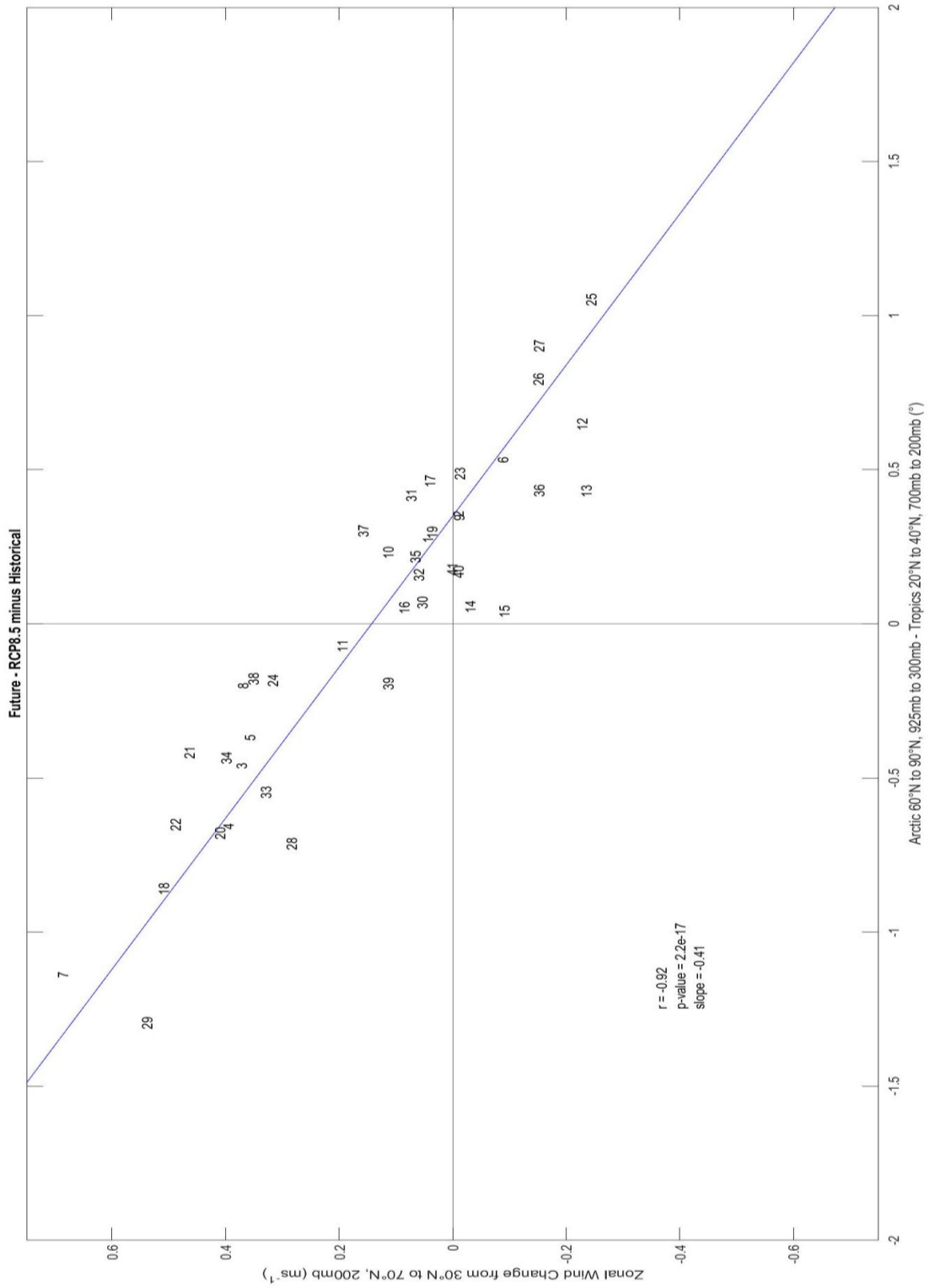

Figure 17: Future era scatter plot for zonal wind (30-70°N, surface to 200mb) versus the warming difference between the given Arctic (60-90°N, 925-300mb) and subtropics (20-40°N, 700-200mb) vertical box. Each number is one climate model (see Table 1).

CHAPTER SIX: RESULTS – SATELLITE ERA

a) Present minus Past Latitude-Pressure Plots

When comparing the difference in temperature for the 91 ensemble members between the Present (1998-2018) and Past (1979-1998) there was a warming for the tropical troposphere and the Arctic surface for each ensemble member 1 (Figures 11-19, odd) as well as the rest of the ensemble members (Figures B1-B33, odd). The warming was not as strong but still significant for the period when compared to the RCP8.5 minus Historical warming latitude-pressure plots, which was expected. A cooling of the lower stratosphere from the mid-latitudes to the Arctic was also present again in some of the plots. As with the RCP8.5 minus Historical warming plots there is a distinct difference from each climate model as well as each ensemble member. When comparing the ensemble members 1 plots to one another, certain climate models again show more warming in the Arctic or the tropics. For example, the GFDL-CM3 (Figure 11) shows both parts of the atmosphere warming, but the Arctic at the surface (~2 K) warms more than the tropics aloft (≤1 K). Most models from the Satellite Era plots shows the Arctic surface warming the most compared to the tropics aloft. Some examples being MIROC-ESM-CHEM (Figure 11), CanEMS2 (Figure 13), FGOALS-s2 (Figure 13), EC-EARTH (Figure 15), Had-GEM2-AO (Figure 15), MIROC5 (Figure 17), and GISS-E2-H-CC (Figure 19). The one notable exception is the climate model IPSL-CM5A-LR (Figure 17) which shows the tropics aloft warming (≥1.5 K) more than the Arctic surface (≤1.25 K). Another noticeable difference with the satellite era compared to the RCP8.5 minus Historical period is how much difference there is between the same climate model group of ensemble members.

The most notable is the CNRM-CM5 (Figure B9, page 111) group of five ensemble members (r1, r2, r4, r6, r10) which ranged from showing little to no warming at the Arctic surface for CNRM-CM5 r2 (≤0.5 K) to significant warming at the Arctic surface for CNRM-CM5 r10 (~2 K). Again, this was expected and is presumably due to the small signal to noise ratio between each ensemble member. Warming for the tropics aloft, with subtle differences, was more uniform compared to the Arctic surface for the CNRM-CM5 ensemble members. The satellite era warming latitude-pressure plots show that climate model outputs and ensemble members differed on how much warming occurred from the tropics aloft and Arctic surface but ultimately indicated that more warming occurred for the Arctic surface compared to the tropics aloft. This would seem to indicate that the Arctic surface is winning the tug-of-war in the satellite era for climate models.

When comparing the change in zonal wind speed for the 91 ensemble members from the averaged Present (1998-2018) and averaged Past (1979-1998) there were notable similarities and differences between each ensemble member. This is similar to what occurred with the RCP8.5 minus Historical Era latitude pressure plots. The similarities were again with the Southern jet with most models showing a strengthening of the westerlies and poleward shift of the jet. However, CNRM-CM5 (Figure 19), CanEMS2 (Figure 21), FIO-ESM (Figure 23), IPSL-CM5B-LR (Figure 25), and INM-CM4 (Figure 27) showed the reverse or a small amount of strengthening for the westerlies in the Southern Hemisphere. The Northern mid-latitude jet again showed difference with the strength and movement of the westerlies. The ACCESS1.3 (Figure 19), FGOALS-s2

(Figure 21), Had-GEM2-AO (Figure 23), IPSL-CM5A-MR (Figure 25), and NorESM1-M (Figure 27) are some examples that had weakening or a small amount of strengthening (≤ 0.5 ms^{-1}). The strengthening of the westerlies in the Northern Hemisphere was not as strong (≤ 2 ms^{-1}) as with RCP8.5 minus Historical, which was expected. Some models that showed strengthening of the westerlies were ACCESS1.3 (Figure 19), BCC-CSM1.1 (Figure 21), GFDL-ESM2M (Figure 23), IPSL-CM5A-LR (Figure 25), and NorESM1-ME (Figure 27). Another noticeable difference compared to the RCP8.5 minus Historical was the difference between the same climate model ensemble members. For example, CESM-WACCM (Figure B8, page 110) had three ensemble members (r2, r3, r4) that showed differing strengthening of the westerlies for both hemispheres.

b) Present minus Past Correlation Scatter Plots

This part of the study for the satellite era focused on the stronger correlated vertical box metrics determined in the RCP8.5 minus Historical part of the study. The vertical box metrics of 30°N to 70°N for ΔU and 20°N to 40°N for ΔT-Tr were kept and did not change since these metrics led to the strongest correlation values for the future era. This part of the study focused on the changing of the pressure levels for ΔT-Ar and ΔT-Tr vertical boxes to determine if these strong correlations were present in the satellite era (Table 6). Correlations found in the satellite era were not as strong compared to the future era but still highly correlated (-0.7078 to -0.7869, Table 6). The somewhat lower correlation was probably due to the low signal to noise ratio and the use of 91 ensemble members instead of 41 as was done in the future era. The vertical boxes that resulted in the strongest correlated value for every degree of warming difference for the satellite

era were not the same as the future era (Table 6, Figure 28-30). The only vertical box metric to change was the ΔT-Ar for the bottom pressure level that went from 850mb to 700mb (Figure 29) and from 700mb to 600mb (Figure 30). This indicates that the Arctic mid-troposphere is more correlated in the satellite era compared to the future era. This was not expected when following the tug-of-war idea and the previous studies focused on the strength of the westerlies.

The satellite era correlation scatter plots only show climate models that had more than one ensemble member (Figures 28-30). When observational data, reanalysis and/or satellite, is combined with these plots it should allow certain models to be dismissed depending on which part of the atmosphere is winning the tug-of-war. For example, for Figure 28 if observational data indicates that the tropics is winning the tug-of-war than MIROC5 (#31) could be dismissed because it shows the Arctic winning the tug-of-war. If the Arctic was winning the tug-of-war than CSIRO-Mk3-6-0 (#7) could be ruled out because most members show the tropics winning the tug-of-war. A drawback to this would be for models that have ensemble members indicating both. For example, HadGEM2-ES (#27) and IPSL-CM5A-LR (#28) have two members each indicating the opposing side of the atmosphere winning the tug-of-war. Thus, with the implementation of observational data with the satellite era results, we may be able to determine which climate models are better at forecasting the strength of the mid-latitude jet.

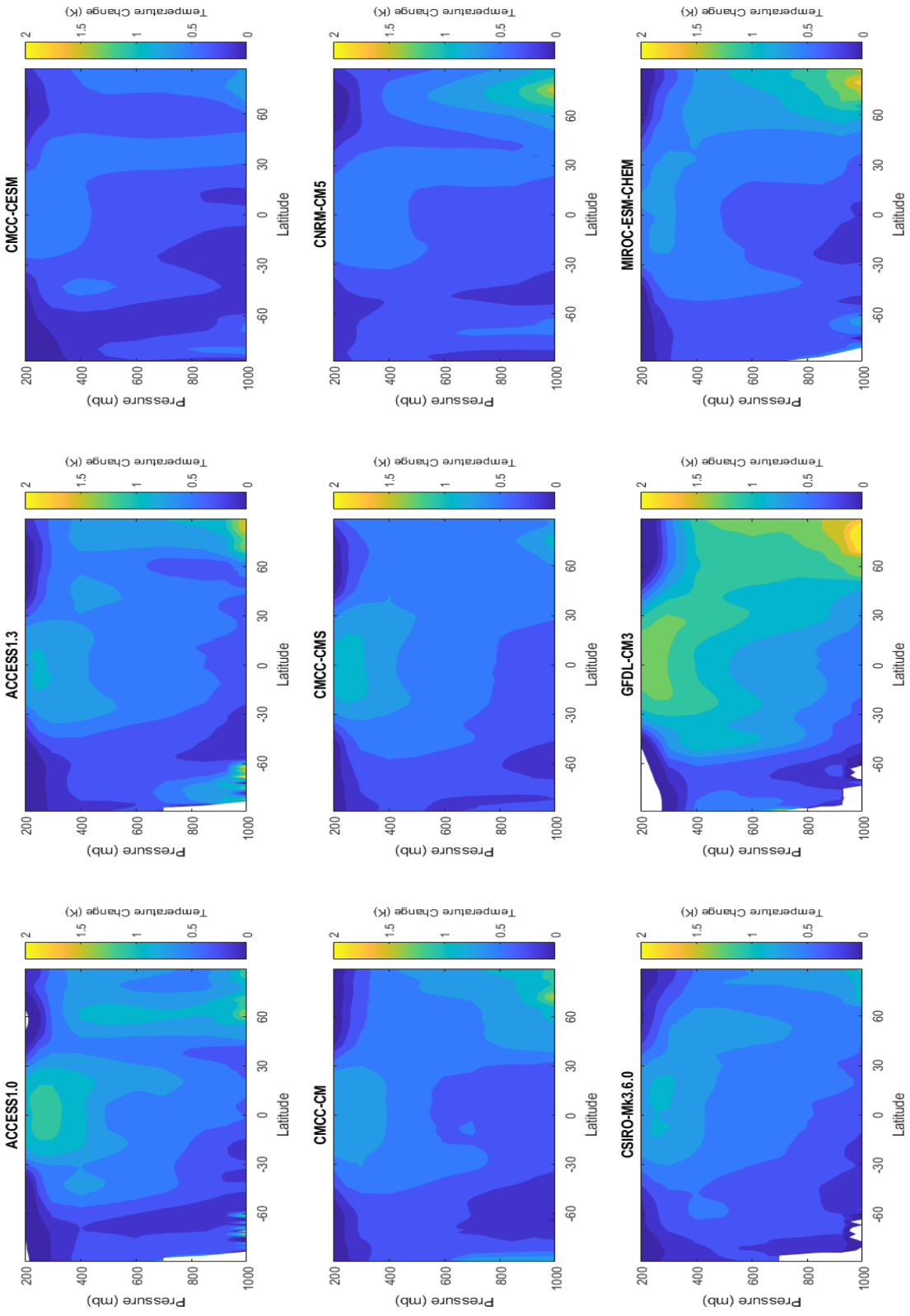

Figure 18: Warming between the present (1999-2018) and past (1979-1998) climate model r1 output for models 1-9 of 41.

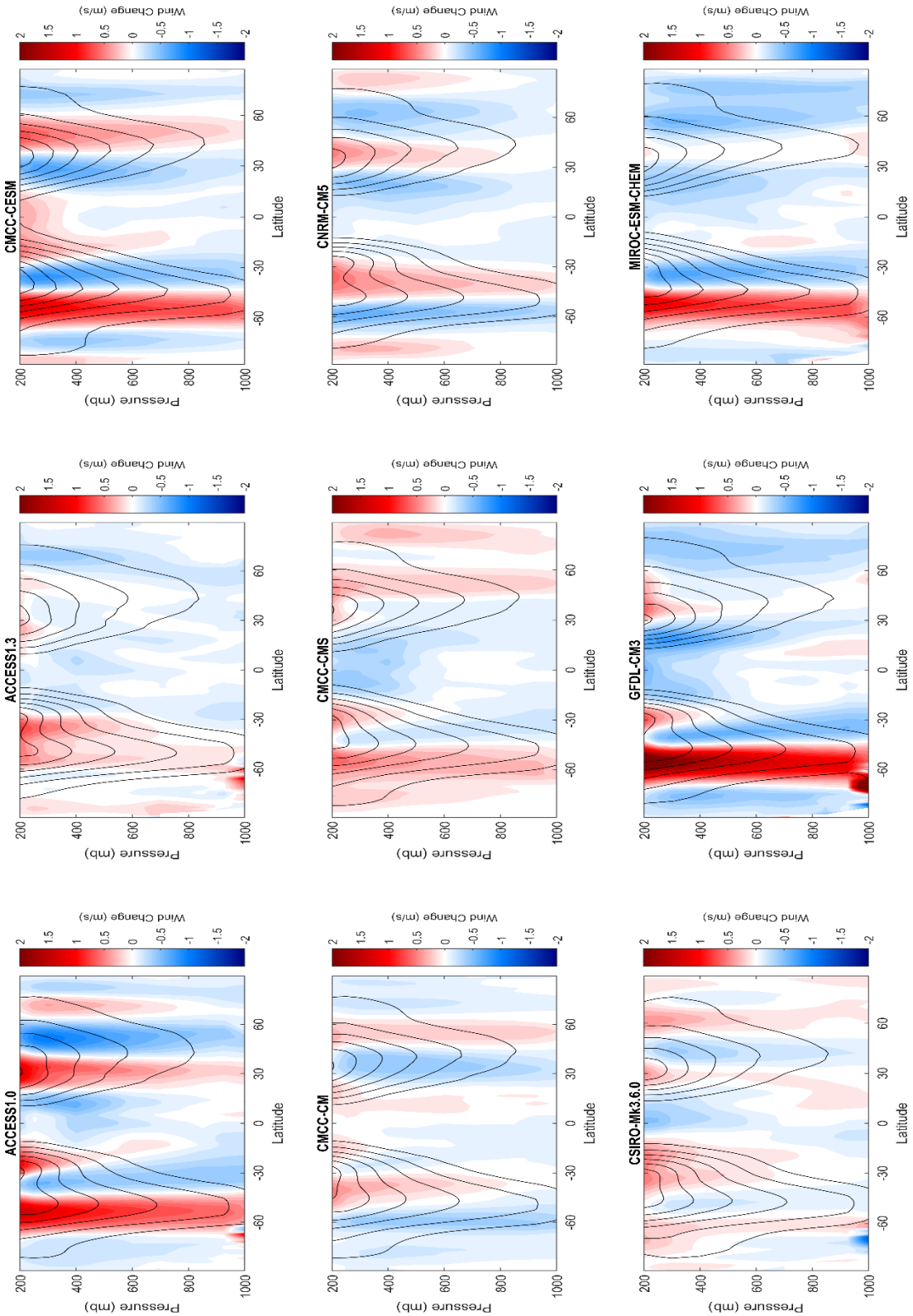

Figure 19: Zonal wind change between the present (1999-2018) and past (1979-1998) climate model r1 output for models 1-9 of 41. The black contours are the Historical zonal wind mean and are in increments of 5 ms-1.

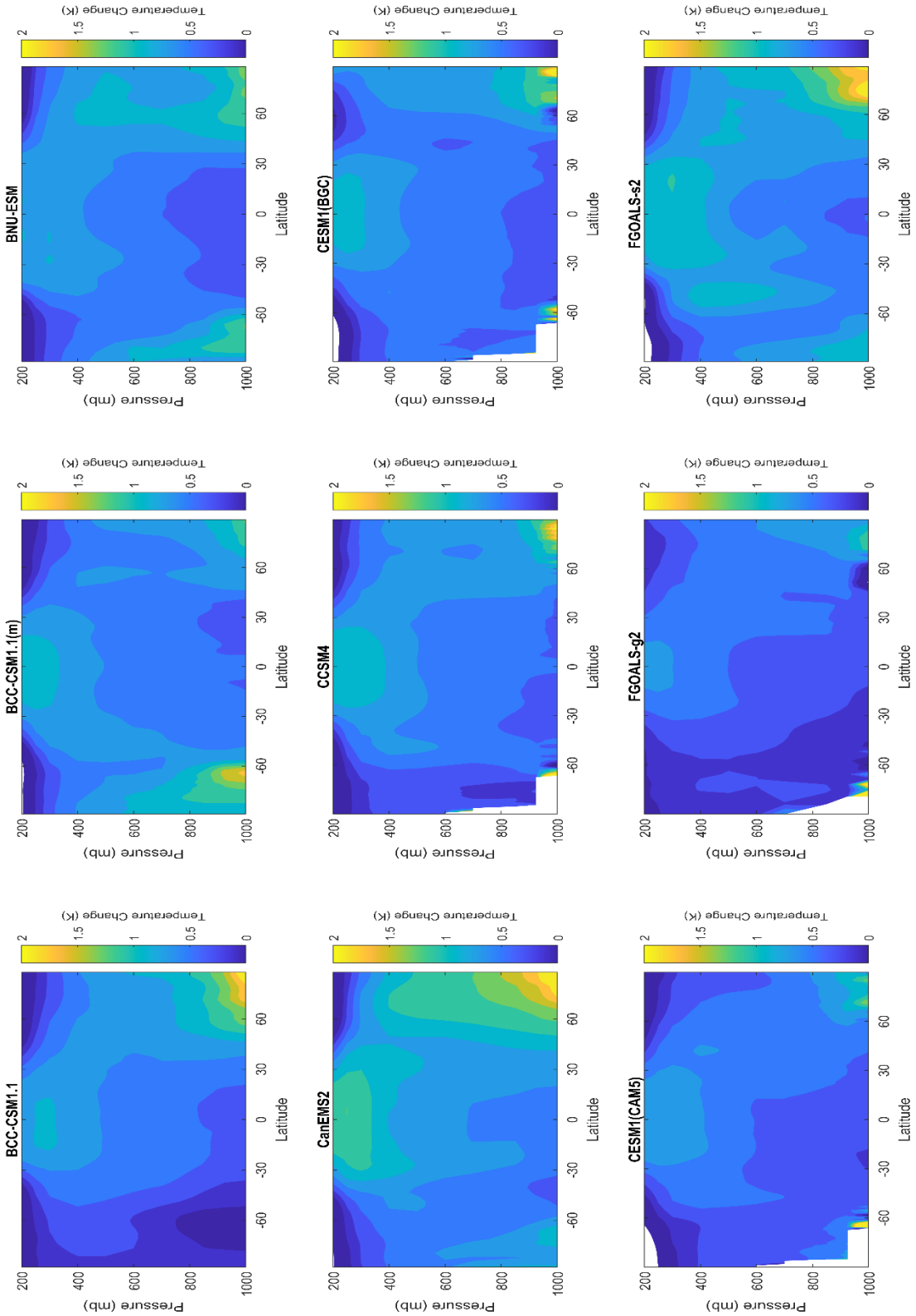

Figure 20: Same as Figure 18 but for models 10 through 18 of 41.

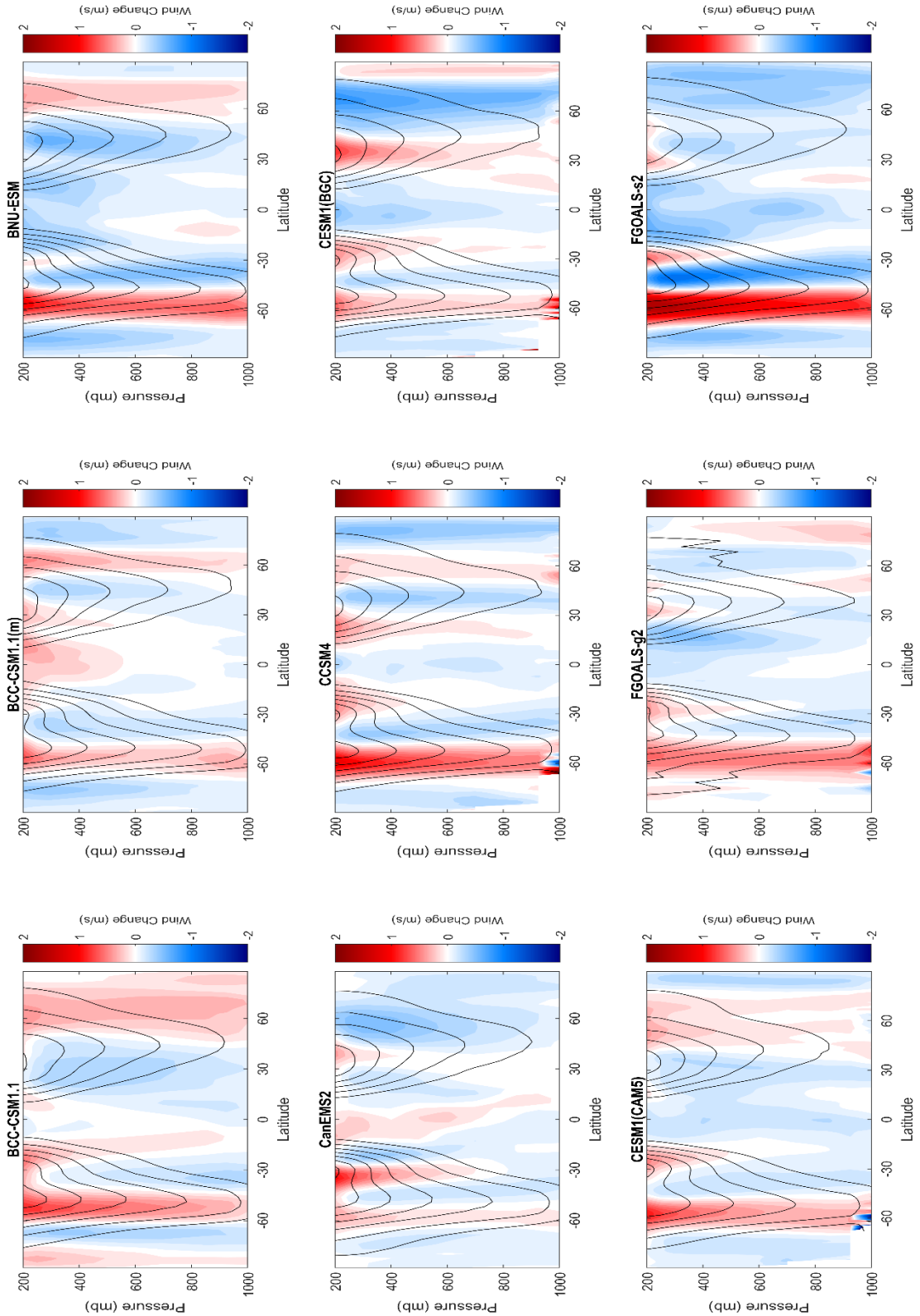

Figure 21: Same as Figure 19 but for models 10 through 18 of 41.

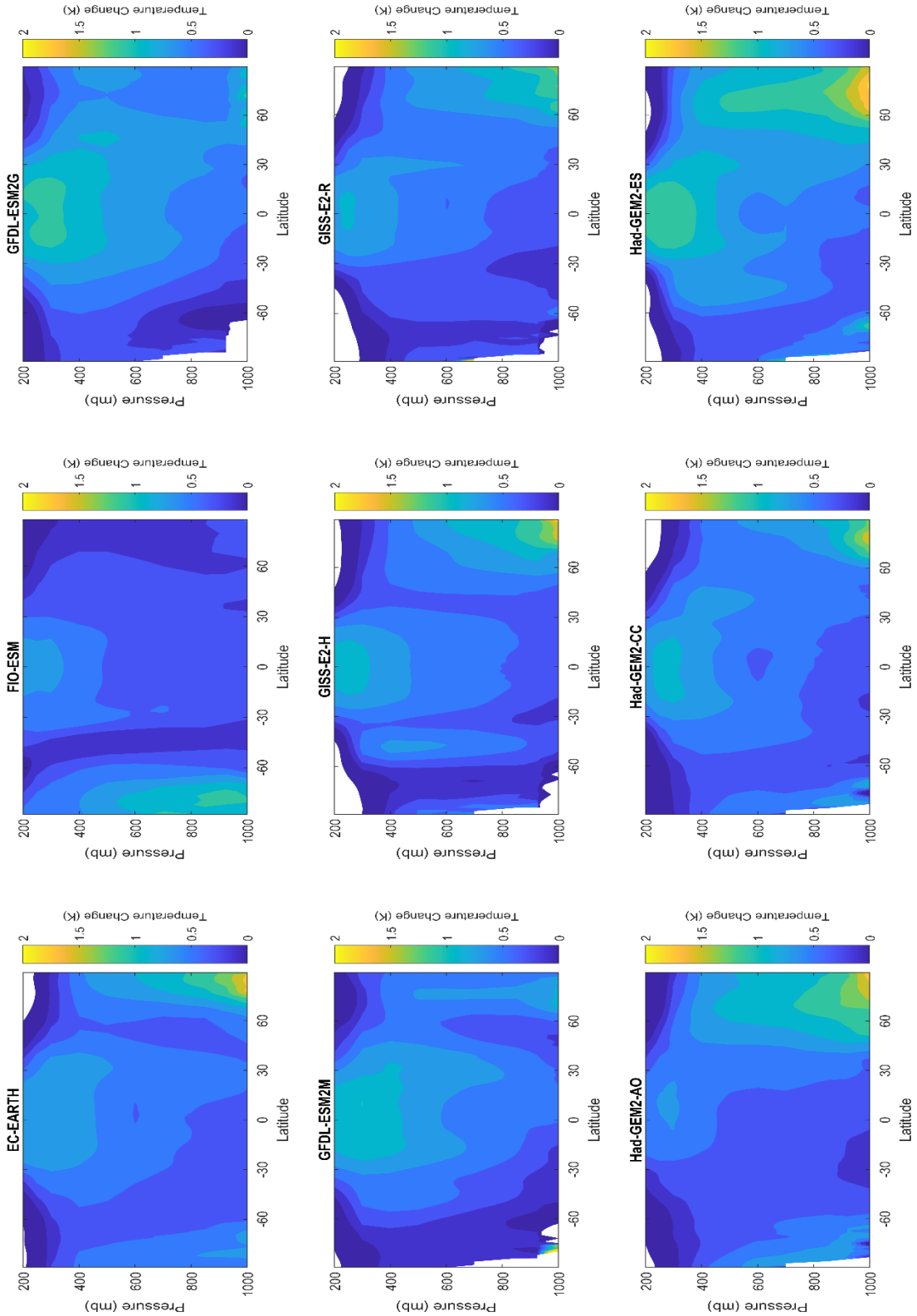

Figure 22: Same as Figure 18 but for models 19 through 27 of 41.

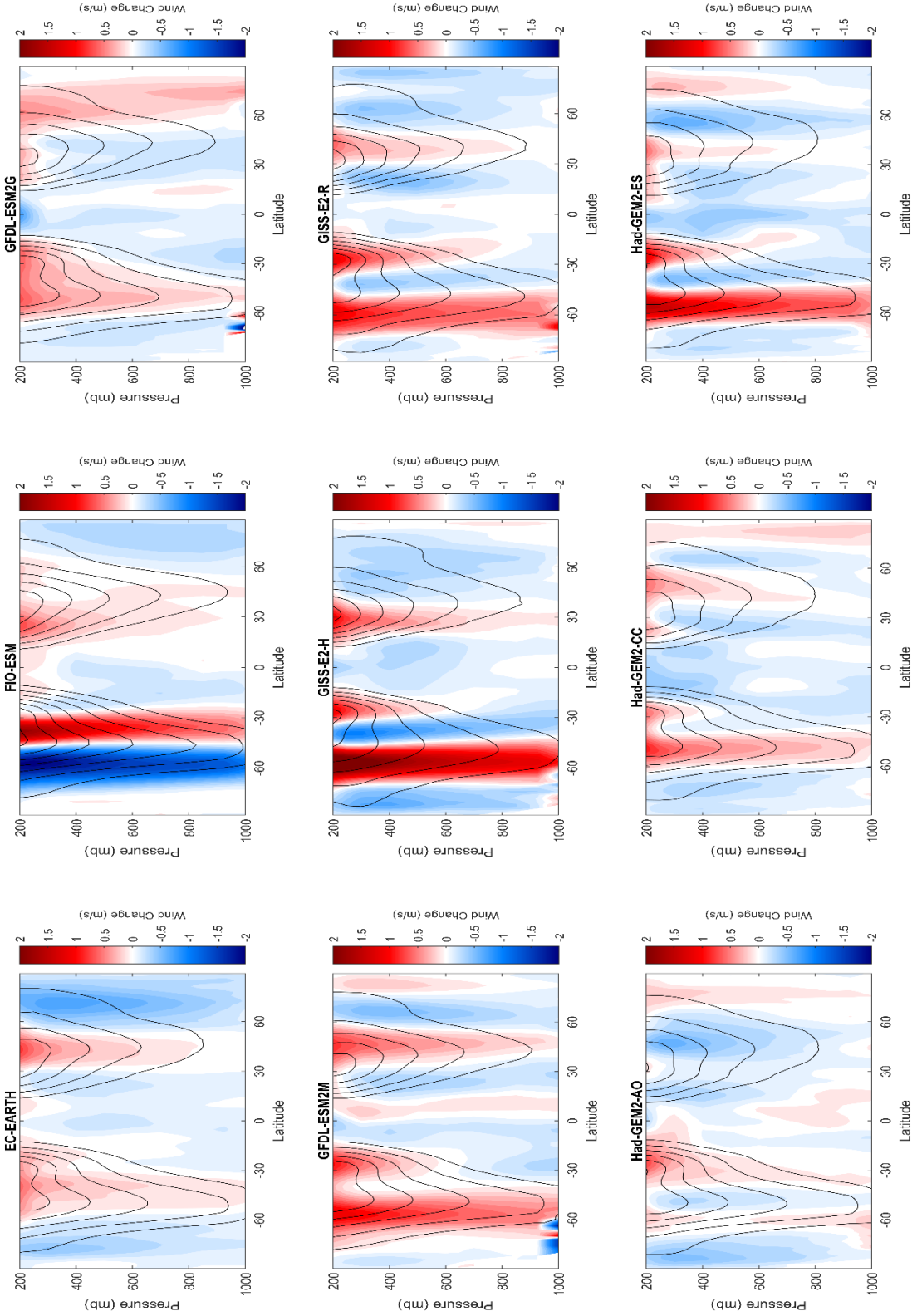

Figure 23: Same as Figure 19 but for models 19 through 27 of 41.

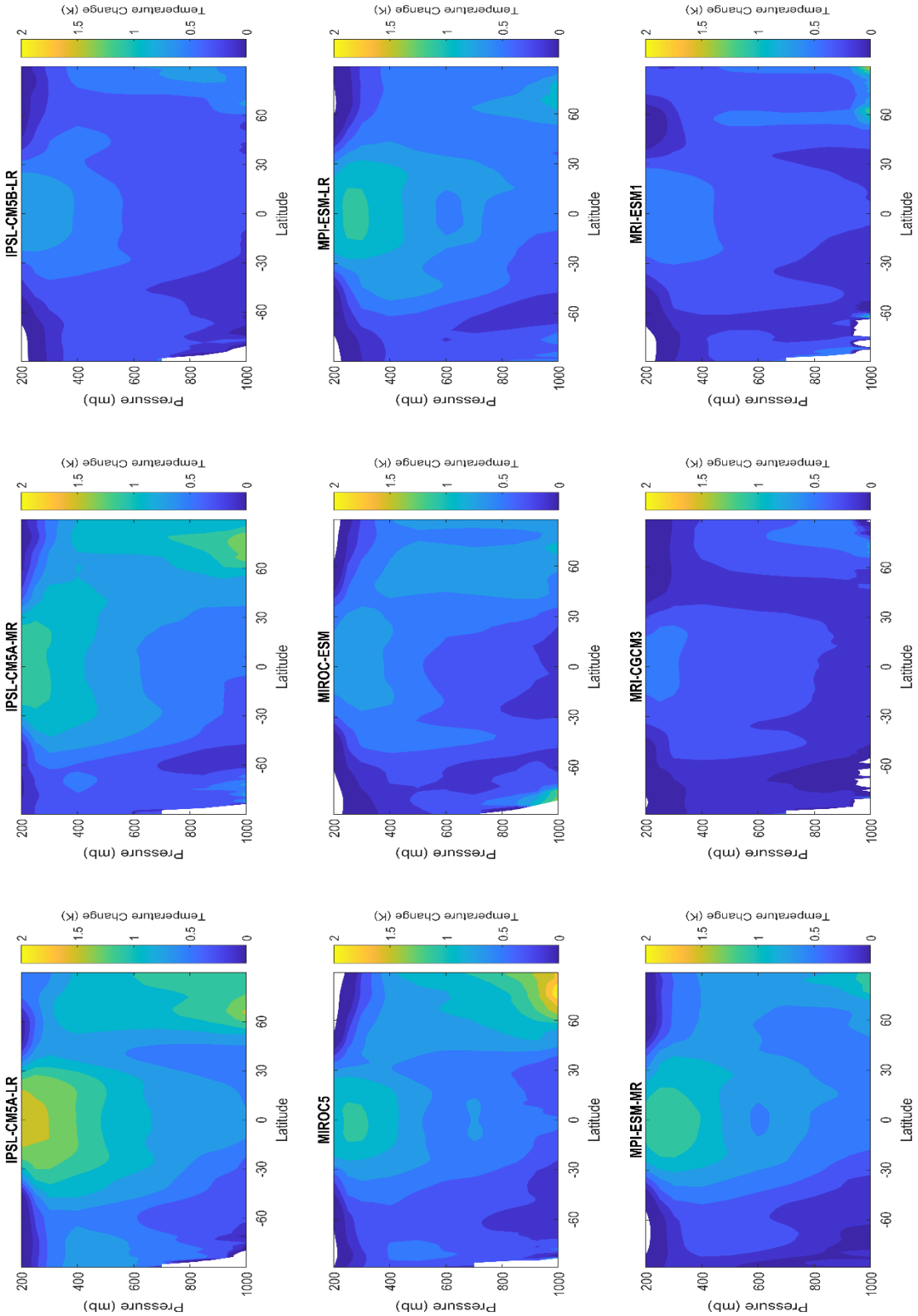

Figure 24: Same as Figure 18 but for models 28 through 36 of 41.

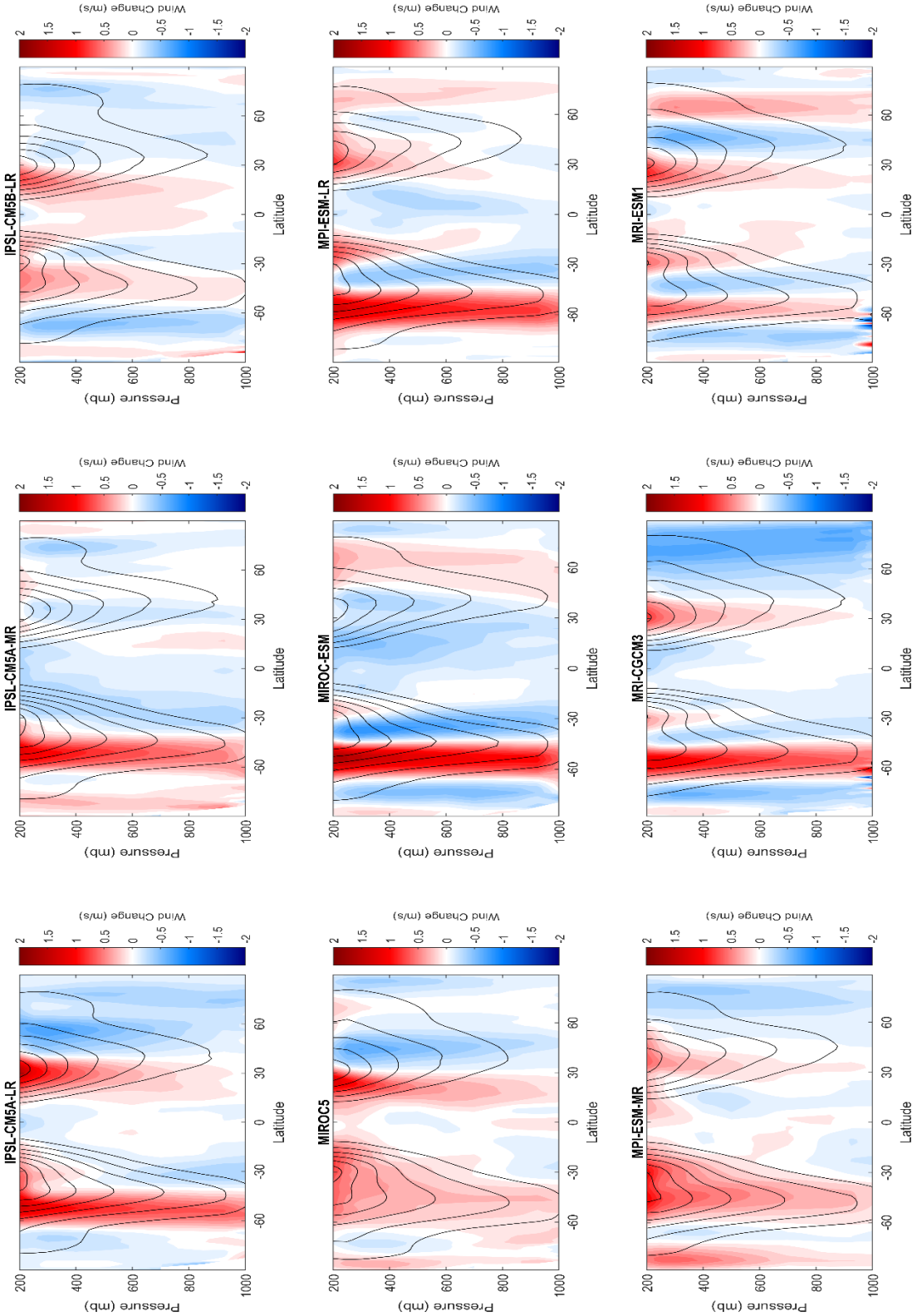

Figure 25: Same as Figure 19 but for models 28 through 36 of 41.

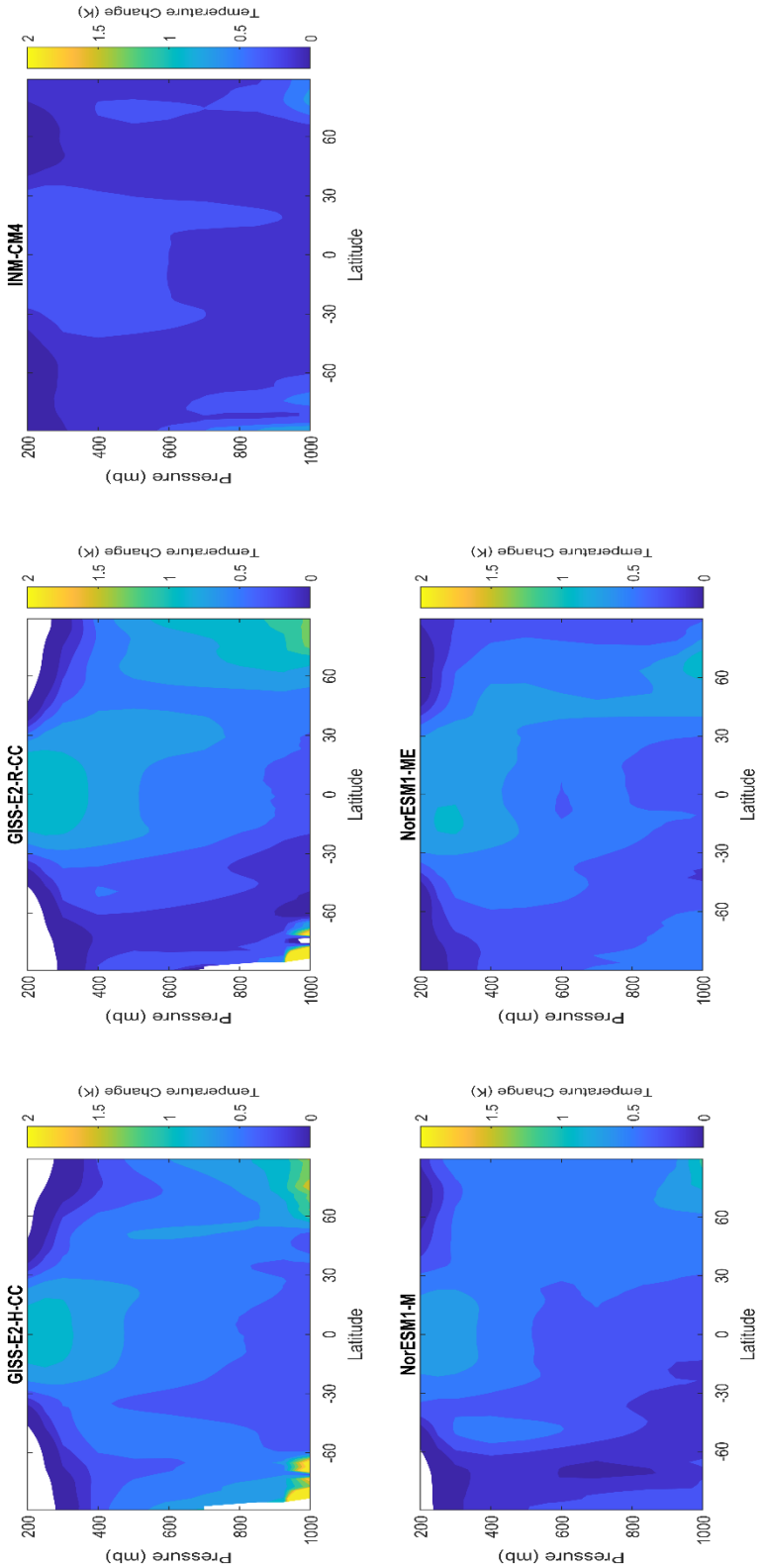

Figure 26: Same as Figure 18 but for models 36 through 41 of 41.

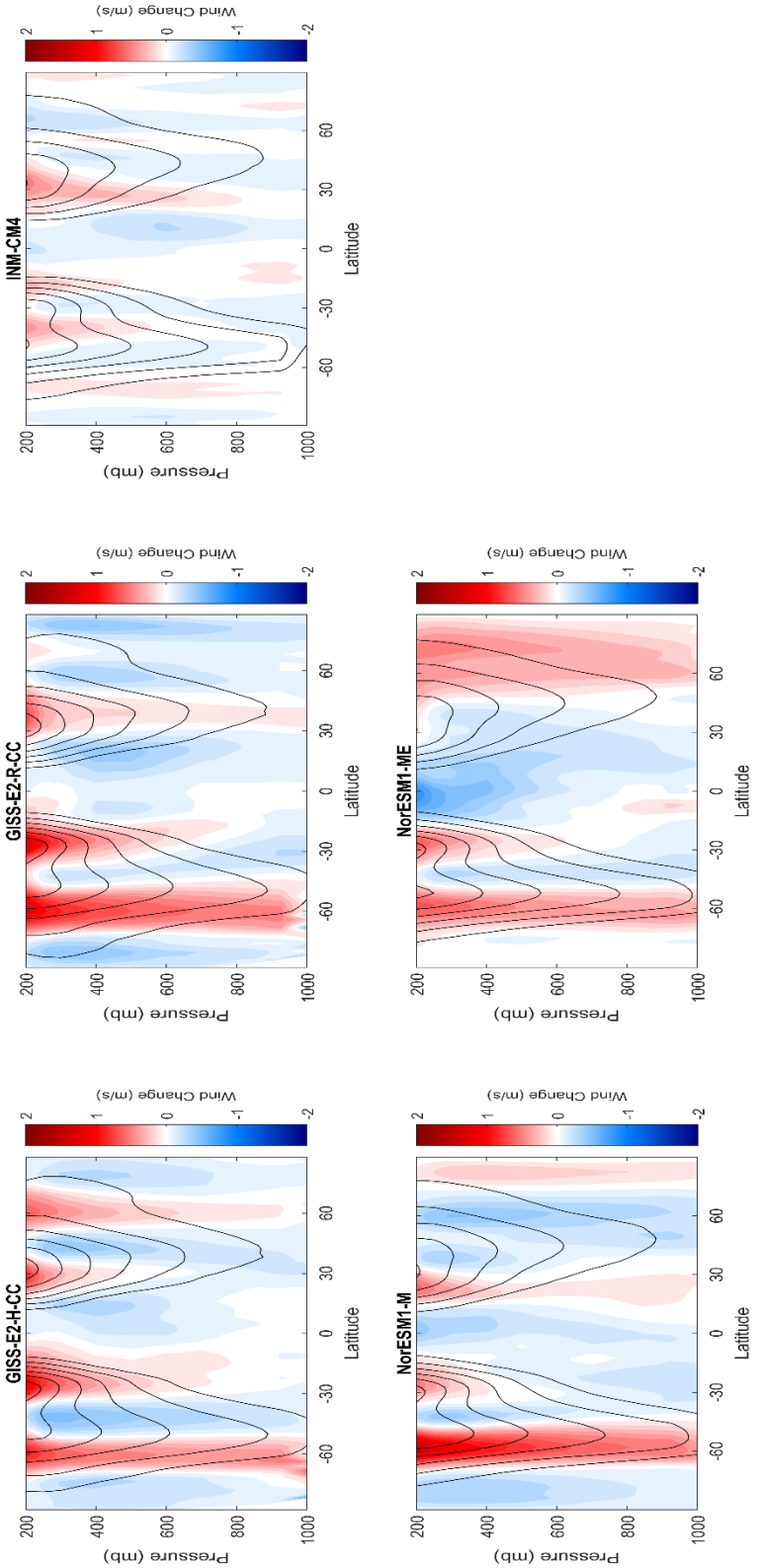

Figure 27: Same as Figure 19 but for models 36 through 41 of 41.

Table 6: Satellite era list of vertical box metrics for change in zonal wind speed (ΔU), the warming difference of the Arctic (ΔT-Ar) and the subtropics (ΔT-Tr), and the resulting correlation between the ΔU vertical box and the difference between ΔT-Ar and the ΔT-Tr vertical box. Red indicates metric that was changed compared to the vertical box before.

ΔU (M/S)	ΔT-Ar (K)				ΔT-Tr (K)				STATISTICS	
Press. (mb)	1st Lat (°)	2nd Lat (°)	1st Press. (mb)	2nd Press. (mb)	1st Lat (°)	2nd Lat (°)	1st Press. (mb)	2nd Press. (mb)	Correlation	P-value
200	60	90	1000	200	20	40	1000	200	-0.7078	4.32E-15
300	60	90	1000	200	20	40	1000	200	-0.6077	1.69E-10
400	60	90	1000	200	20	40	1000	200	-0.5629	6.33E-09
200	60	90	925	200	20	40	1000	200	-0.6866	5.81E-14
300	60	90	925	200	20	40	1000	200	-0.5682	4.25E-09
400	60	90	925	200	20	40	1000	200	-0.5266	8.25E-08
200	60	90	925	300	20	40	1000	200	-0.7410	4.57E-17
300	60	90	925	300	20	40	1000	200	-0.7088	3.81E-15
400	60	90	925	300	20	40	1000	200	-0.6664	5.59E-13
200	60	90	925	400	20	40	1000	200	-0.6889	4.40E-14
300	60	90	925	400	20	40	1000	200	-0.6785	1.47E-13
400	60	90	925	400	20	40	1000	200	-0.6394	9.03E-12
200	60	90	925	300	20	40	925	200	-0.7363	9.06E-17
300	60	90	925	300	20	40	925	200	-0.6966	1.76E-14
400	60	90	925	300	20	40	925	200	-0.6530	2.31E-12
200	60	90	925	300	20	40	850	200	-0.7318	1.73E-16
300	60	90	925	300	20	40	850	200	-0.6848	7.12E-14
400	60	90	925	300	20	40	850	200	-0.6400	8.52E-12
200	60	90	925	300	20	40	700	200	-0.7245	4.75E-16
300	60	90	925	300	20	40	700	200	-0.6697	3.93E-13
400	60	90	925	300	20	40	700	200	-0.6236	4.06E-11
200	60	90	925	300	20	40	600	200	-0.7082	4.15E-15
300	60	90	925	300	20	40	600	200	-0.6489	3.50E-12
400	60	90	925	300	20	40	600	200	-0.6023	2.69E-10
200	60	90	850	300	20	40	850	200	-0.7643	1.20E-18
300	60	90	850	300	20	40	850	200	-0.7063	5.29E-15
400	60	90	850	300	20	40	850	200	-0.6598	1.14E-12
200	60	90	700	300	20	40	850	200	-0.7869	2.31E-20
300	60	90	700	300	20	40	850	200	-0.7127	2.32E-15
400	60	90	700	300	20	40	850	200	-0.6642	7.15E-13
200	60	90	600	300	20	40	850	200	-0.7827	5.06E-20
300	60	90	600	300	20	40	850	200	-0.6903	3.72E-14
400	60	90	600	300	20	40	850	200	-0.6410	7.68E-12

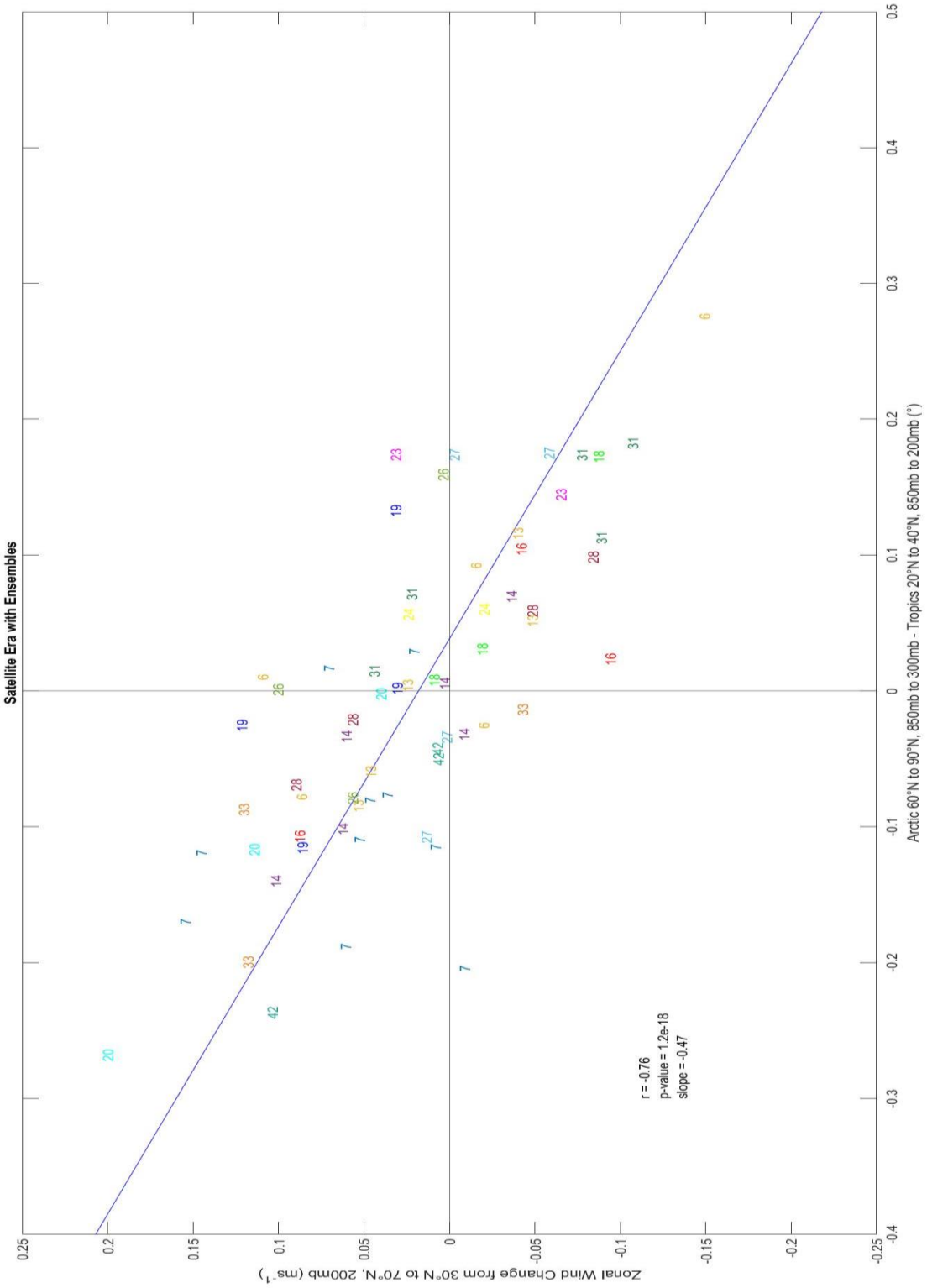

Figure 28: Satellite era scatter plot for zonal wind (30-70°N, surface to 200mb) versus the warming difference between the given Arctic (60-90°N, 850-300mb) and subtropics (20-40°N, 850-200mb) vertical box. Each number is one climate model (see Table 1).

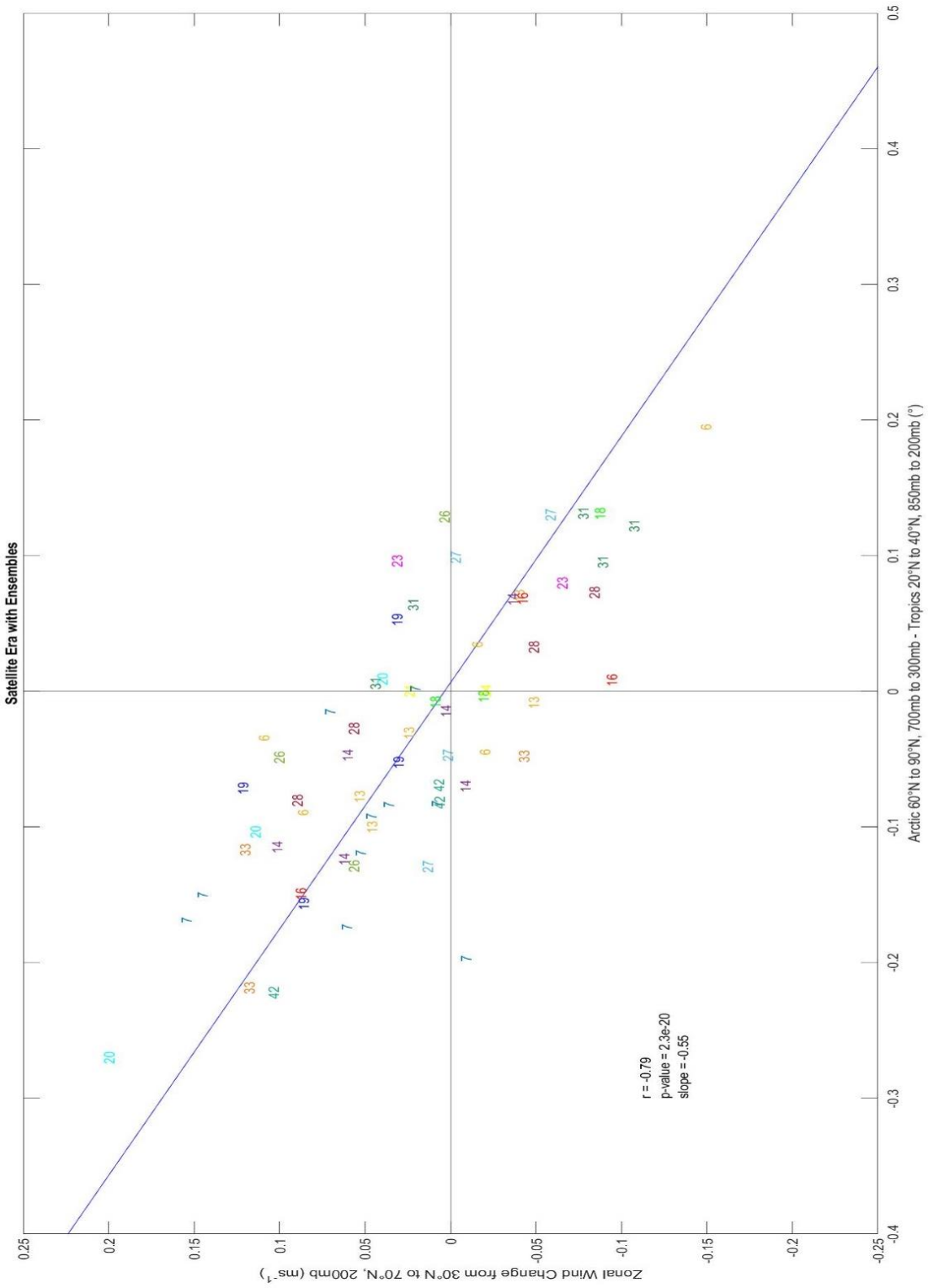

Figure 29: Satellite era scatter plot for zonal wind (30-70°N, surface to 200mb) versus the warming difference between the given Arctic (60-90°N, 700-300mb) and subtropics (20-40°N, 850-200mb) vertical box. Each number is one climate model (see Table 1).

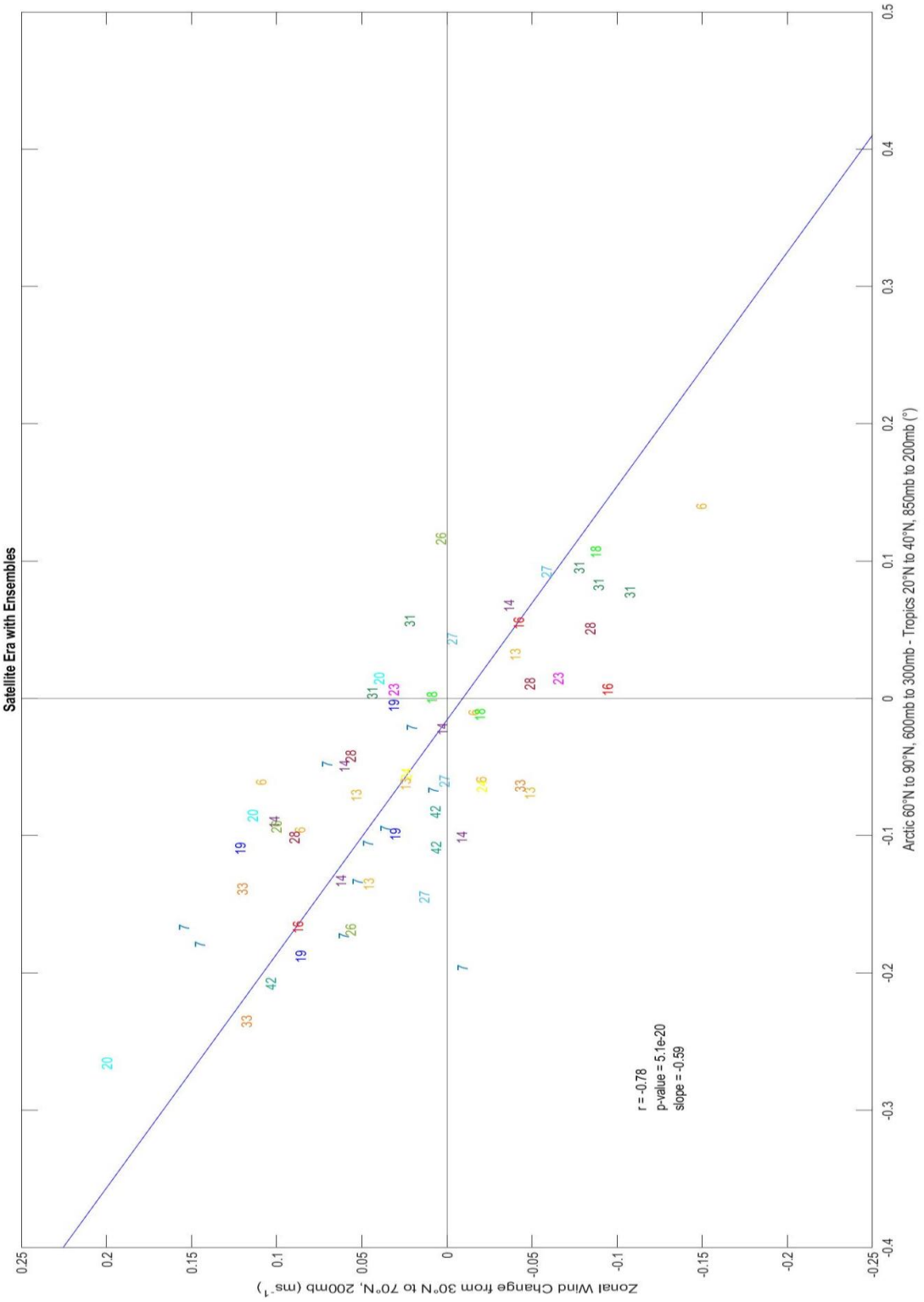

Figure 30: Satellite era scatter plot for zonal wind (30-70°N, surface to 200mb) versus the warming difference between the given Arctic (60-90°N, 600-300mb) and subtropics (20-40°N, 850-200mb) vertical box. Each number is one climate model (see Table 1).

CHAPTER SEVEN: DISCUSSION

This study has allowed us to answer some or part of the questions we asked at the end of the background section. The latitude-pressure plots show for both the future and satellite era that climate models differ on which part of the atmosphere warms the most, the strength of the westerlies, and the equatorward or poleward movement of the Northern mid-latitude jet. For the future era there were many CMIP5 climate models that indicated a stronger warming for the Arctic surface from the latitude-pressure plots. However, the statistical analysis indicates that the tropical and Arctic mid-troposphere warming plays a larger role compared to the tropical upper troposphere and Arctic surface warming in the strengthening of the westerlies for more models. This analysis also indicates that the tropical mid-troposphere warming is more correlated with strength of the westerlies for the Northern mid-latitude jet. For the satellite era the same can be said as was for the future era. Most of the pressure-latitude plots indicated that the surface of the Arctic is warming the most. Yet, the warming of the tropics and Arctic mid-troposphere has a stronger influence on the strengthening of the westerlies than the warming of the tropical and Arctic surface. Thus, this would indicate that the tropics mid-troposphere warming is winning the tug-of-war in CMIP5 climate models. While correlation is not causation and this study was just using CMIP5 climate models, more data and information is needed to determine a winner of the tug-of-war for the real world. To achieve a more valid answer to which part of the atmosphere is warming the most and which part will win the tug-of-war the next step is to add observational and re-analysis data to a future study.

CHAPTER EIGHT: FUTURE WORK

For future work to expand this study we suggest using two new datasets: reanalysis projects and Microwave Sounding Unit (MSU) analysis.

For the reanalysis part there are six reanalysis projects that show promise for climate reanalysis. Those are the ERA-Interim, CFSR, MERRA-2, JRA-55, ERA5, and 20CRv3 for the Satellite Era (1979-2018). The above shows promise and should consider using the two twenty-year sections from the satellite era, Past (1979-1998) and Present (1999-2018), again to determine the warming difference and change in zonal wind speed for the Arctic and tropics. The findings would then be plotted with the CMIP5 satellite era correlation scatter plot to see which climate model's ensemble members line up with reanalysis results. The goal for this section is to see which model outputs match or do not match with the reanalysis results. This may lead to being able to predict the future mid-latitude jet using the tug-of-war framework.

The suggestion for the MSU datasets is again to use the Present (1999-2018) and Past (1979-1998) from the satellite era. Then take the average temperature difference for each MSU climate model and observational MSU as was done for the climate models and could be done for the reanalysis section. Climate models do not output MSU satellite data, therefore synthetic MSU data was developed by Santer et al. (2018). This future study would use a similar method to the vertical box method that was developed for the warming difference and change in zonal wind speed in the CMIP5 climate models to make a correlation scatter plot. Instead of different latitudes and pressure levels the future study will be using different latitudes and the T_{24} (TTT) channel for the upper

troposphere (tropics/subtropics) and T_{2LT} (TLT) channel for the lower troposphere (Arctic) to determine the warming difference. The channels T_{2LT} (TLT) and T_{24} (TTT) are defined by a weighting function in Figure 1 of (Fu et al. 2011). The MSU uses broad vertical channels to measure the temperature of the atmosphere rather than specific pressure levels. By using the MSU data this may allow the narrowing of climate models and possibly rule out various models as well.

This future work will help determine which part of the atmosphere may warm the most in the future and win the tug-of-war: Arctic or tropics. This may allow us to determine which climate model or ensemble member may be the closest to predicting the winner of the tug-of-war. By understanding which part of the atmosphere warms the most we may be able to determine the effect this will have on the mid-latitude jet along with the weather and climate of the future.

REFERENCES

Armour, K. C., J. Marshall, J. R. Scott, A. Donohoe, and E. R. Newsom, 2016: Southern Ocean warming delayed by circumpolar upwelling and equatorward transport. *Nature Geosci*, **9**, 549–554, https://doi.org/10.1038/ngeo2731.

Barnes, E. A., and L. M. Polvani, 2015: CMIP5 Projections of Arctic Amplification, of the North American/North Atlantic Circulation, and of Their Relationship. *Journal of Climate*, **28**, 5254–5271, https://doi.org/10.1175/JCLI-D-14-00589.1.

Butler, A. H., D. W. J. Thompson, and R. Heikes, 2010: The Steady-State Atmospheric Circulation Response to Climate Change–like Thermal Forcings in a Simple General Circulation Model. *Journal of Climate*, **23**, 3474–3496, https://doi.org/10.1175/2010JCLI3228.1.

Ceppi, P., and D. L. Hartmann, 2016: Clouds and the Atmospheric Circulation Response to Warming. *Journal of Climate*, **29**, 783–799, https://doi.org/10.1175/JCLI-D-15-0394.1.

Cohen, J., and Coauthors, 2014: Recent Arctic amplification and extreme mid-latitude weather. *Nature Geosci*, **7**, 627–637, https://doi.org/10.1038/ngeo2234.

Collins, M., and Coauthors, 2013: Long-term Climate Change: Projections, Commitments and Irreversibility. 108.

Deser, C., R. A. Tomas, and L. Sun, 2015: The Role of Ocean–Atmosphere Coupling in the Zonal-Mean Atmospheric Response to Arctic Sea Ice Loss. *Journal of Climate*, **28**, 2168–2186, https://doi.org/10.1175/JCLI-D-14-00325.1.

Feldstein, S. B., and S. Lee, 2014: Intraseasonal and Interdecadal Jet Shifts in the Northern Hemisphere: The Role of Warm Pool Tropical Convection and Sea Ice. *Journal of Climate*, **27**, 6497–6518, https://doi.org/10.1175/JCLI-D-14-00057.1.

Francis, J. A., 2017: Why Are Arctic Linkages to Extreme Weather Still up in the Air? *Bulletin of the American Meteorological Society*, **98**, 2551–2557, https://doi.org/10.1175/BAMS-D-17-0006.1.

Francis, J. A., and S. J. Vavrus, 2015: Evidence for a wavier jet stream in response to rapid Arctic warming. *Environ. Res. Lett.*, **10**, 014005, https://doi.org/10.1088/1748-9326/10/1/014005.

Fu, Q., and P. Lin, 2011: Poleward Shift of Subtropical Jets Inferred from Satellite-Observed Lower-Stratospheric Temperatures. *Journal of Climate*, **24**, 5597–5603, https://doi.org/10.1175/JCLI-D-11-00027.1.

Fu, Q., S. Manabe, and C. M. Johanson, 2011: On the warming in the tropical upper troposphere: Models versus observations: ON TROPICAL UPPER TROPOSPHERIC WARMING. *Geophys. Res. Lett.*, **38**, https://doi.org/10.1029/2011GL048101.

Gelaro, R., and Coauthors, 2017: The Modern-Era Retrospective Analysis for Research and Applications, Version 2 (MERRA-2). *J. Climate*, **30**, 5419–5454, https://doi.org/10.1175/JCLI-D-16-0758.1.

Graversen, R. G., T. Mauritsen, M. Tjernström, E. Källén, and G. Svensson, 2008: Vertical structure of recent Arctic warming. *Nature*, **451**, 53–56, https://doi.org/10.1038/nature06502.

Harvey, B. J., L. C. Shaffrey, and T. J. Woollings, 2014: Equator-to-pole temperature differences and the extra-tropical storm track responses of the CMIP5 climate models. *Climate Dynamics*, **43**, 1171–1182, https://doi.org/10.1007/s00382-013-1883-9.

Harvey, B. J., L. C. Shaffrey, and T. J. Woollings, 2015: Deconstructing the climate change response of the Northern Hemisphere wintertime storm tracks. *Climate Dynamics*, **45**, 2847–2860, https://doi.org/10.1007/s00382-015-2510-8.

Held, I. M., 1993: Large-Scale Dynamics and Global Warming. **74**, 15.

Hersbach, H., and Coauthors, 2019: Global reanalysis: goodbye ERA-Interim, hello ERA5. https://doi.org/10.21957/VF291HEHD7.

Kobayashi, S., and Coauthors, 2015: The JRA-55 Reanalysis: General Specifications and Basic Characteristics. *Journal of the Meteorological Society of Japan*, **93**, 5–48, https://doi.org/10.2151/jmsj.2015-001.

Lu, J., G. A. Vecchi, and T. Reichler, 2007: Expansion of the Hadley cell under global warming. *Geophys. Res. Lett.*, **34**, L06805, https://doi.org/10.1029/2006GL028443.

Peings, Y., J. Cattiaux, S. J. Vavrus, and G. Magnusdottir, 2018: Projected squeezing of the wintertime North-Atlantic jet. *Environ. Res. Lett.*, **13**, 074016, https://doi.org/10.1088/1748-9326/aacc79.

Riahi, K., and Coauthors, 2011: RCP 8.5—A scenario of comparatively high greenhouse gas emissions. *Climatic Change*, **109**, 33–57, https://doi.org/10.1007/s10584-011-0149-y.

Saha, S., and Coauthors, 2014: The NCEP Climate Forecast System Version 2. *Journal of Climate*, **27**, 2185–2208, https://doi.org/10.1175/JCLI-D-12-00823.1.

Santer, B. D., and Coauthors, 2013: Identifying human influences on atmospheric temperature. *Proceedings of the National Academy of Sciences*, **110**, 26–33, https://doi.org/10.1073/pnas.1210514109.

Santer, B. D., and Coauthors, 2018: Human influence on the seasonal cycle of tropospheric temperature. *Science*, **361**, eaas8806, https://doi.org/10.1126/science.aas8806.

Schwalm, C. R., S. Glendon, and P. B. Duffy, 2020: RCP8.5 tracks cumulative CO_2 emissions. *Proc Natl Acad Sci USA*, **117**, 19656–19657, https://doi.org/10.1073/pnas.2007117117.

Screen, J. A., and Coauthors, 2018: Consistency and discrepancy in the atmospheric response to Arctic sea-ice loss across climate models. *Nature Geosci*, **11**, 155–163, https://doi.org/10.1038/s41561-018-0059-y.

Shaw, T. A., and Z. Tan, 2018: Testing Latitudinally Dependent Explanations of the Circulation Response to Increased CO_2 Using Aquaplanet Models. *Geophys. Res. Lett.*, **45**, 9861–9869, https://doi.org/10.1029/2018GL078974.

Shaw, T. A., and Coauthors, 2016: Storm track processes and the opposing influences of climate change. *Nature Geosci*, **9**, 656–664, https://doi.org/10.1038/ngeo2783.

Sherwood, S. C., and N. Nishant, 2015: Atmospheric changes through 2012 as shown by iteratively homogenized radiosonde temperature and wind data (IUKv2). *Environ. Res. Lett.*, **10**, 054007, https://doi.org/10.1088/1748-9326/10/5/054007.

Slivinski, L. C., and Coauthors, 2019: Towards a more reliable historical reanalysis: Improvements for version 3 of the Twentieth Century Reanalysis system. *Q.J.R. Meteorol. Soc.*, **145**, 2876–2908, https://doi.org/10.1002/qj.3598.

Staten, P. W., 2018: Re-examining tropical expansion. *NatUre Climate Change*, **8**, 8.

Taylor, K. E., R. J. Stouffer, and G. A. Meehl, 2012: An Overview of CMIP5 and the Experiment Design. *Bulletin of the American Meteorological Society*, **93**, 485–498, https://doi.org/10.1175/BAMS-D-11-00094.1.

Yim, B. Y., H. S. Min, B.-M. Kim, J.-H. Jeong, and J.-S. Kug, 2016a: Sensitivity of Arctic warming to sea ice concentration: Arctic Warming Sensitivity to SIC. *J. Geophys. Res. Atmos.*, **121**, 6927–6942, https://doi.org/10.1002/2015JD023953.

Yim, B. Y., H. S. Min, and J.-S. Kug, 2016b: Inter-model diversity in jet stream changes and its relation to Arctic climate in CMIP5. *Climate Dynamics*, **47**, 235–248, https://doi.org/10.1007/s00382-015-2833-5.

APPENDIX A: FUTURE ERA

Tropics Latitude Equator to 20N		
Zonal Wind 200mb	Correlation	P-value
Arctic 600 to 400mb - Tropics 400 to 200mb	-0.535	3.13E-04
Arctic 600 to 400mb - Tropics 500 to 200mb	-0.5767	7.93E-05
Arctic 600 to 400mb - Tropics 600 to 200mb	-0.5903	4.86E-05
Arctic 700 to 300mb - Tropics 400 to 200mb	-0.5408	2.62E-04
Arctic 700 to 300mb - Tropics 500 to 200mb	-0.5854	5.80E-05
Arctic 700 to 300mb - Tropics 600 to 200mb	-0.604	2.90E-05
Arctic 700 to 400mb - Tropics 400 to 200mb	-0.5541	1.71E-04
Arctic 700 to 400mb - Tropics 500 to 200mb	-0.5971	3.78E-05
Arctic 700 to 400mb - Tropics 600 to 200mb	-0.6127	2.06E-05
Arctic 700 to 500mb - Tropics 400 to 200mb	-0.5607	1.37E-04
Arctic 700 to 500mb - Tropics 500 to 200mb	-0.6024	3.09E-05
Arctic 700 to 500mb - Tropics 600 to 200mb	-0.6179	1.68E-05

Table A1 - Correlation analysis for zonal wind range latitude 40-70N with the given pressure level and warming vertical boxes.

Tropics Latitude Equator to 20N		
Zonal Wind 300mb	Correlation	P-value
Arctic 600 to 400mb - Tropics 400 to 200mb	-0.4645	0.0022
Arctic 600 to 400mb - Tropics 500 to 200mb	-0.5121	6.21E-04
Arctic 600 to 400mb - Tropics 600 to 200mb	-0.5302	3.63E-04
Arctic 700 to 300mb - Tropics 400 to 200mb	-0.4622	0.0023
Arctic 700 to 300mb - Tropics 500 to 200mb	-0.5109	6.41E-04
Arctic 700 to 300mb - Tropics 600 to 200mb	-0.5323	3.40E-04
Arctic 700 to 400mb - Tropics 400 to 200mb	-0.49	1.10E-03
Arctic 700 to 400mb - Tropics 500 to 200mb	-0.5391	2.76E-04
Arctic 700 to 400mb - Tropics 600 to 200mb	-0.5595	1.43E-04
Arctic 700 to 500mb - Tropics 400 to 200mb	-0.5035	7.91E-04
Arctic 700 to 500mb - Tropics 500 to 200mb	-0.5518	1.84E-04
Arctic 700 to 500mb - Tropics 600 to 200mb	-0.5723	9.24E-05

Table A2 – As in Table A1 but with zonal wind to 300mb.

Tropics Latitude Equator to 20N		
Zonal Wind 400mb	Correlation	P-value
Arctic 600 to 400mb - Tropics 400 to 200mb	-0.4561	0.0027
Arctic 600 to 400mb - Tropics 500 to 200mb	-0.5007	8.57E-04
Arctic 600 to 400mb - Tropics 600 to 200mb	-0.5152	5.68E-04
Arctic 700 to 300mb - Tropics 400 to 200mb	-0.4542	0.0029
Arctic 700 to 300mb - Tropics 500 to 200mb	-0.4999	8.74E-04
Arctic 700 to 300mb - Tropics 600 to 200mb	-0.5179	5.25E-04
Arctic 700 to 400mb - Tropics 400 to 200mb	-0.4837	1.40E-03
Arctic 700 to 400mb - Tropics 500 to 200mb	-0.5302	3.64E-04
Arctic 700 to 400mb - Tropics 600 to 200mb	-0.5473	2.13E-04
Arctic 700 to 500mb - Tropics 400 to 200mb	-0.4992	8.91E-04
Arctic 700 to 500mb - Tropics 500 to 200mb	-0.5453	2.27E-04
Arctic 700 to 500mb - Tropics 600 to 200mb	-0.563	1.27E-04

Table A3 - As in Table A1 but with zonal wind to 400mb.

Tropics Latitude 20S to 20N		
Zonal Wind 200mb	Correlation	P-value
Arctic 600 to 400mb - Tropics 400 to 200mb	-0.5274	3.95E-04
Arctic 600 to 400mb - Tropics 500 to 200mb	-0.5687	1.05E-04
Arctic 600 to 400mb - Tropics 600 to 200mb	-0.5834	6.24E-05
Arctic 700 to 300mb - Tropics 400 to 200mb	-0.5339	3.24E-04
Arctic 700 to 300mb - Tropics 500 to 200mb	-0.5782	7.53E-05
Arctic 700 to 300mb - Tropics 600 to 200mb	-0.5978	3.68E-05
Arctic 700 to 400mb - Tropics 400 to 200mb	-0.5466	2.18E-04
Arctic 700 to 400mb - Tropics 500 to 200mb	-0.5891	5.07E-05
Arctic 700 to 400mb - Tropics 600 to 200mb	-0.6058	2.71E-05
Arctic 700 to 500mb - Tropics 400 to 200mb	-0.5533	1.75E-04
Arctic 700 to 500mb - Tropics 500 to 200mb	-0.5947	4.13E-05
Arctic 700 to 500mb - Tropics 600 to 200mb	-0.6112	2.19E-05

Table A4 - Correlation analysis for zonal wind range latitude 40-70N with the given pressure level and warming vertical boxes.

Tropics Latitude 20S to 20N		
Zonal Wind 300mb	Correlation	P-value
Arctic 600 to 400mb - Tropics 400 to 200mb	-0.4573	0.0026
Arctic 600 to 400mb - Tropics 500 to 200mb	-0.5042	7.76E-04
Arctic 600 to 400mb - Tropics 600 to 200mb	-0.5235	4.44E-04
Arctic 700 to 300mb - Tropics 400 to 200mb	-0.4559	0.0027
Arctic 700 to 300mb - Tropics 500 to 200mb	-0.5038	7.85E-04
Arctic 700 to 300mb - Tropics 600 to 200mb	-0.5264	4.08E-04
Arctic 700 to 400mb - Tropics 400 to 200mb	-0.4828	1.40E-03
Arctic 700 to 400mb - Tropics 500 to 200mb	-0.5312	3.52E-04
Arctic 700 to 400mb - Tropics 600 to 200mb	-0.5527	1.79E-04
Arctic 700 to 500mb - Tropics 400 to 200mb	-0.4964	9.63E-04
Arctic 700 to 500mb - Tropics 500 to 200mb	-0.5441	2.36E-04
Arctic 700 to 500mb - Tropics 600 to 200mb	-0.5657	1.16E-04

Table A5 - As in Table A4 but with zonal wind to 300mb.

Tropics Latitude 20S to 20N		
Zonal Wind 400mb	Correlation	P-value
Arctic 600 to 400mb - Tropics 400 to 200mb	-0.4491	0.0032
Arctic 600 to 400mb - Tropics 500 to 200mb	-0.4929	0.0011
Arctic 600 to 400mb - Tropics 600 to 200mb	-0.5086	6.85E-04
Arctic 700 to 300mb - Tropics 400 to 200mb	-0.4479	0.0033
Arctic 700 to 300mb - Tropics 500 to 200mb	-0.4929	0.0011
Arctic 700 to 300mb - Tropics 600 to 200mb	-0.512	6.22E-04
Arctic 700 to 400mb - Tropics 400 to 200mb	-0.4766	0.0016
Arctic 700 to 400mb - Tropics 500 to 200mb	-0.5223	4.60E-04
Arctic 700 to 400mb - Tropics 600 to 200mb	-0.5406	2.63E-04
Arctic 700 to 500mb - Tropics 400 to 200mb	-0.4923	1.10E-03
Arctic 700 to 500mb - Tropics 500 to 200mb	-0.5376	2.89E-04
Arctic 700 to 500mb - Tropics 600 to 200mb	-0.5564	1.58E-04

Table A6 - As in Table A4 but with zonal wind to 400mb.

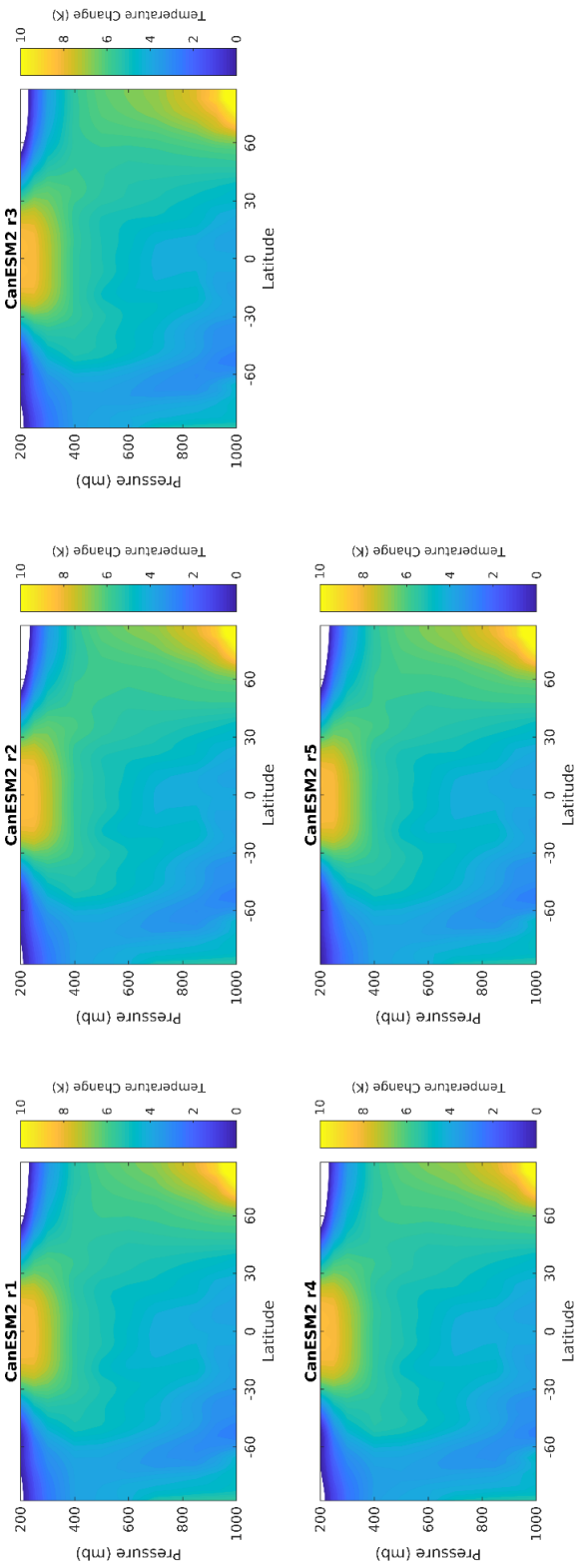

Figure A1 – Warming between the RCP8.5 (2070-2099) and Historical (1975-2004) climate model output for all the ensemble members of CanESM2.

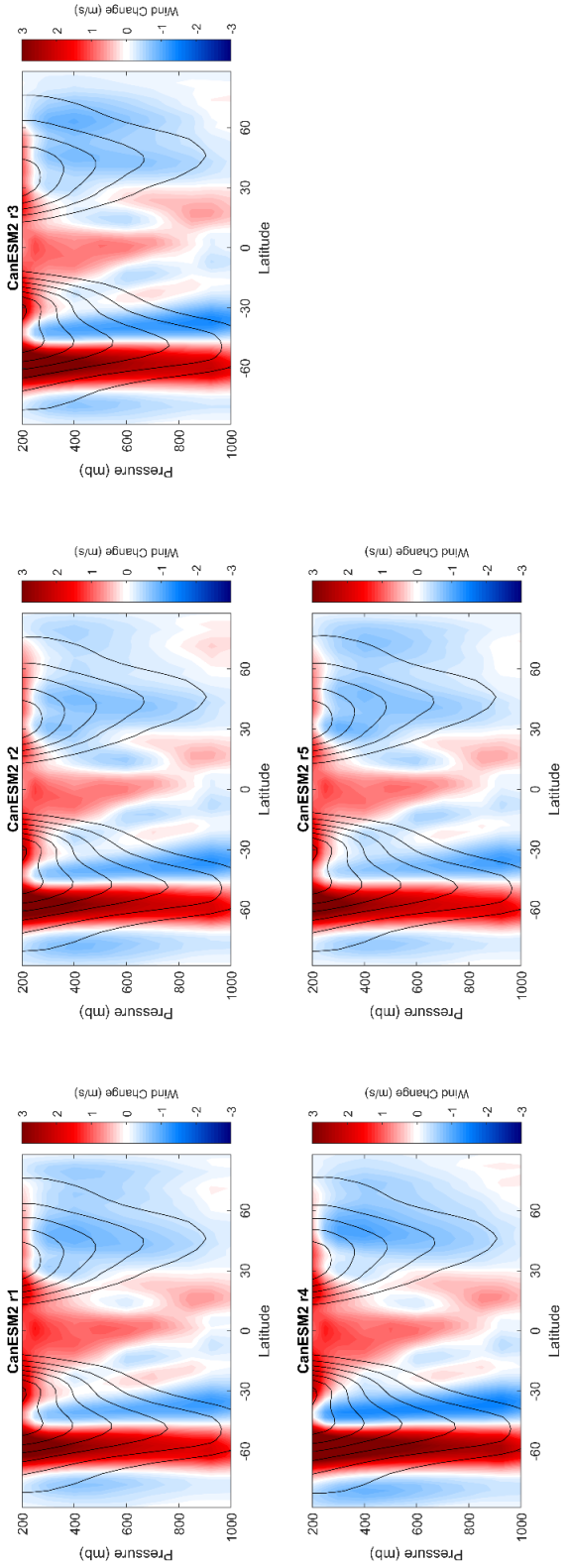

Figure A2 – Zonal wind change between the RCP8.5 (2070-2099) and Historical (1975-2004) climate model output for all the ensemble members of CanESM2. The black contours are the Historical zonal wind mean and are in increments of 5 ms^{-1}

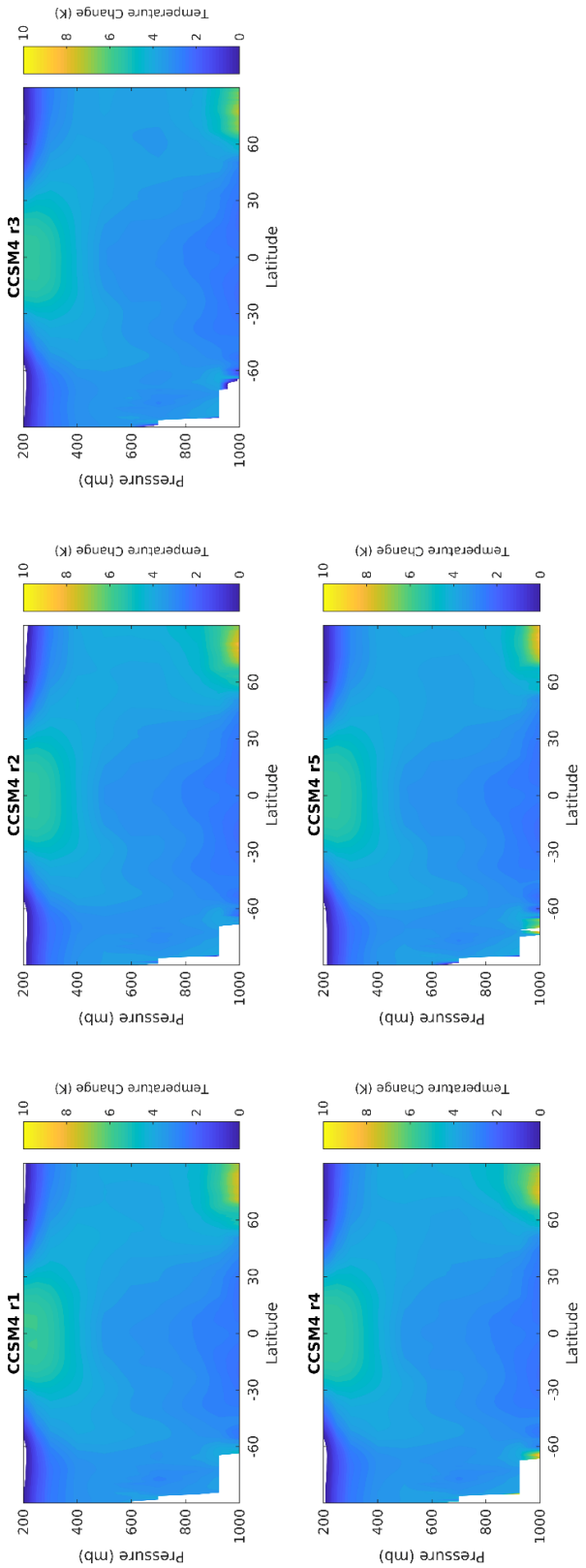

Figure A3 –As in Figure A1 but for all the ensemble members of CCSM4.

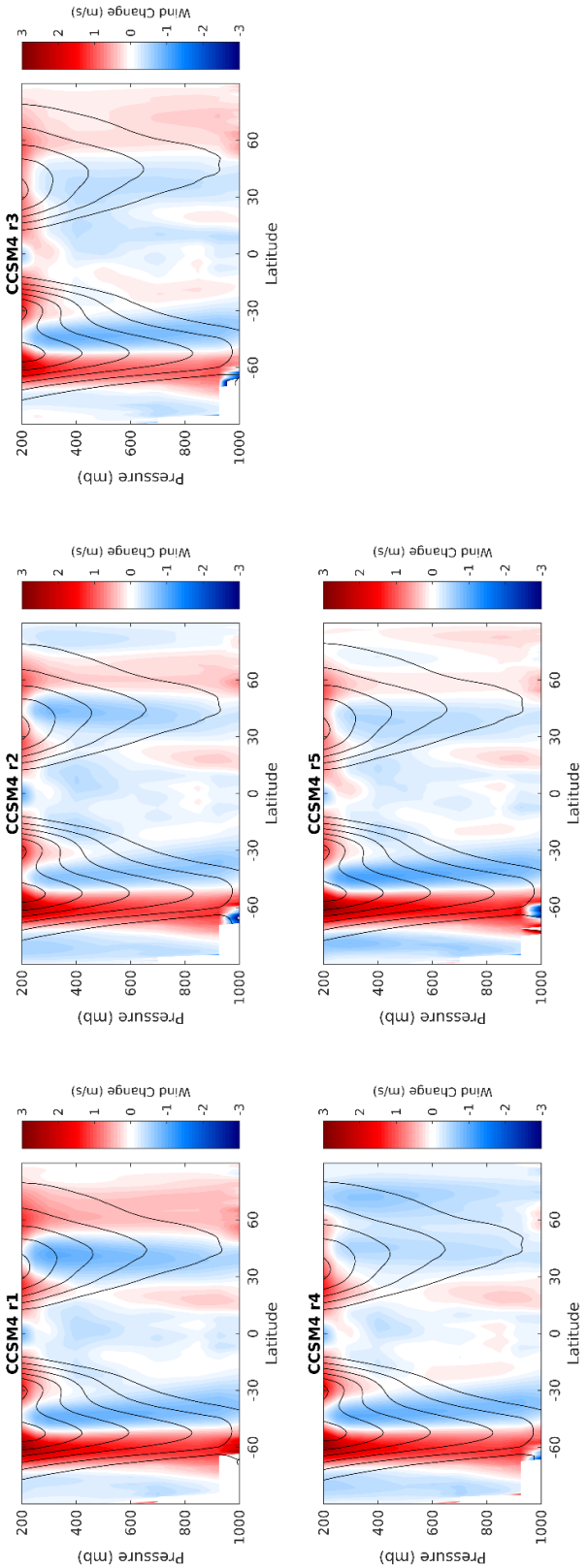

Figure A4 –As in Figure A2 but for all the ensemble members of CCSM4.

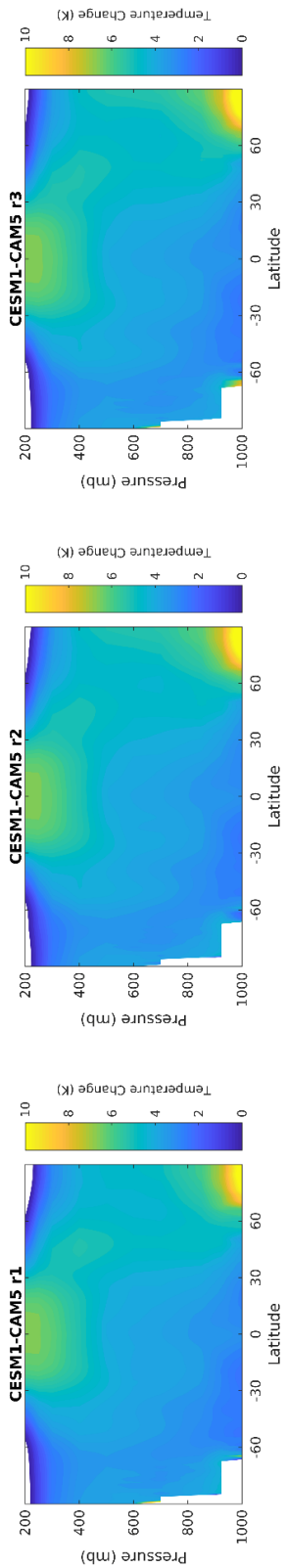

Figure A5 –As in Figure A1 but for all the ensemble members of CESM1-CAM5.

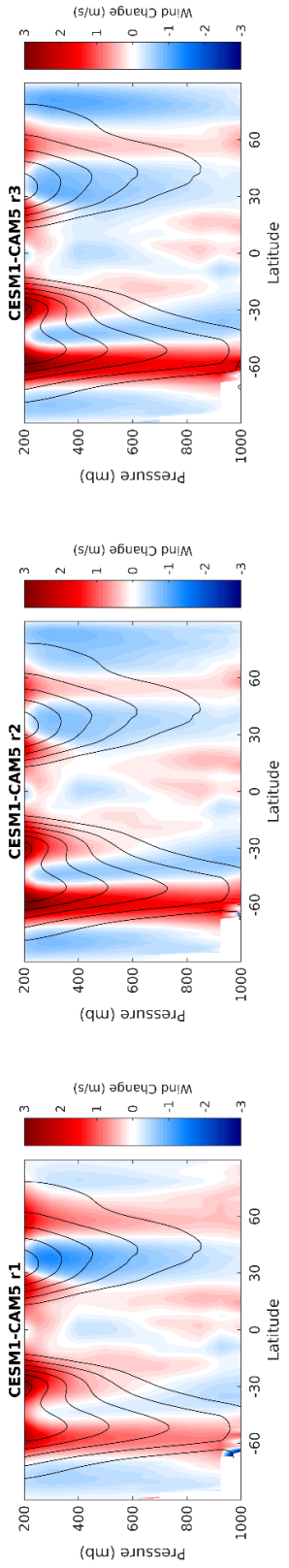

Figure A6 –As in Figure A2 but for all the ensemble members of CESM1-CAM5.

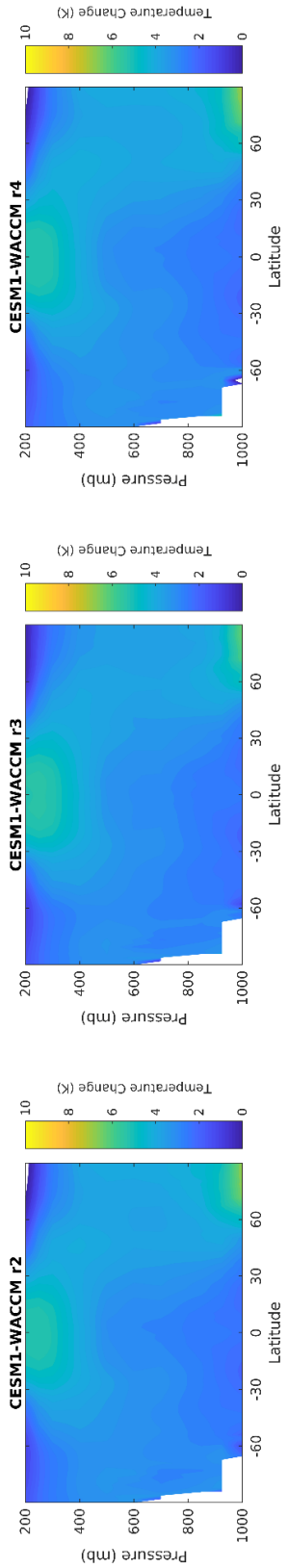

Figure A7 –As in Figure A1 but for all the ensemble members of CESM1-WACCM.

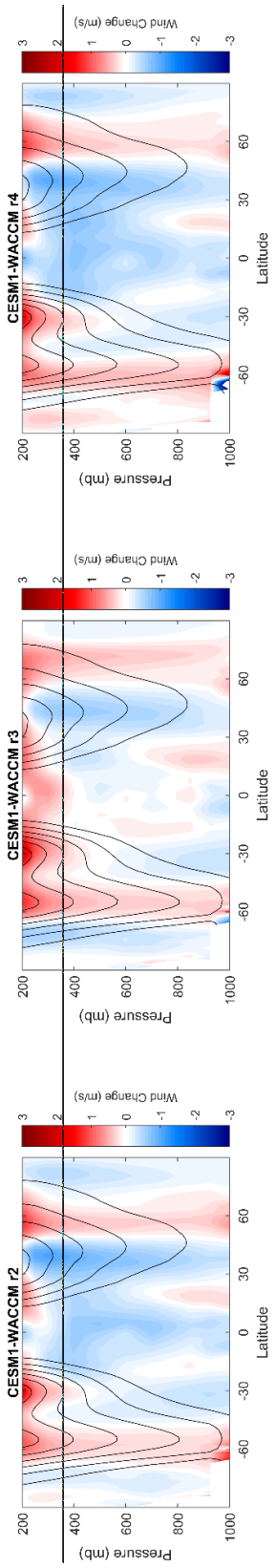

Figure A8 –As in Figure A2 but for all the ensemble members of CESM1-WACCM.

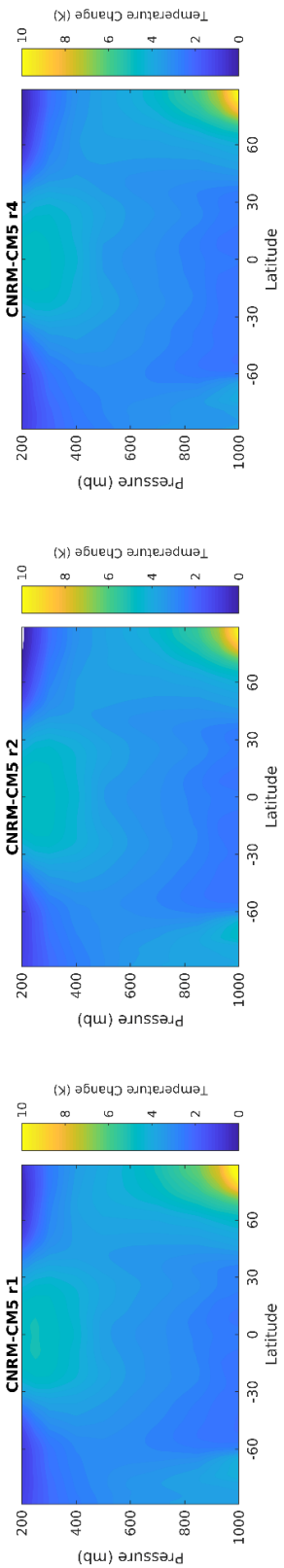

Figure A9 –As in Figure A1 but for all the ensemble members of CNRM-CM5.

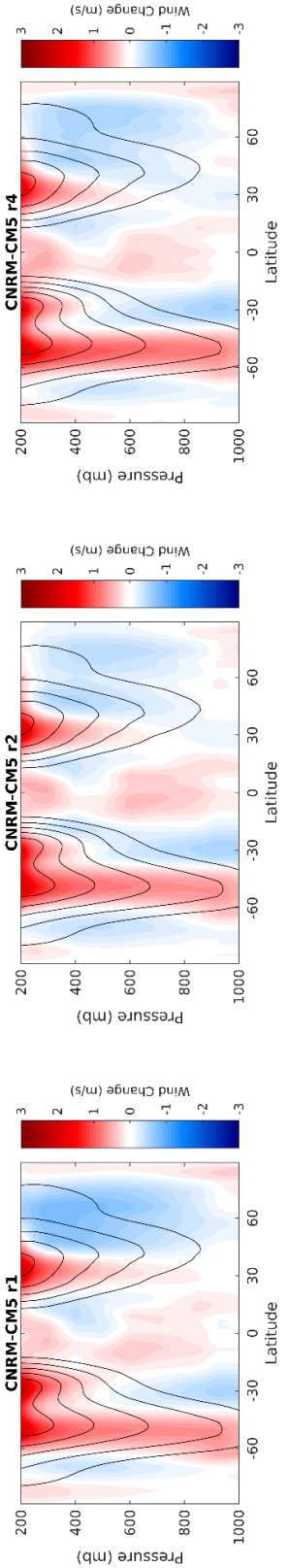

Figure A10 –As in Figure A2 but for all the ensemble members of CNRM-CM5.

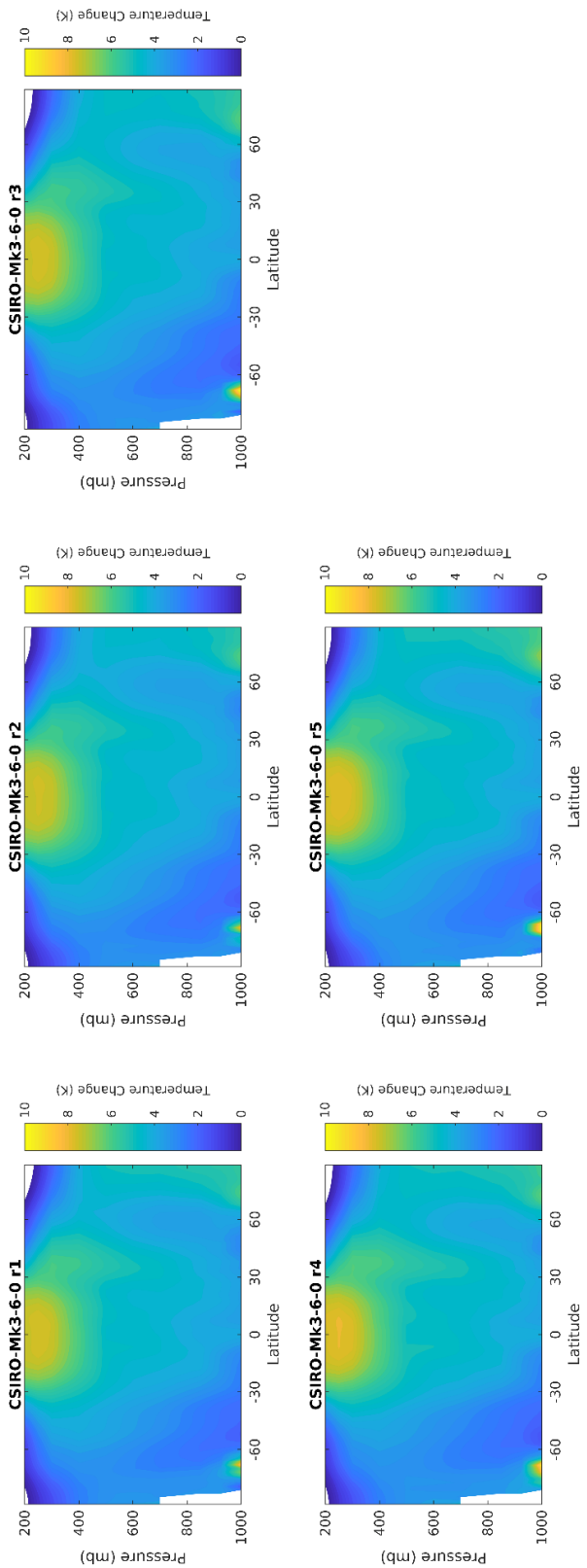

Figure A11 –As in Figure A1 but for all the ensemble members of CSIRO-Mk3-6-0.

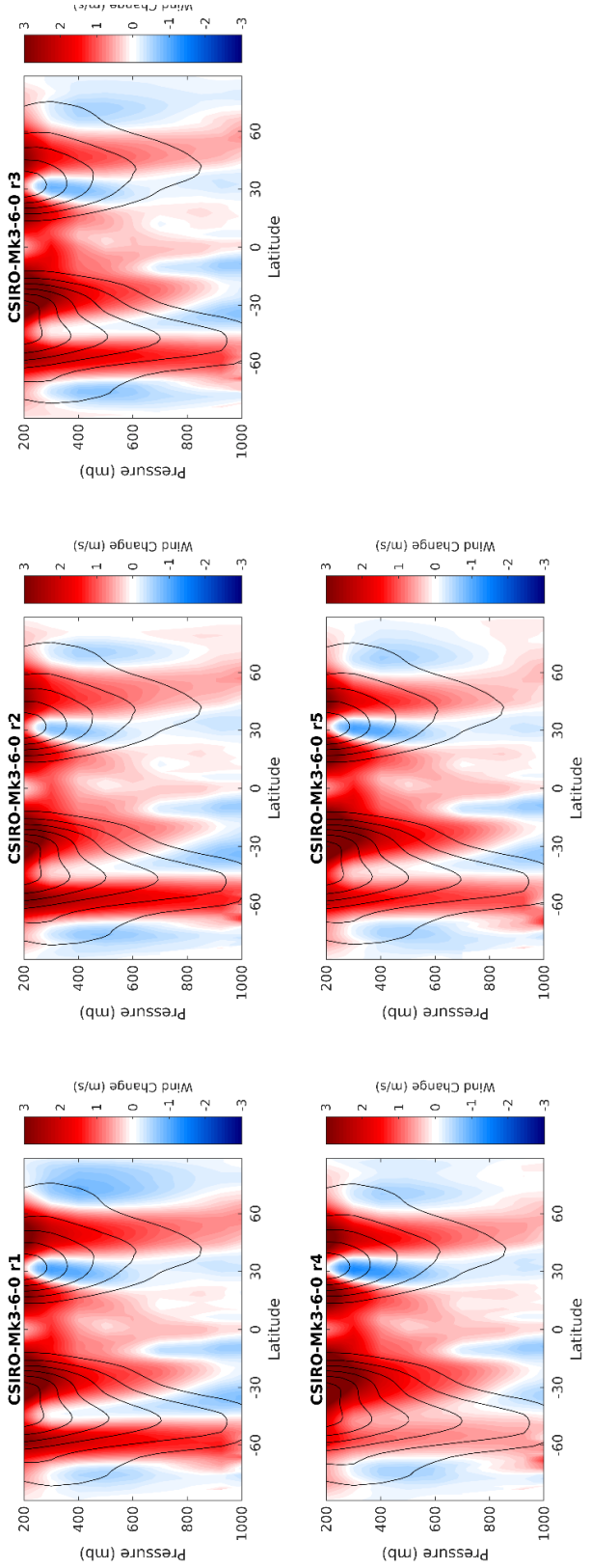

Figure A12 –As in Figure A2 but for all the ensemble members of CSIRO-Mk3-6-0.

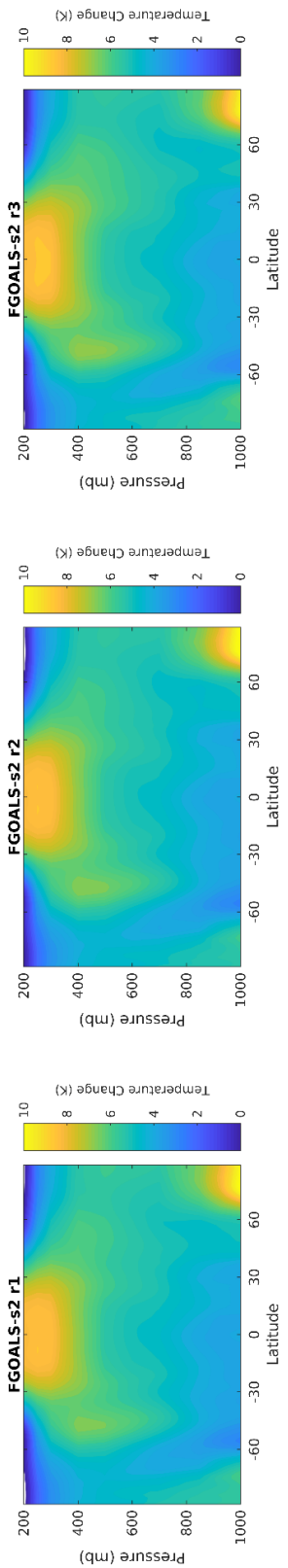

Figure A13 –As in Figure A1 but for all the ensemble members of FGOALS-s2.

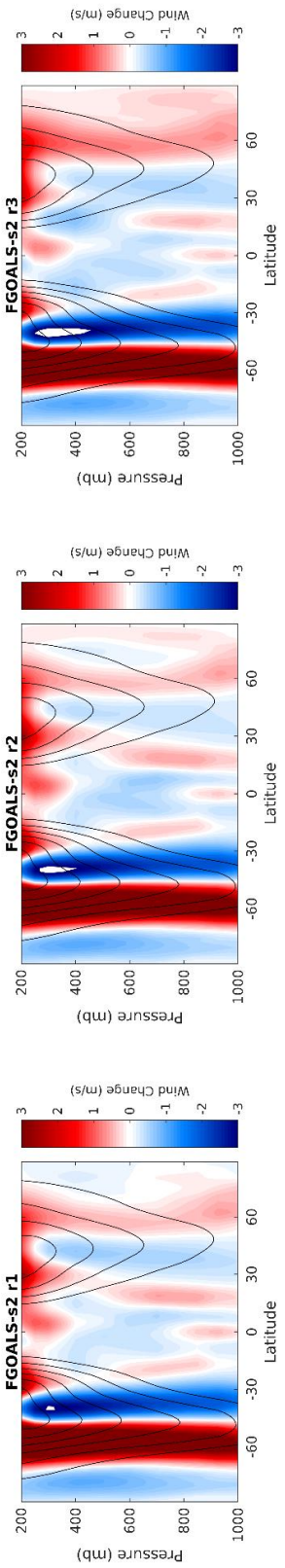

Figure A14 –As in Figure A2 but for all the ensemble members of FGOALS-s2.

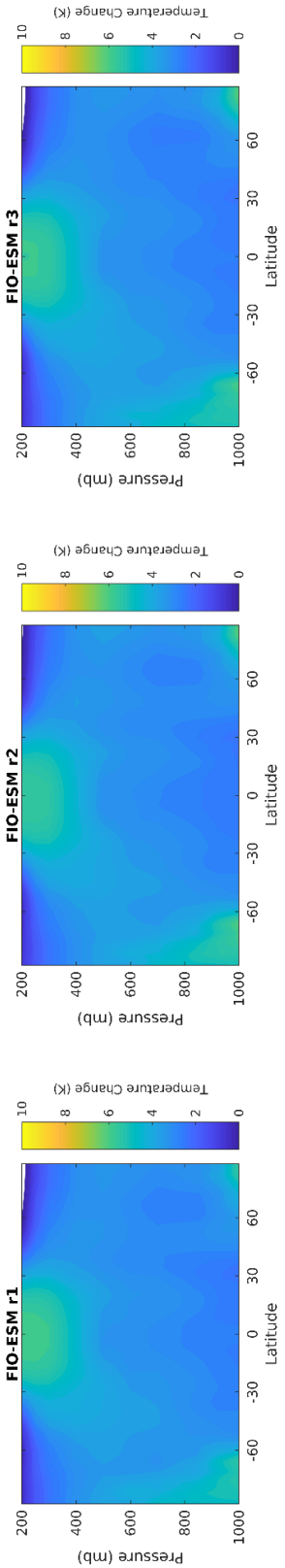

Figure A15 –As in Figure A1 but for all the ensemble members of FIO-ESM.

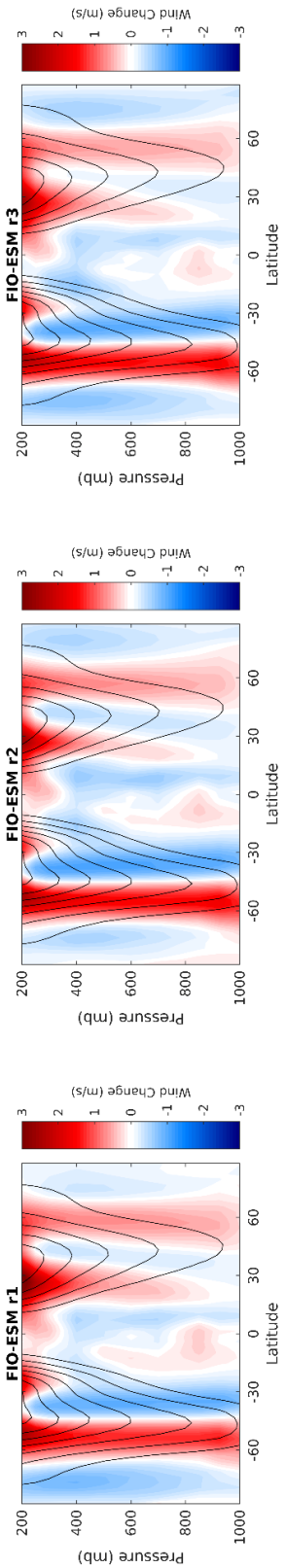

Figure A16 –As in Figure A2 but for all the ensemble members of FIO-ESM.

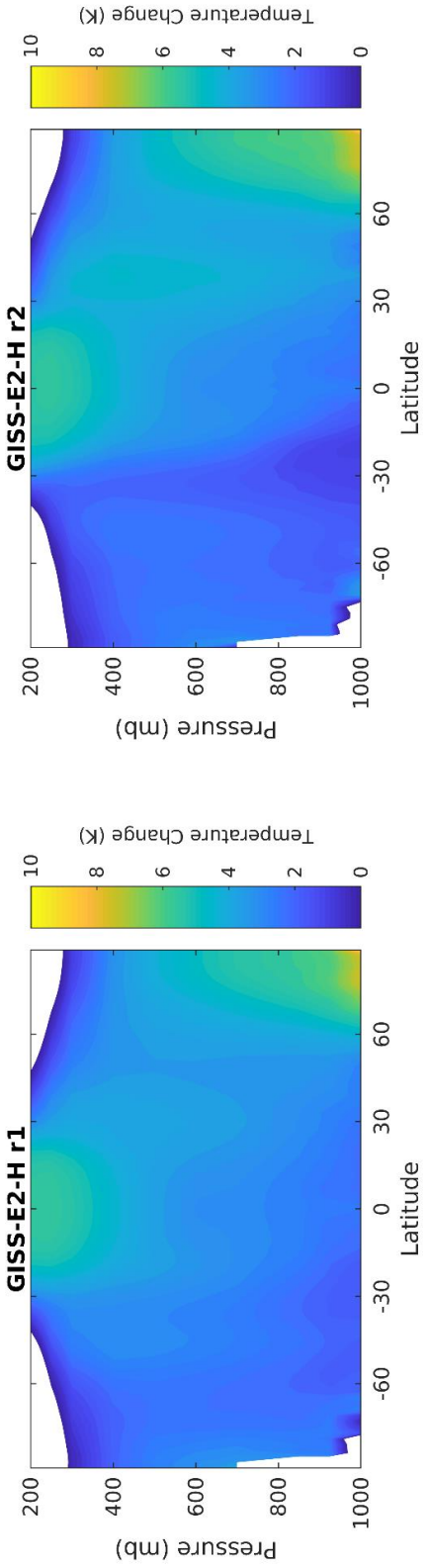

Figure A17 –As in Figure A1 but for all the ensemble members of GISS-E2-H.

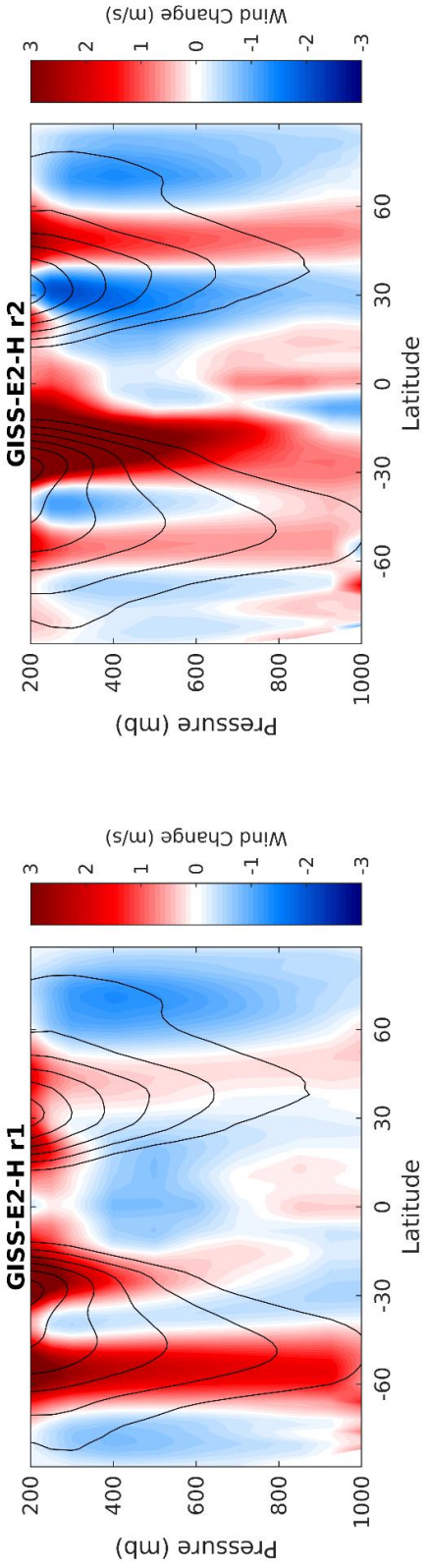

Figure A18 –As in Figure A2 but for all the ensemble members of GISS-E2-H.

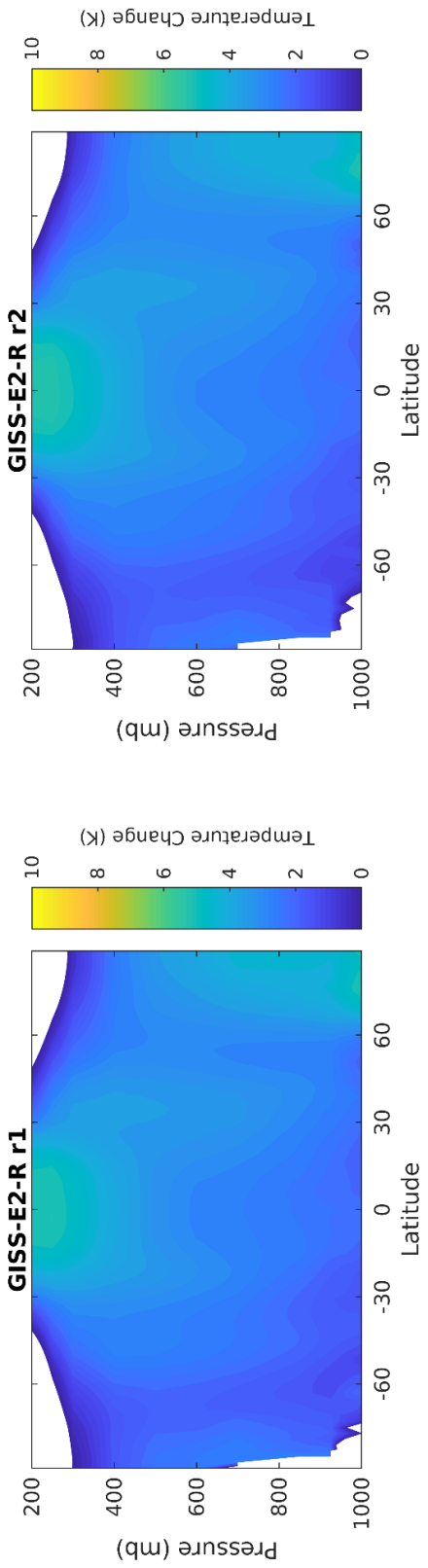

Figure A19 –As in Figure A1 but for all the ensemble members of GISS-E2-R.

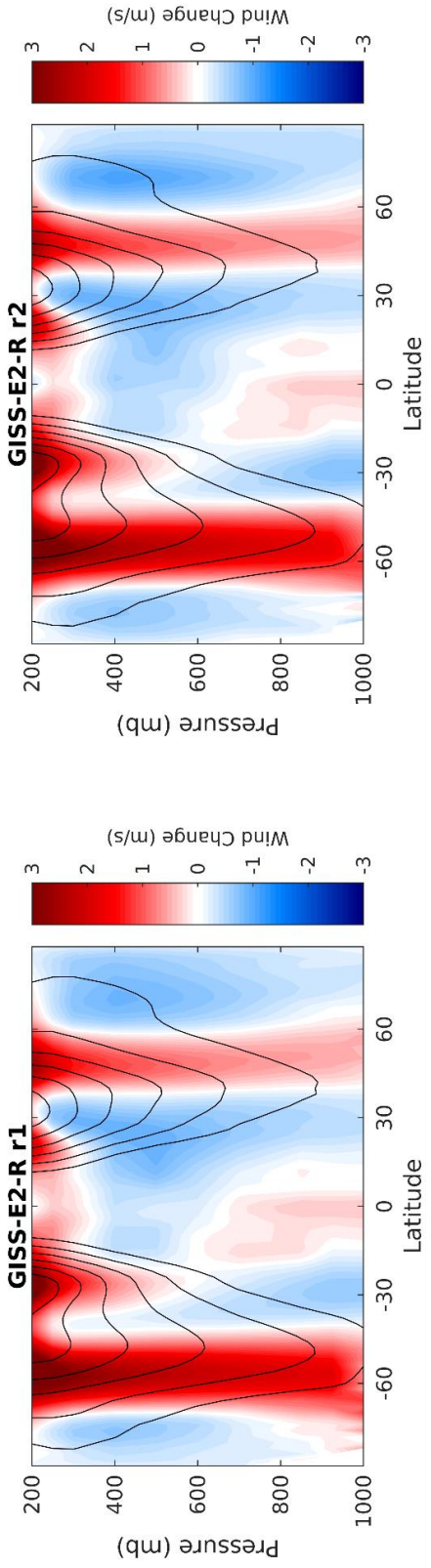

Figure A20 –As in Figure A2 but for all the ensemble members of GISS-E2-R.

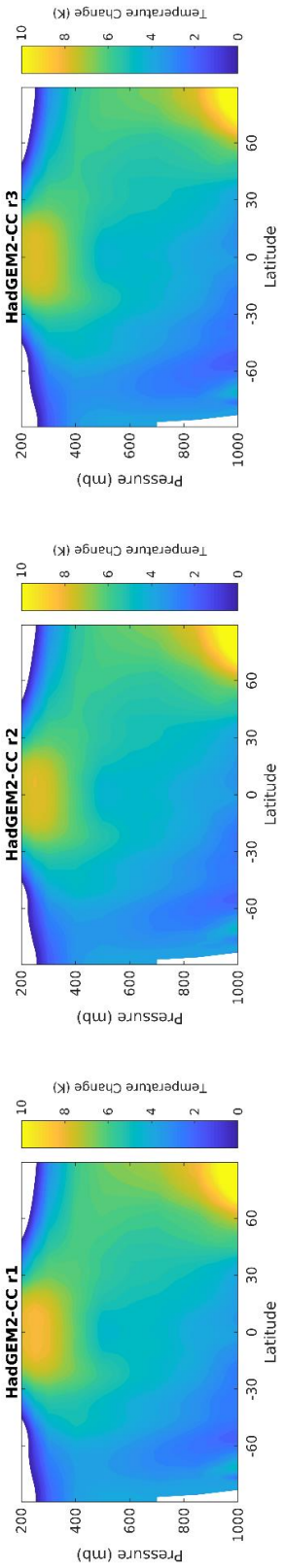

Figure A21 –As in Figure A1 but for all the ensemble members of HadGEM2-CC.

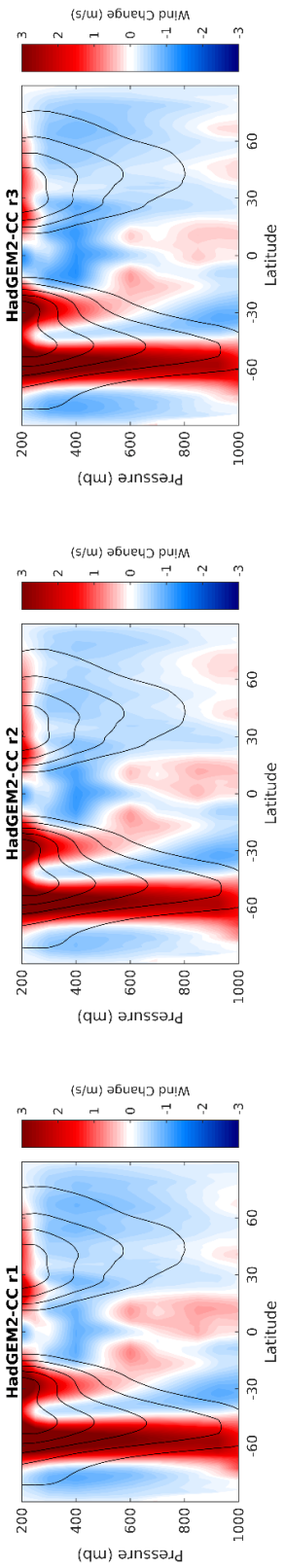

Figure A22 –As in Figure A2 but for all the ensemble members of HadGEM2-CC.

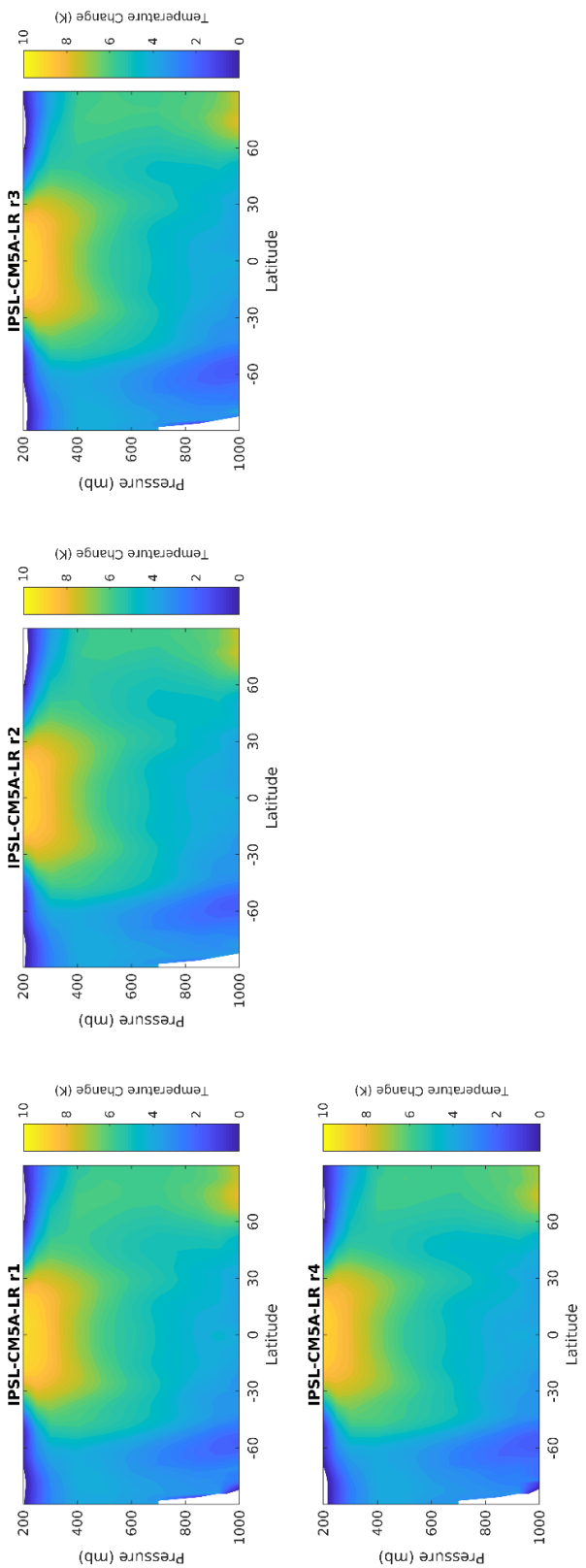

Figure A23 –As in Figure A1 but for all the ensemble members of IPSL-CM5A-LR.

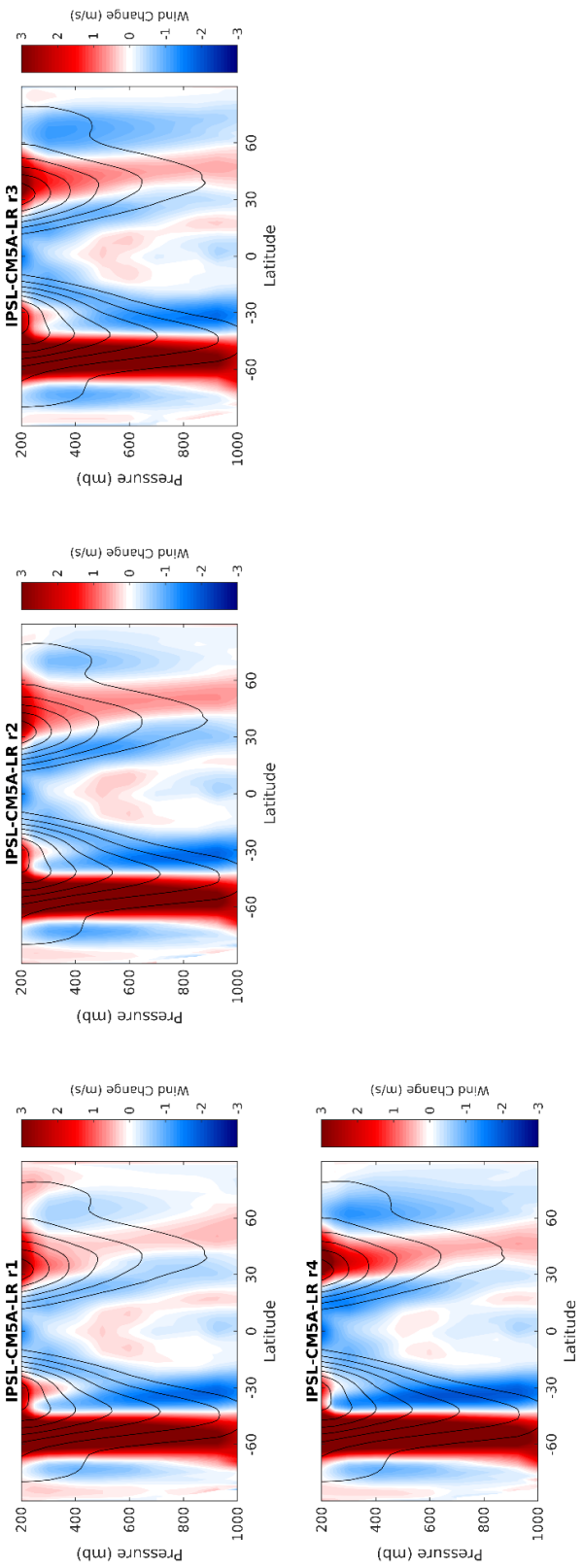

Figure A24 –As in Figure A2 but for all the ensemble members of IPSL-CM5A-LR.

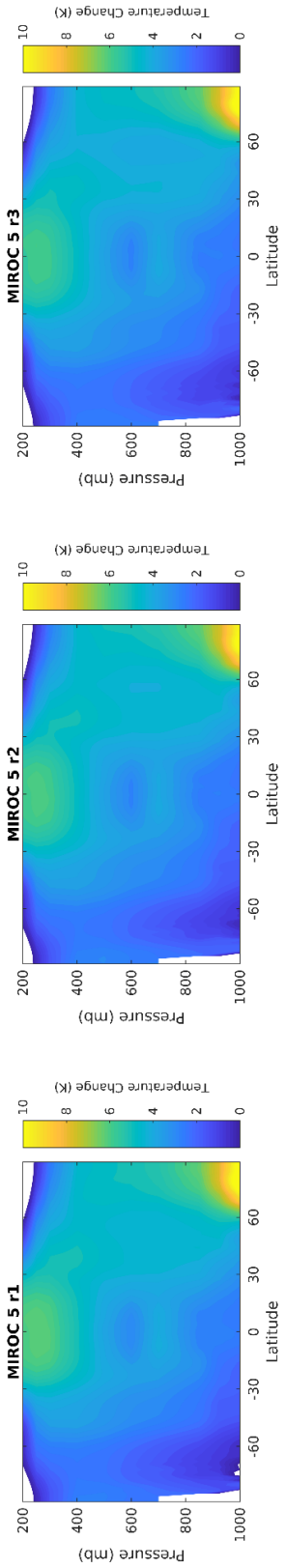

Figure A25 –As in Figure A1 but for all the ensemble members of MIROC 5.

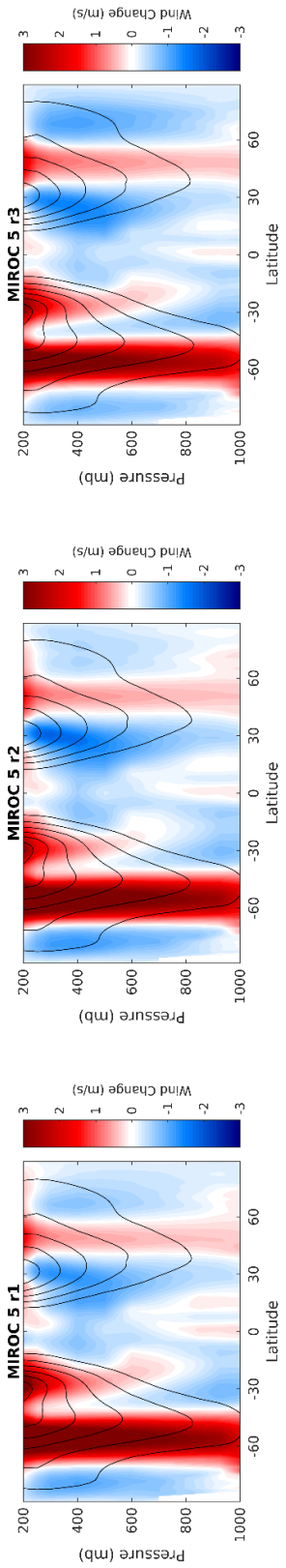

Figure A26 –As in Figure A2 but for all the ensemble members of MIROC 5.

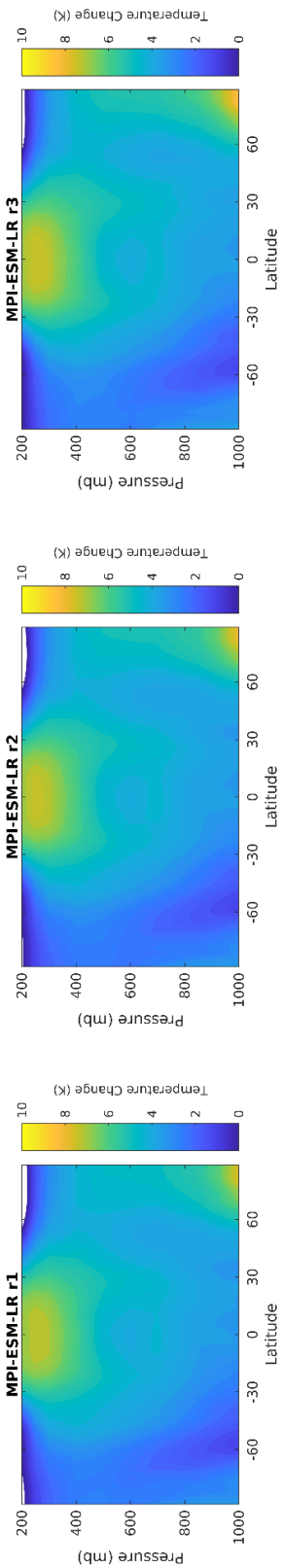

Figure A27 –As in Figure 1 but for all the ensemble members of MPI-ESM-LR.

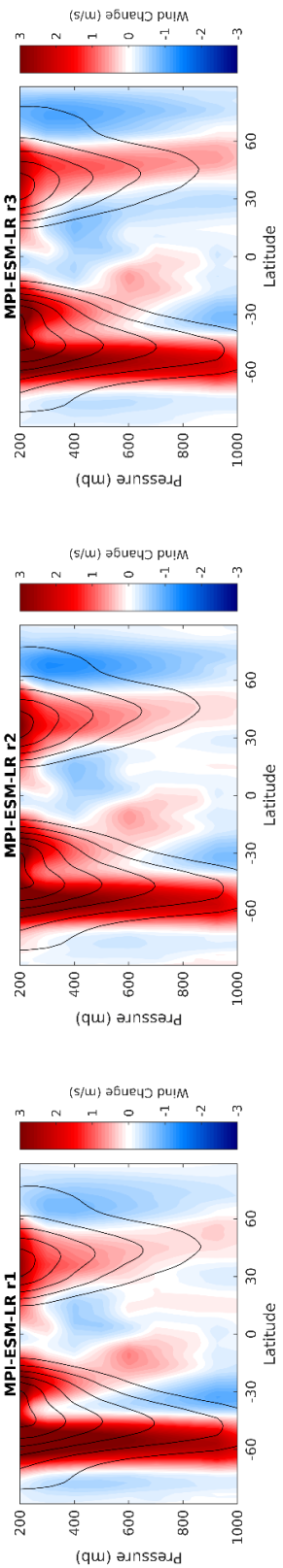

Figure A28 –As in Figure 2 but for all the ensemble members of MPI-ESM-LR.

APPENDIX B: SATELLITE ERA

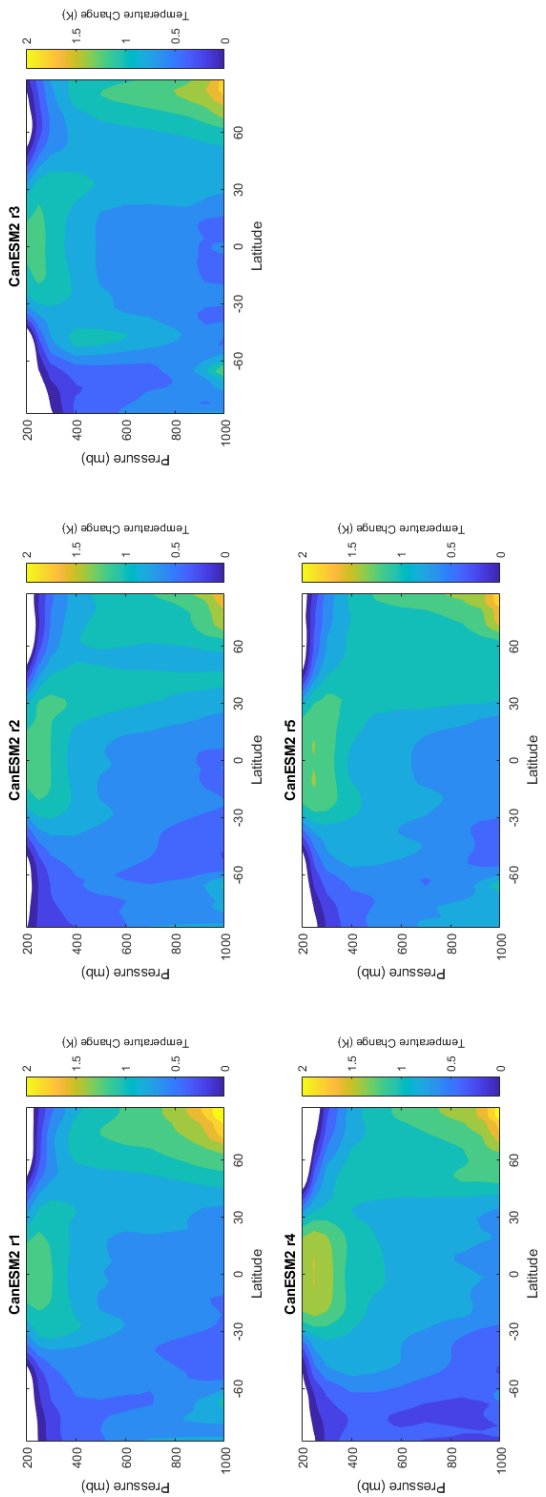

Figure B1 – Warming difference between the Present (1999-2018) and Past (1979-1998) climate model output for all the ensemble members of CanESM2.

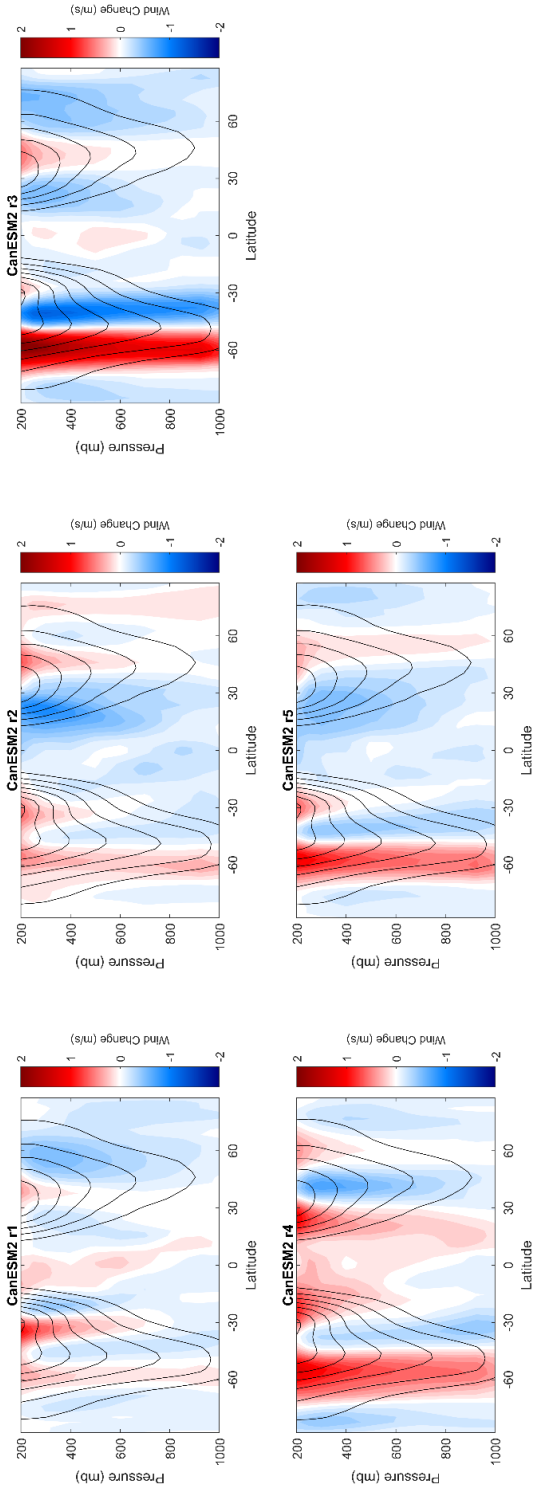

Figure B2 – Zonal wind change between the Present (1999-2018) and Past (1979-1998) climate model output for all the ensemble members of CanESM2. The black contours are the Historical zonal wind mean and are in increments of 5 ms^{-1}.

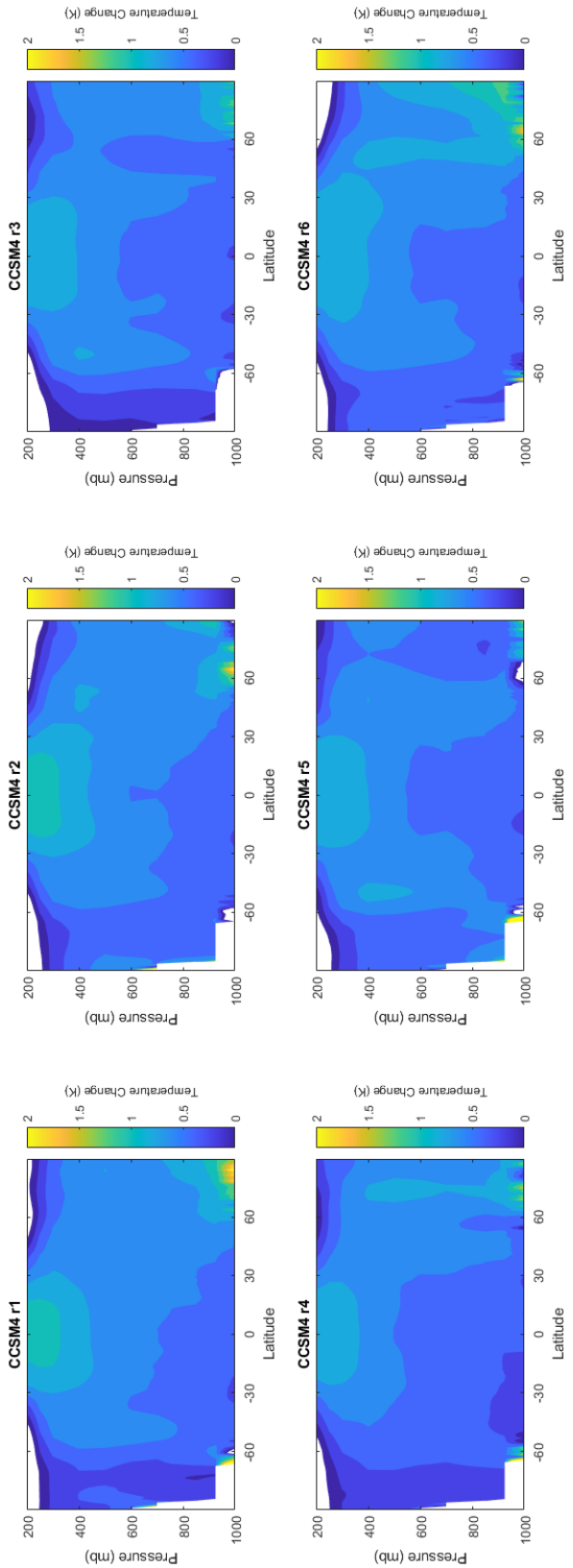

Figure B3 –As in Figure B1 but for all the ensemble members of CCSM4.

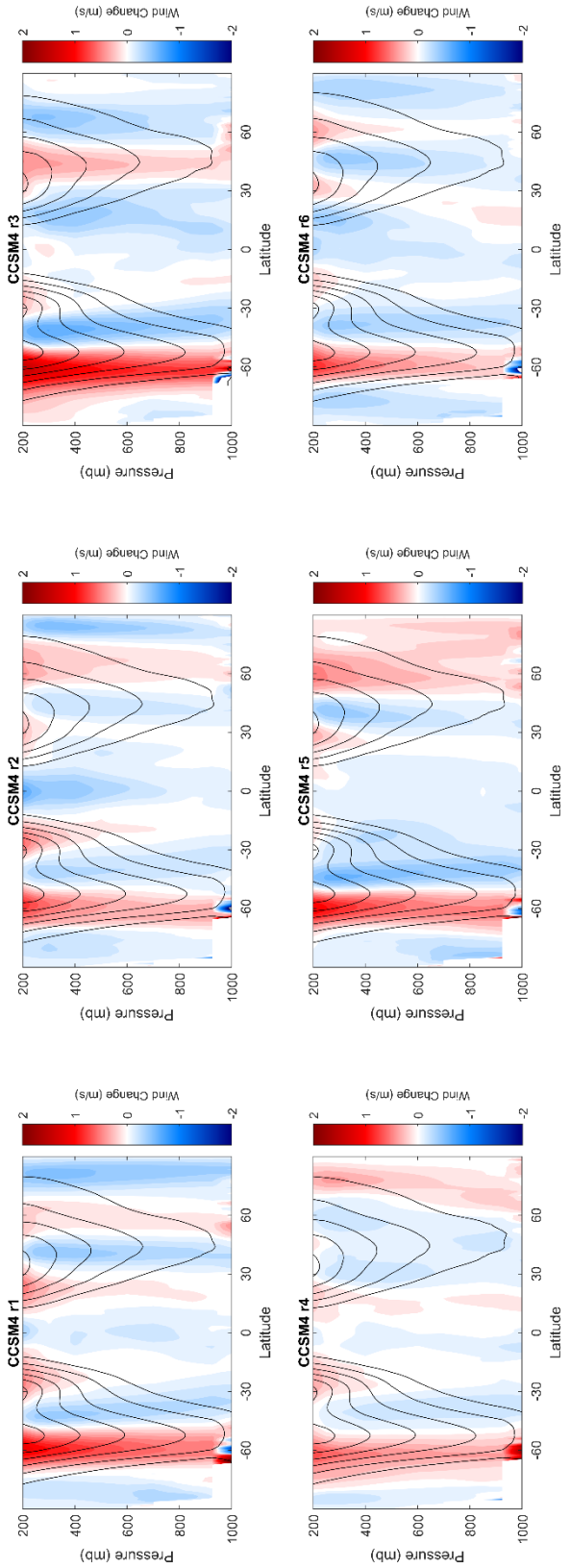

Figure B4 –As in Figure B2 but for all the ensemble members of CCSM4.

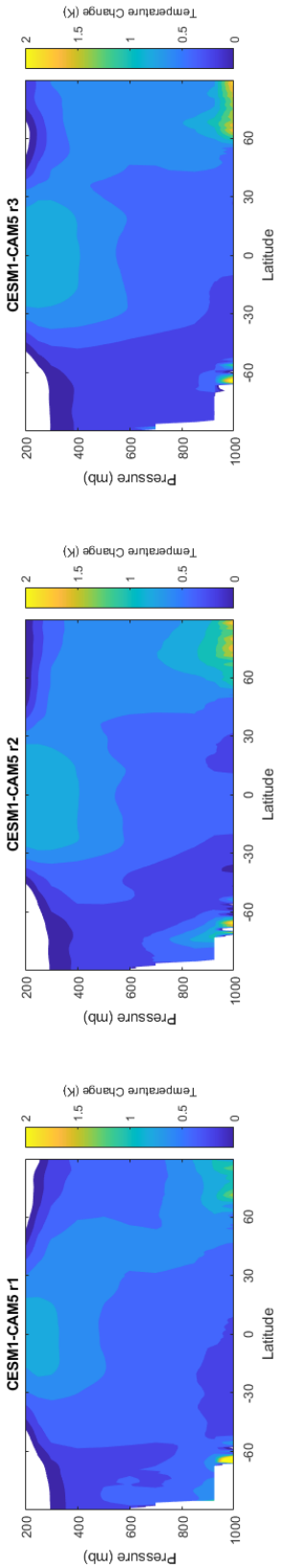

Figure B5 –As in Figure B1 but for all the ensemble members of CESM1-CAM5.

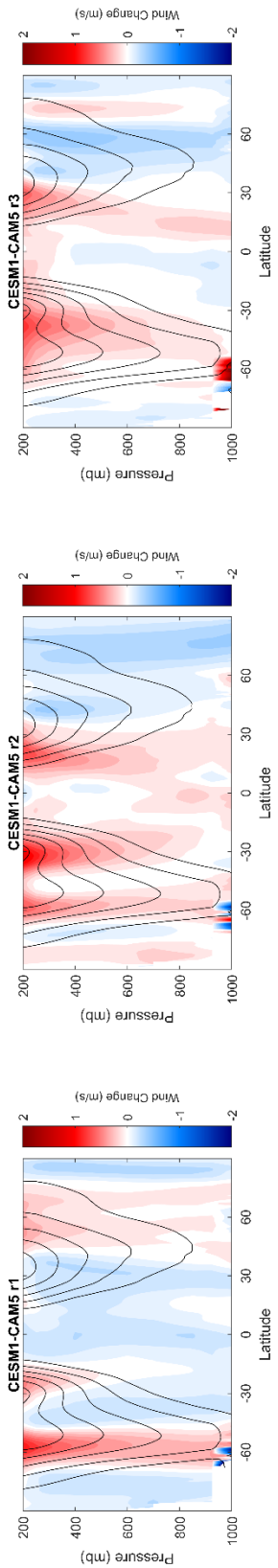

Figure B6 –As in Figure B2 but for all the ensemble members of CESM1-CAM5.

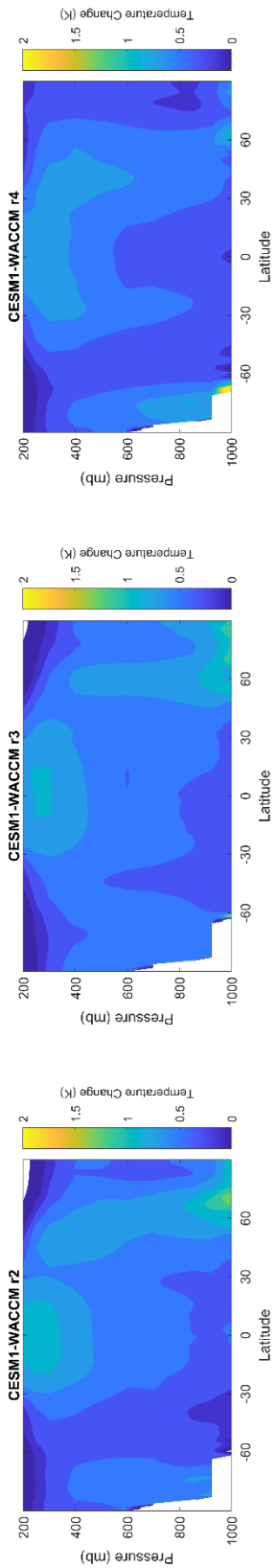

Figure B7 –As in Figure B1 but for all the ensemble members of CESM1-WACCM.

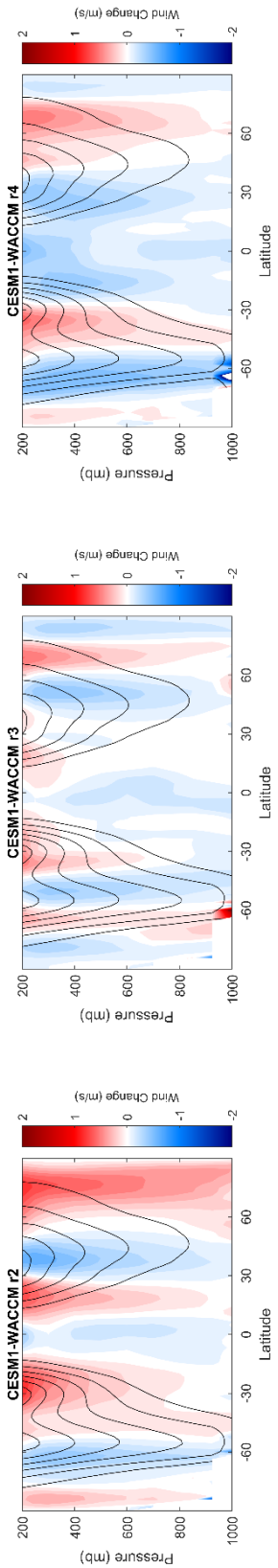

Figure B8 –As in Figure B2 but for all the ensemble members of CESM1-WACCM.

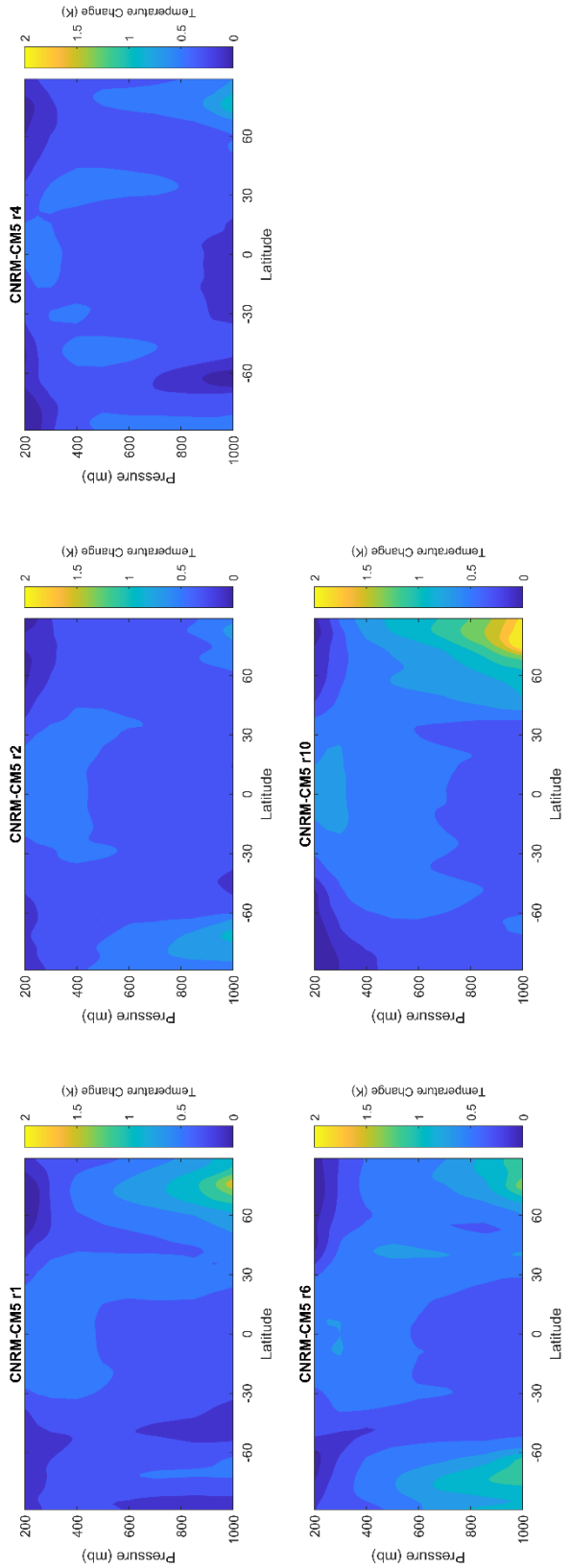

Figure B9 –As in Figure B1 but for all the ensemble members of CNRM-CM5.

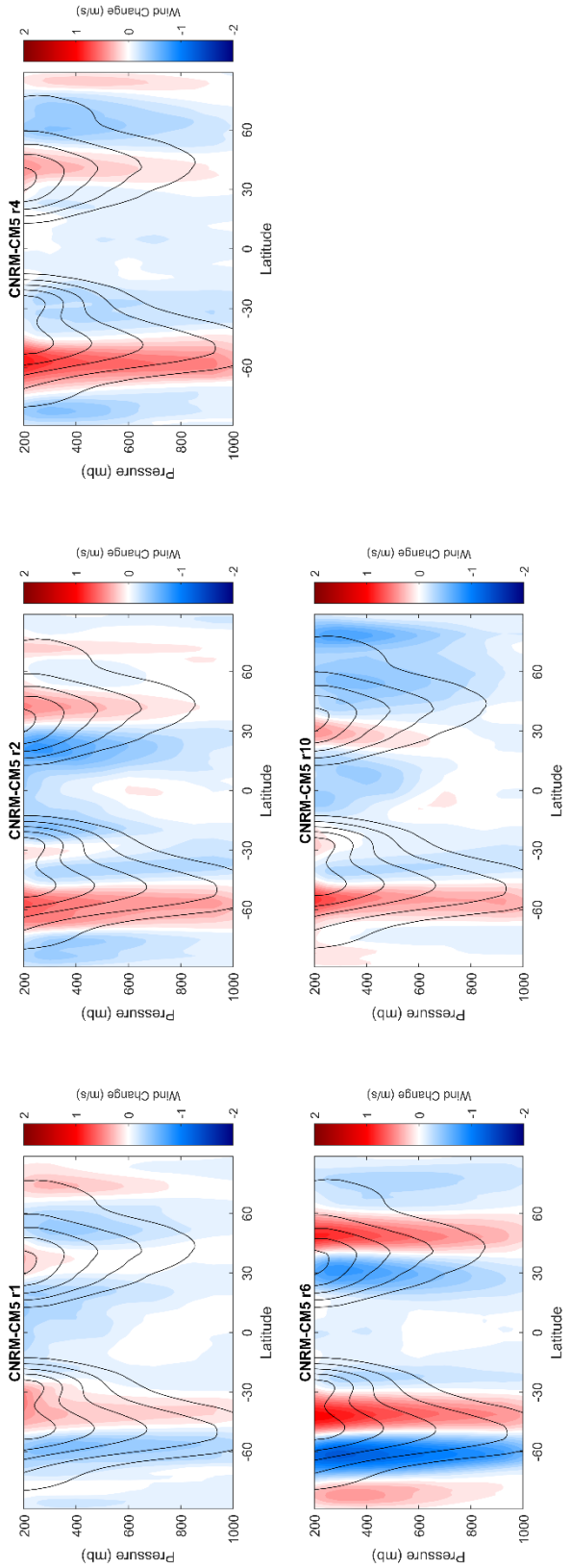

Figure B10 –As in Figure B2 but for all the ensemble members of CNRM-CM5.

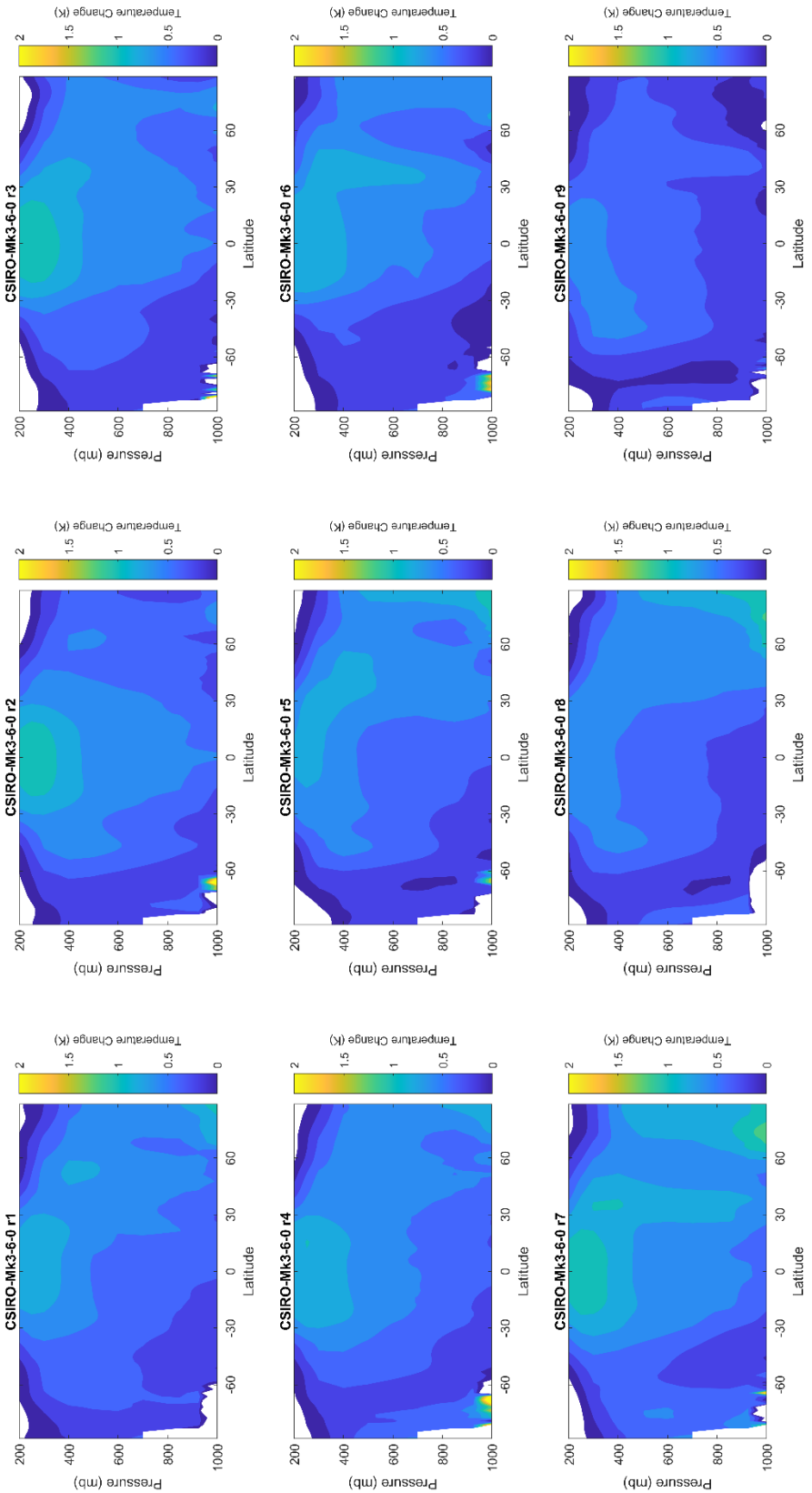

Figure B11 –As in Figure B1 but for all the ensemble members of CSIRO-Mk3-6-0.

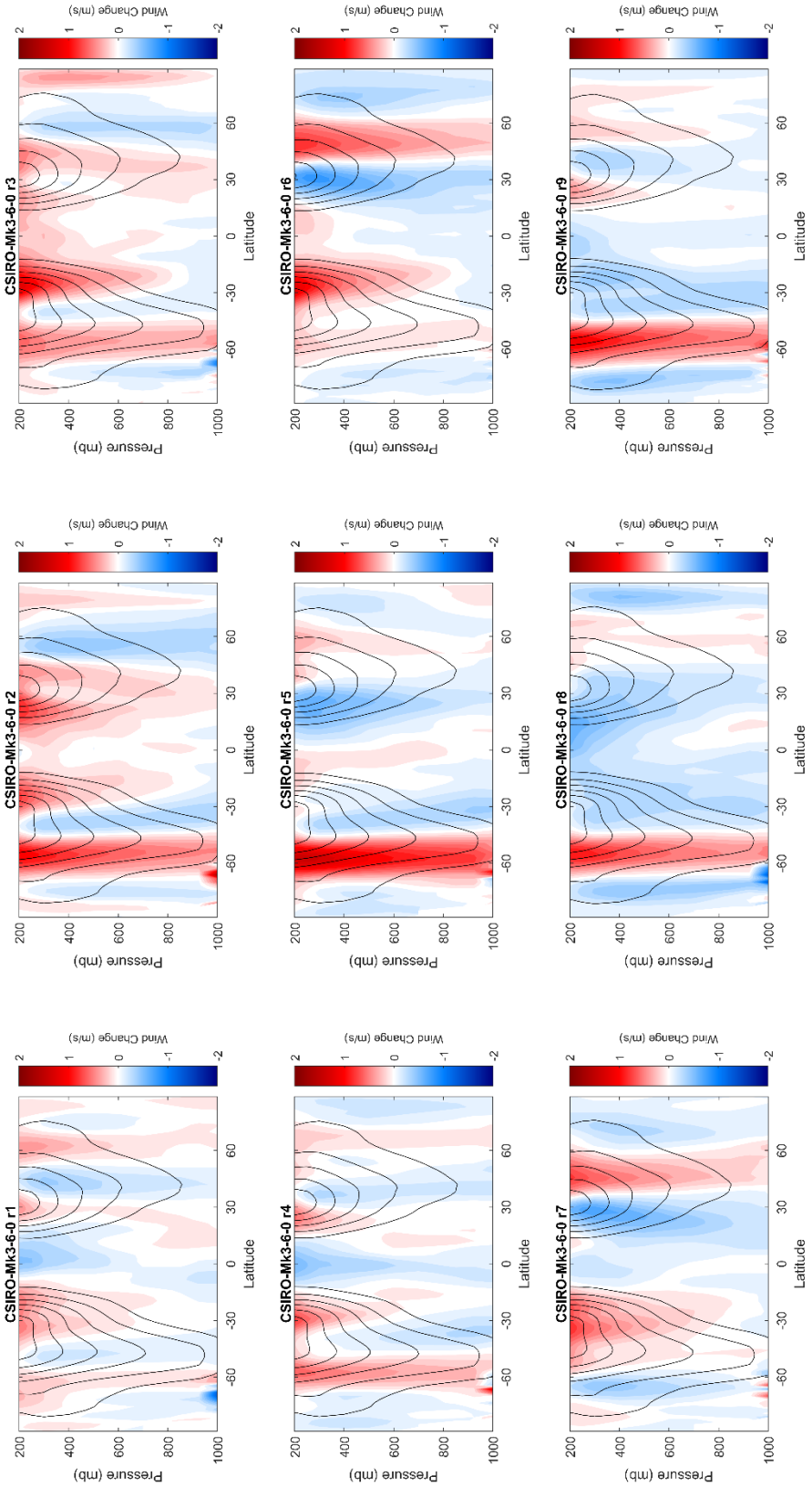

Figure B12 –As in Figure B2 but for all the ensemble members of CSIRO-Mk3-6-0.

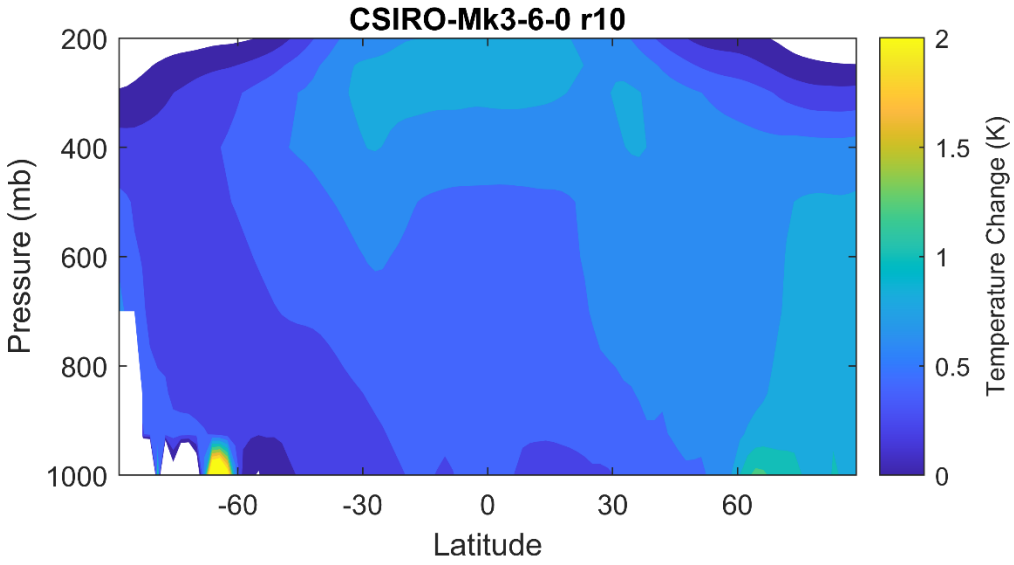

Figure B13 –As in Figure B1 but for ensemble member 10 of CSIRO-Mk3-6-0.

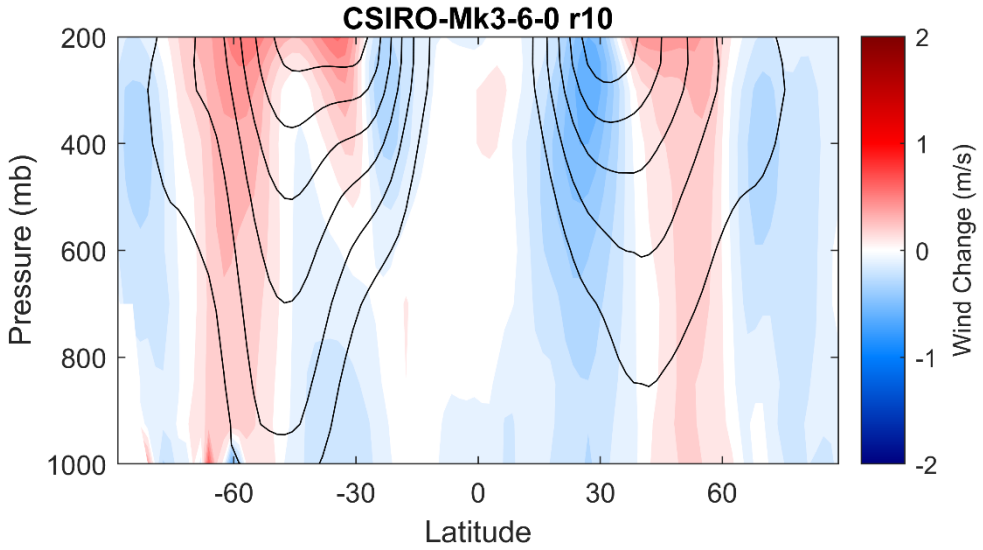

Figure B14 – As in Figure B2 but for ensemble member 10 of CSIRO-Mk3-6-0.

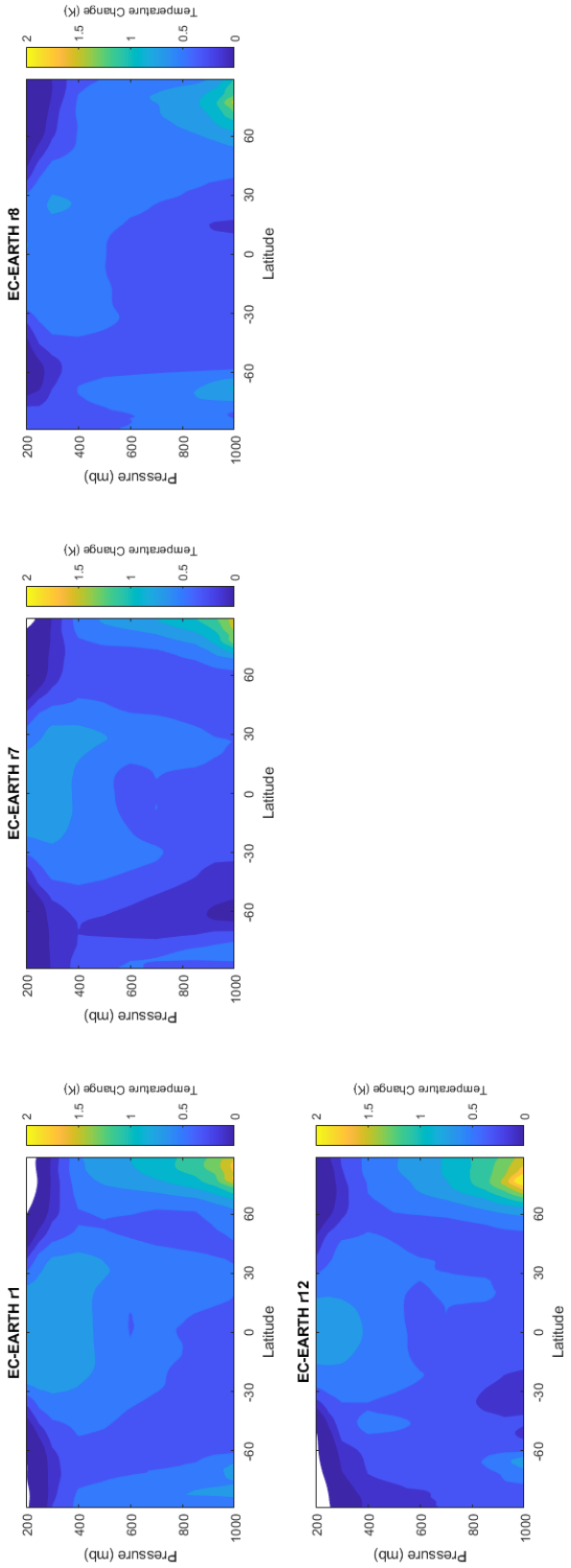

Figure B15 –As in Figure B1 but for all the ensemble members of EC-EARTH.

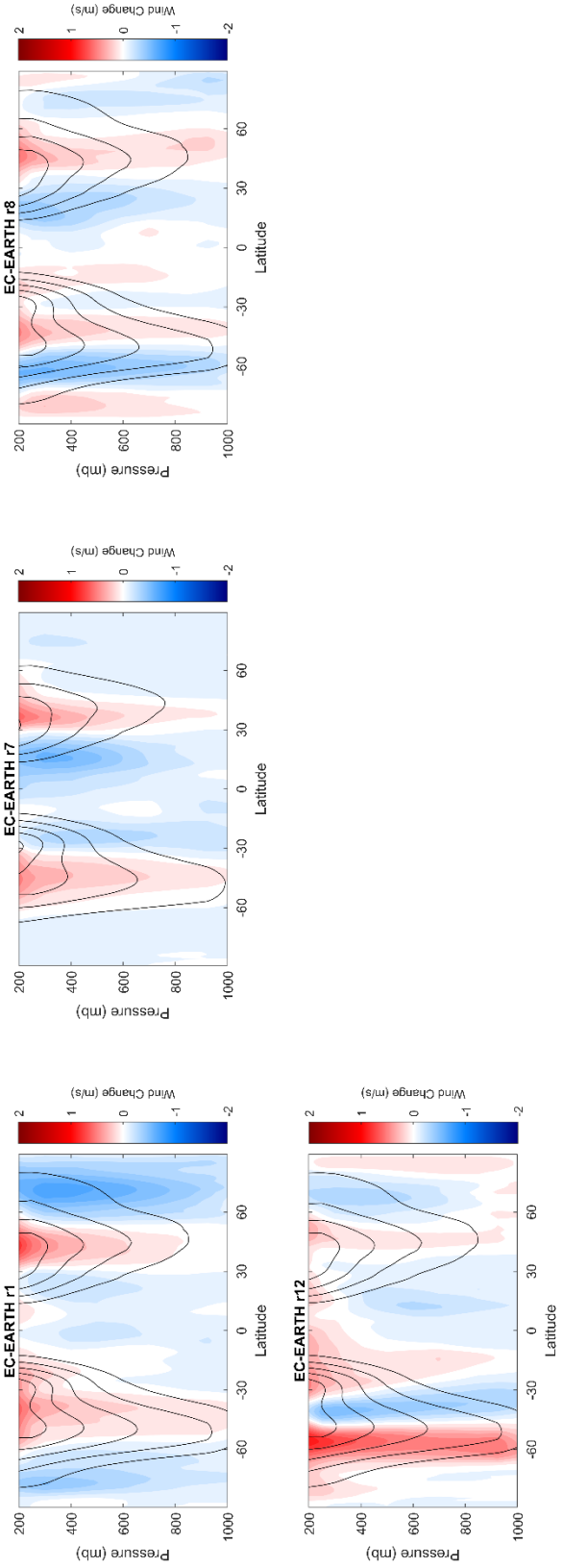

Figure B16 – As in Figure B1 but for all the ensemble members of EC-EARTH.

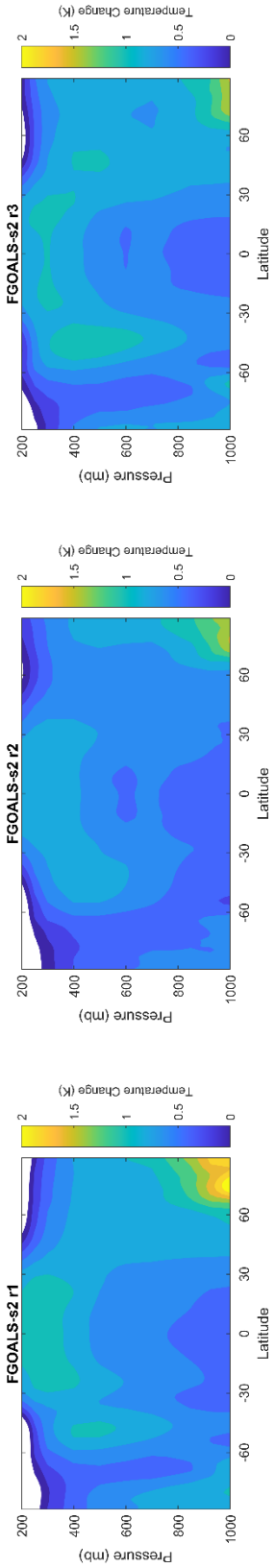

Figure B17 –As in Figure B1 but for all the ensemble members of FGOALS-s2.

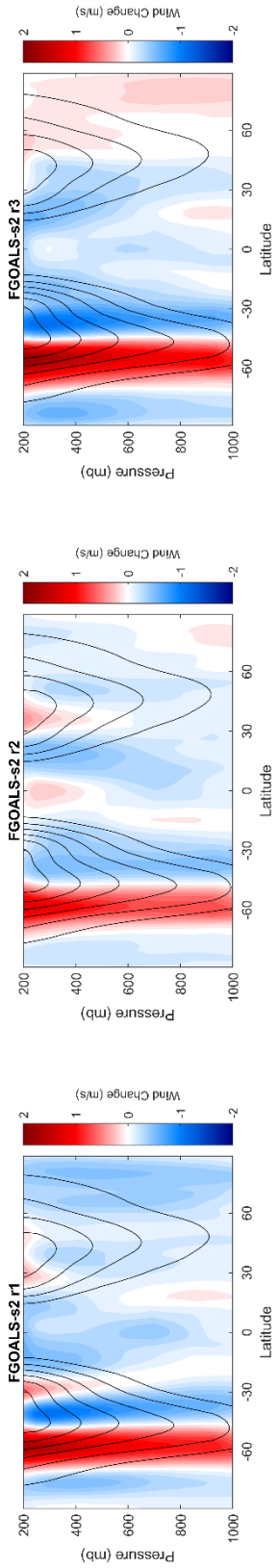

Figure B18 –As in Figure B2 but for all the ensemble members of FGOALS-s2.

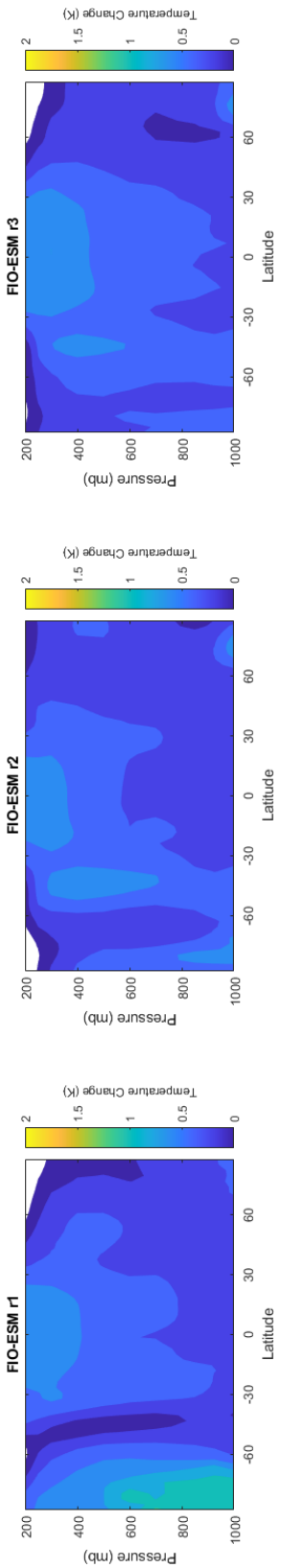

Figure B19 –As in Figure B1 but for all the ensemble members of FIO-ESM.

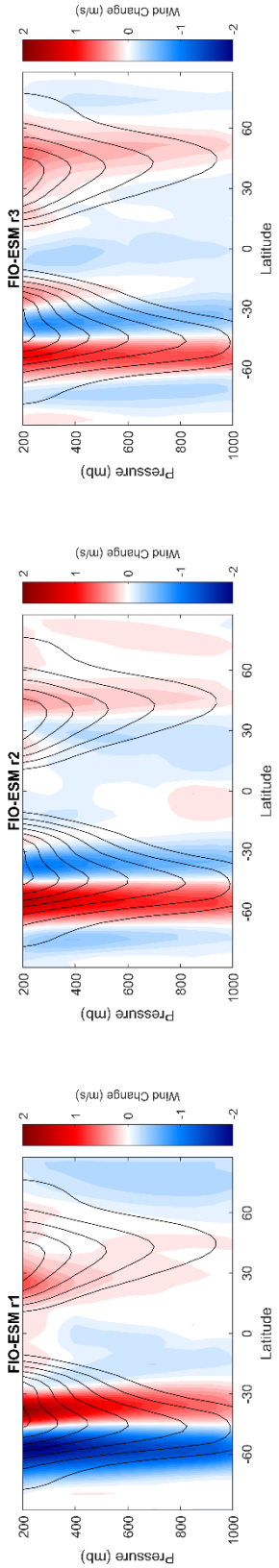

Figure B20 –As in Figure B2 but for all the ensemble members of FIO-ESM.

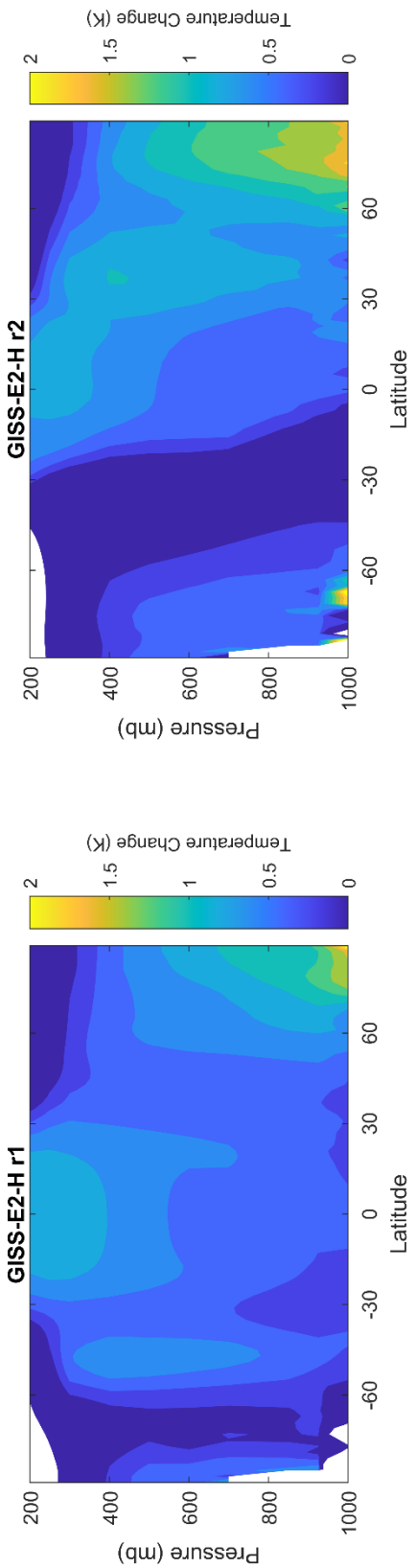

Figure B21 –As in Figure B1 but for all the ensemble members of GISS-E2-H.

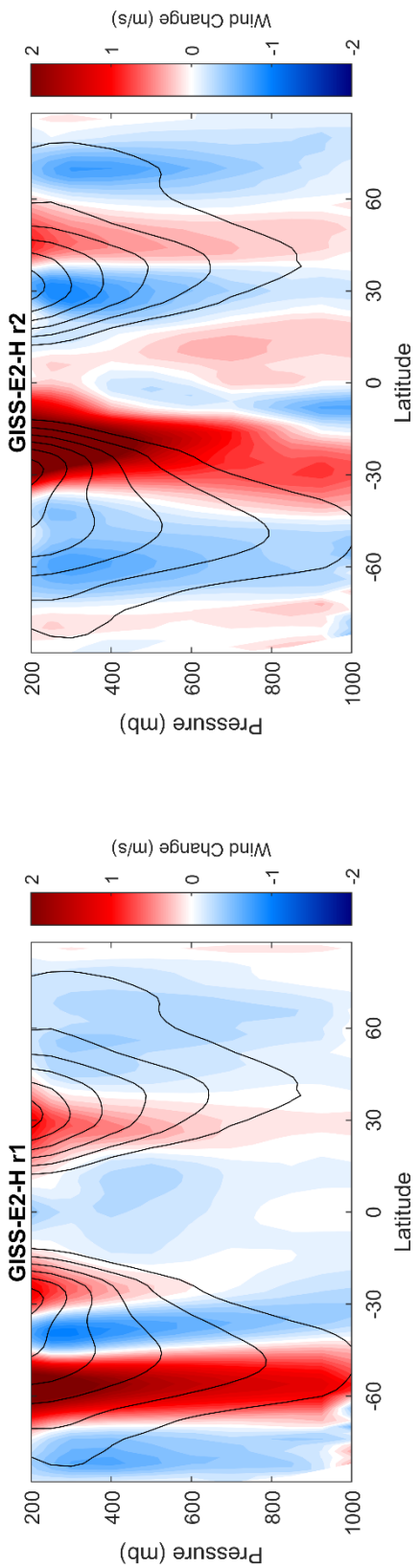

Figure B22 –As in Figure B2 but for all the ensemble members of GISS-E2-H.

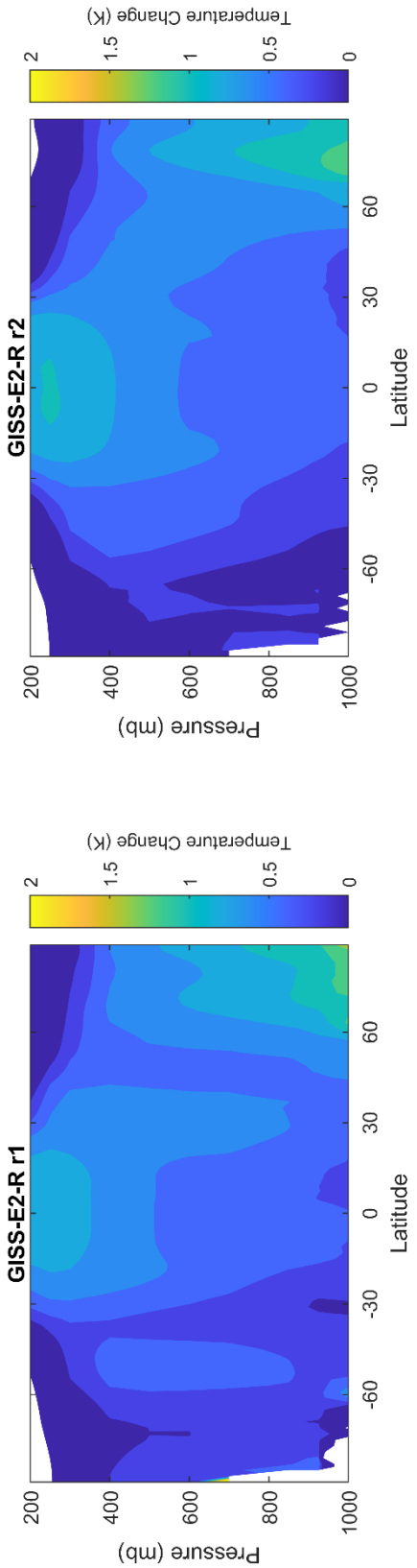

Figure B23 –As in Figure B1 but for all the ensemble members of GISS-E2-R.

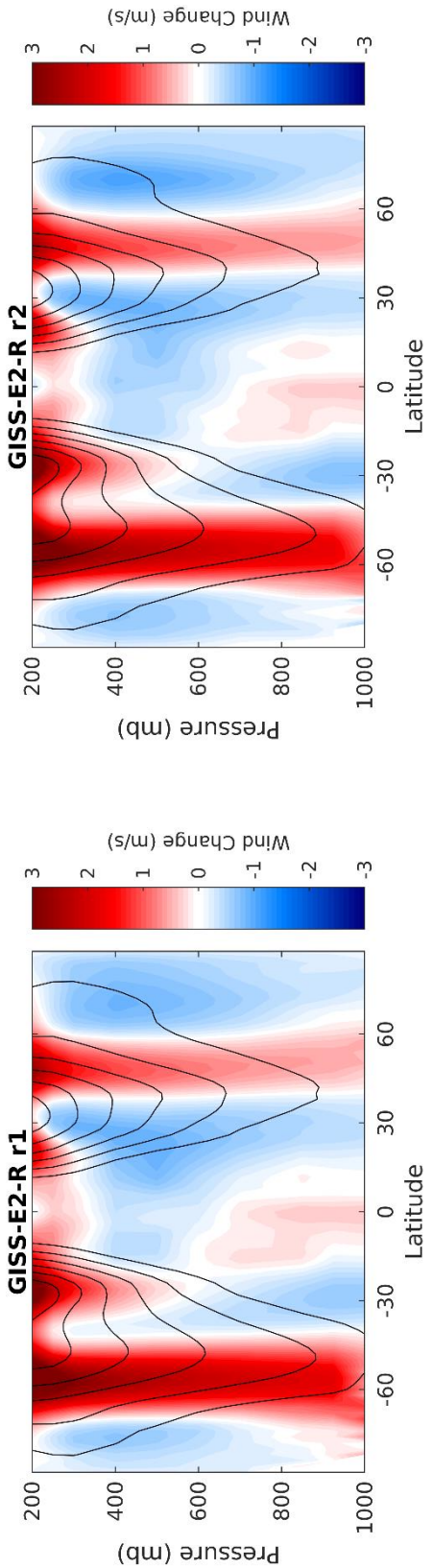

Figure B24 –As in Figure B2 but for all the ensemble members of GISS-E2-R.

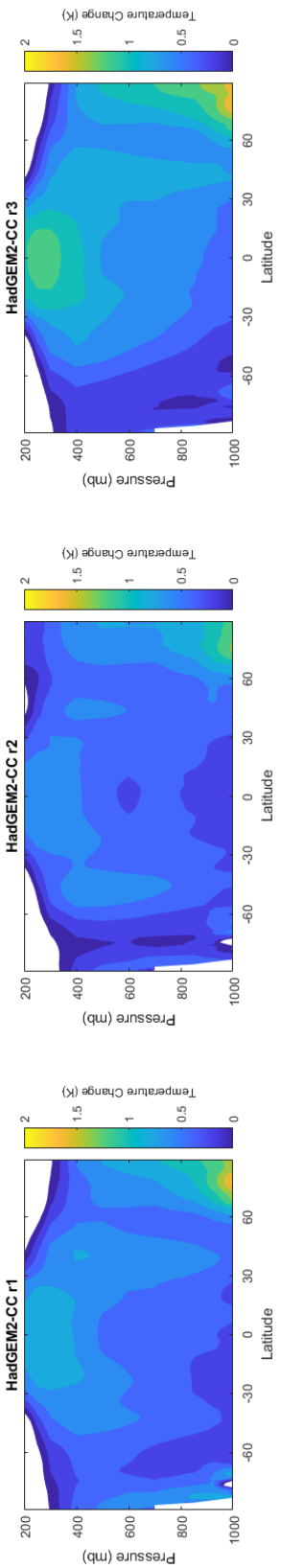

Figure B25 –As in Figure B1 but for all the ensemble members of HadGEM2-CC.

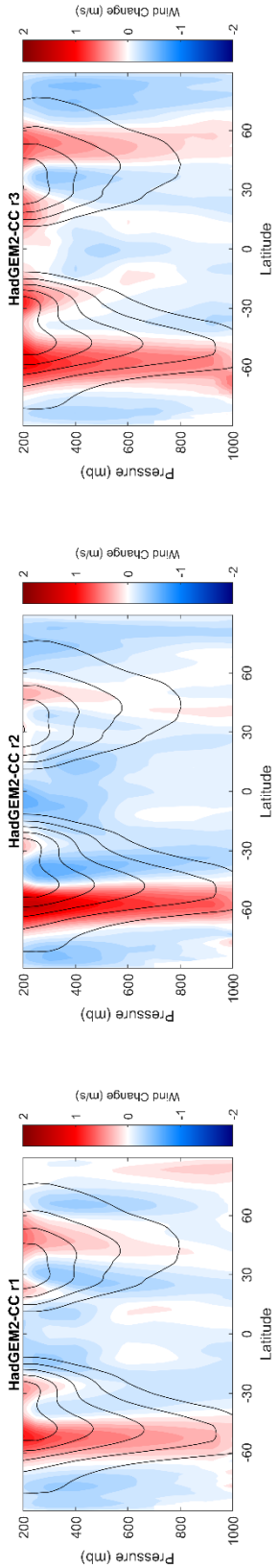

Figure B26 –As in Figure B2 but for all the ensemble members of HadGEM2-CC.

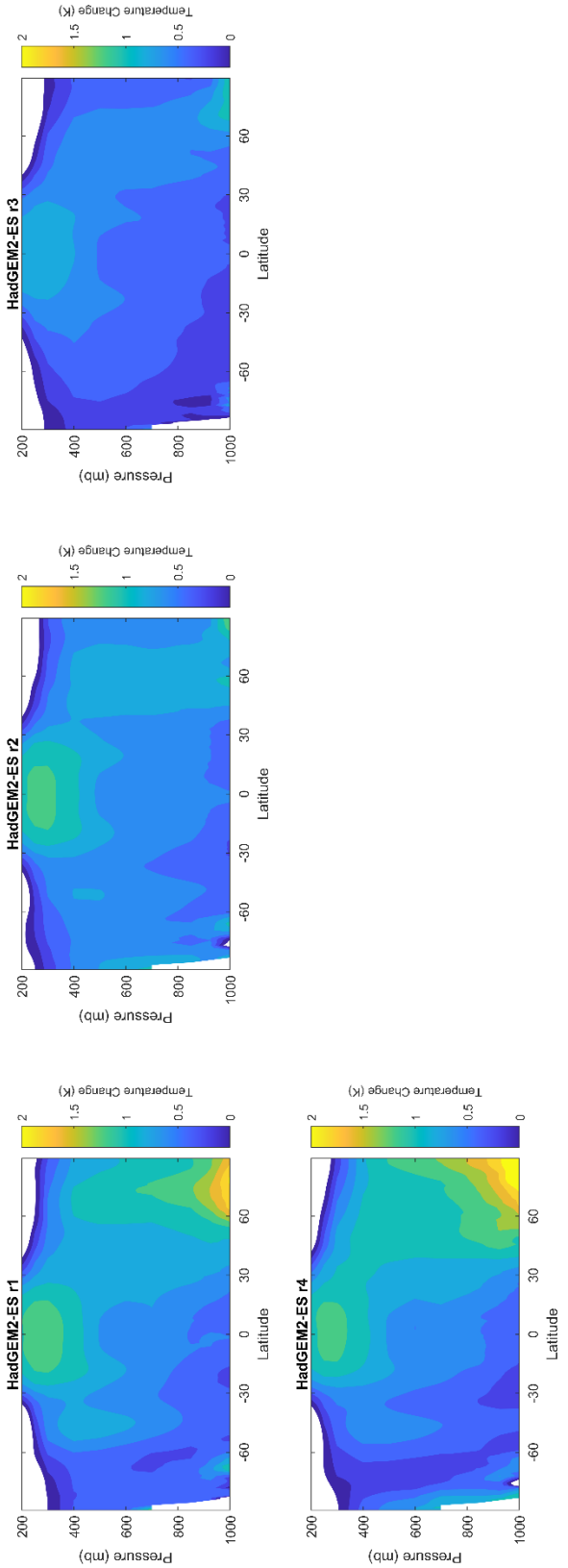

Figure B27 –As in Figure B1 but for all the ensemble members of HadGEM2-ES.

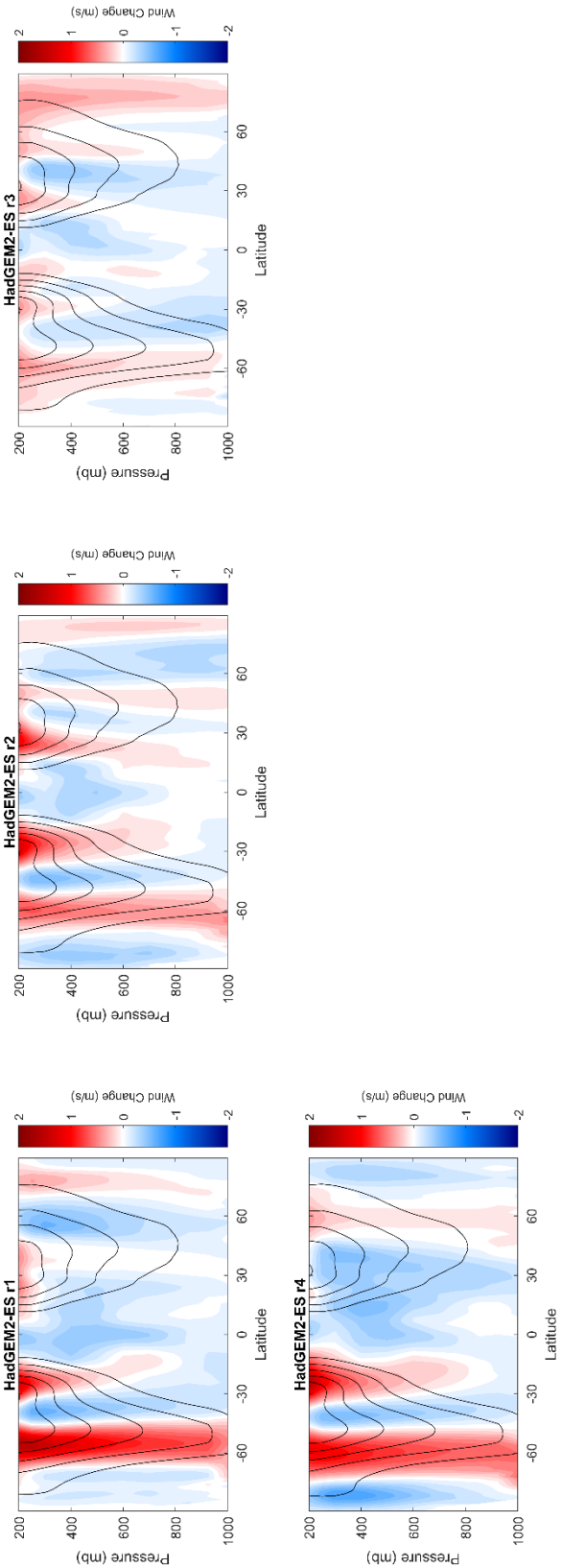

Figure B28 –As in Figure B2 but for all the ensemble members of HadGEM2-ES.

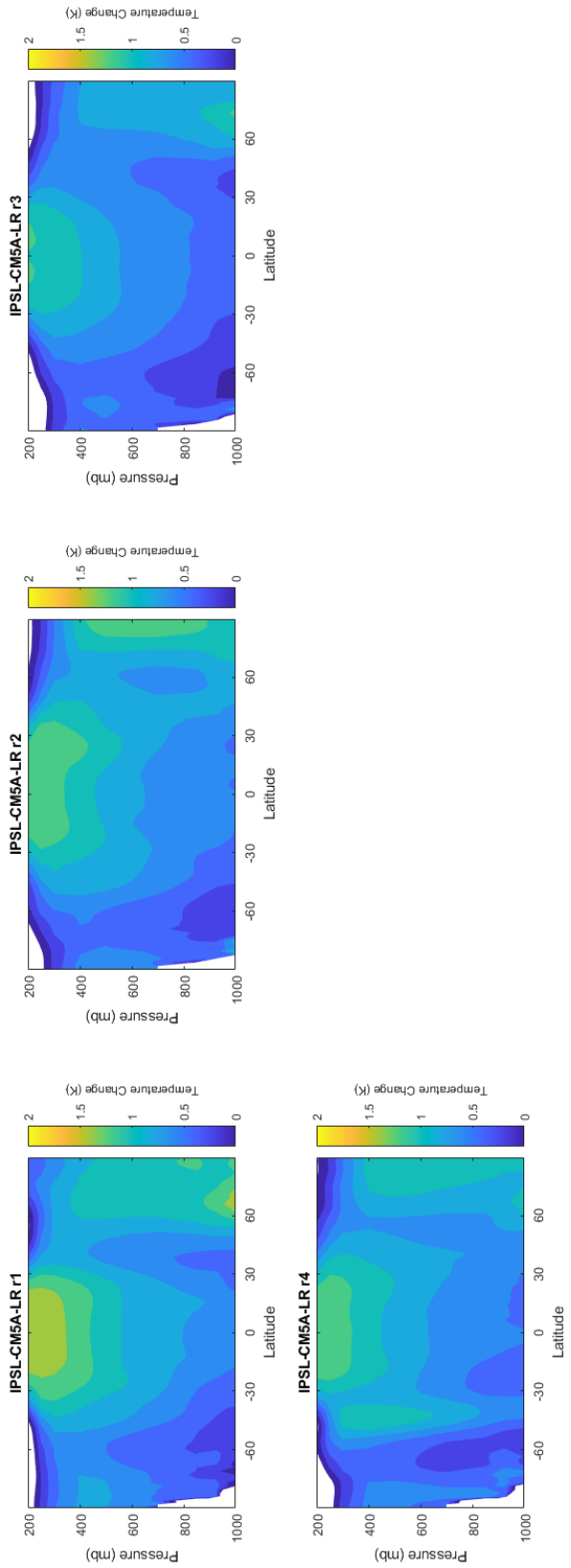

Figure B29 –As in Figure B1 but for all the ensemble members of IPSL-CM5A-LR.

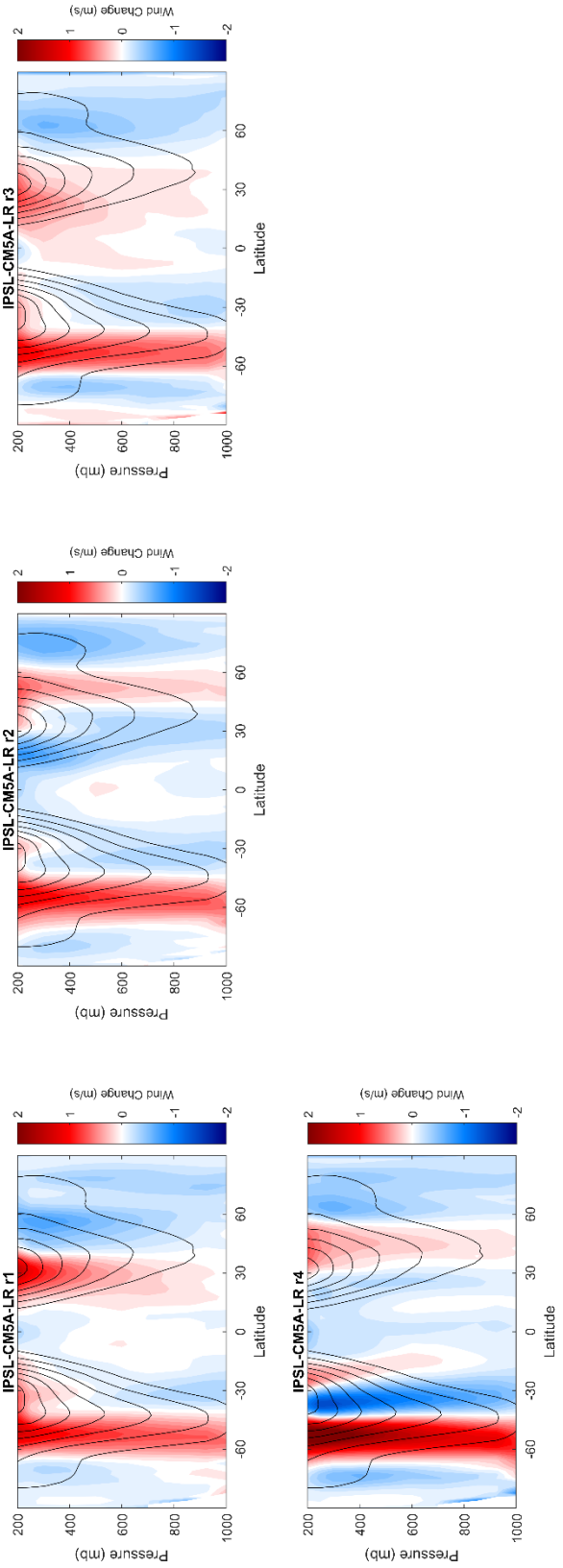

Figure B30 –As in Figure B2 but for all the ensemble members of IPSL-CM5A-LR.

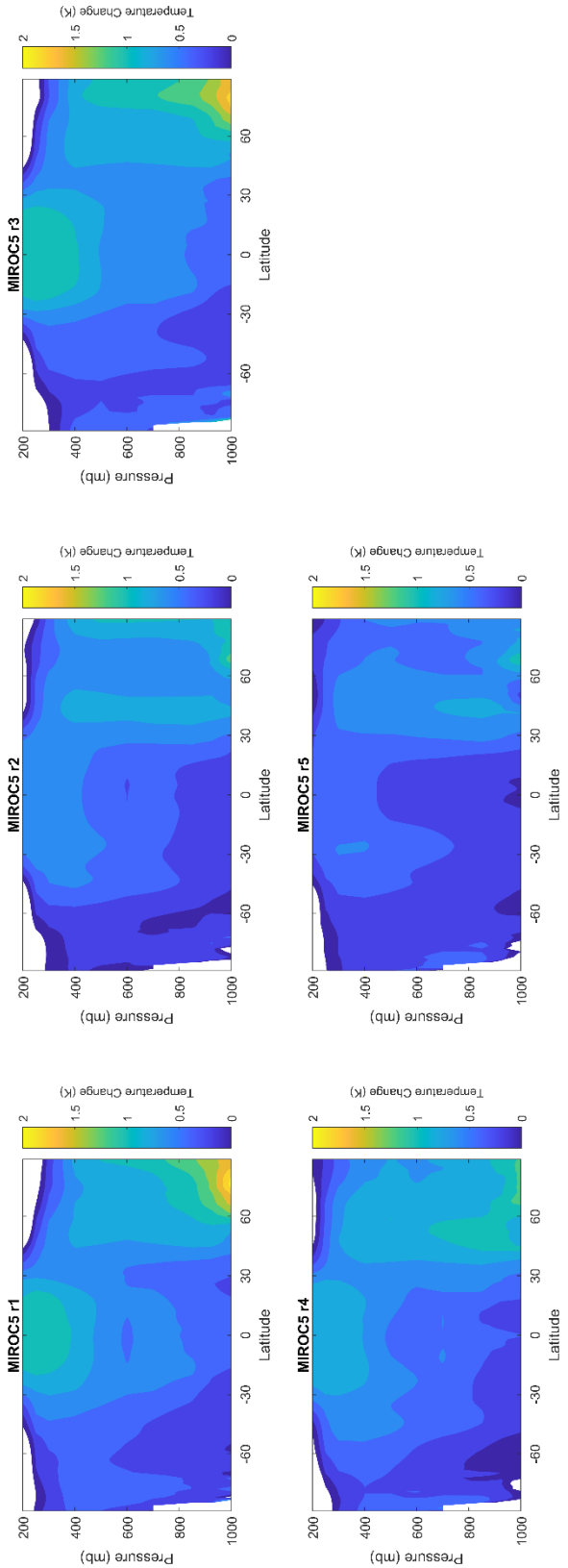

Figure B31 –As in Figure B1 but for all the ensemble members of MIROC 5.

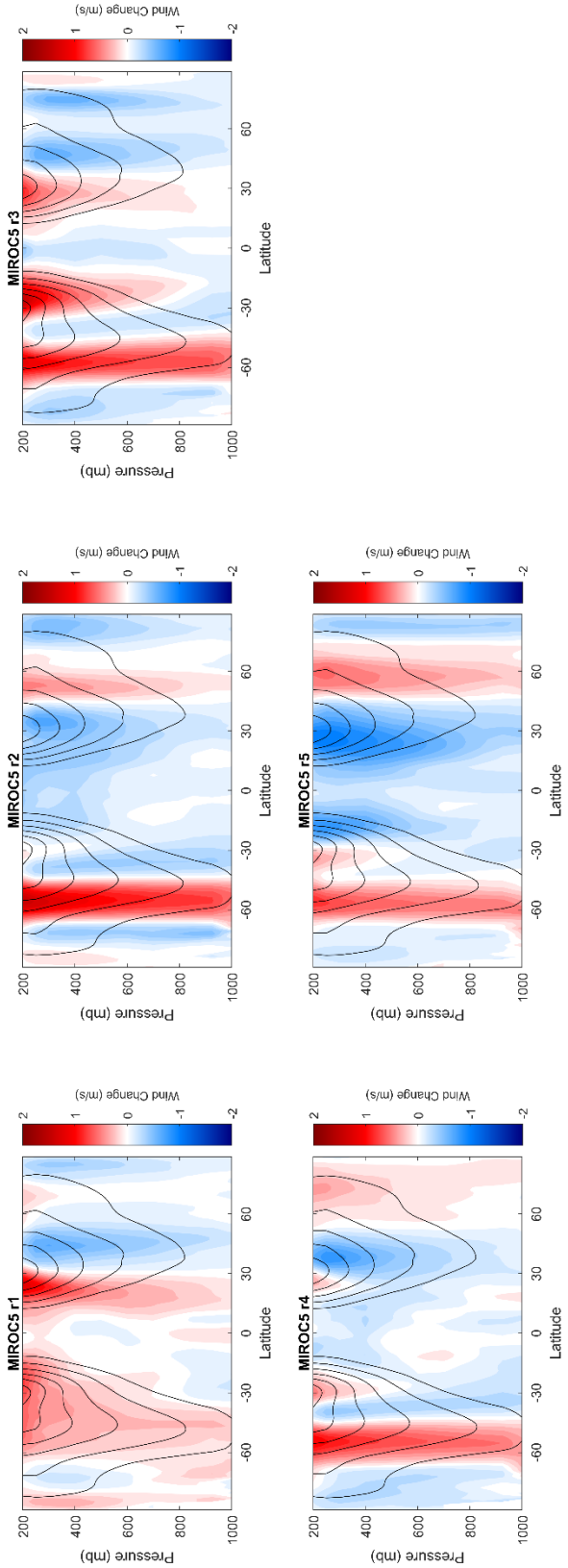

Figure B32 –As in Figure B2 but for all the ensemble members of MIROC 5.

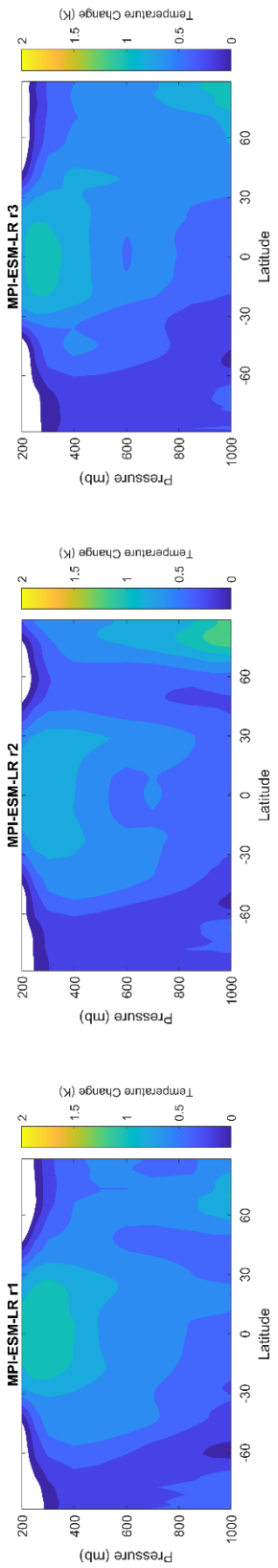

Figure B33 –As in Figure B1 but for all the ensemble members of MPI-ESM-LR.

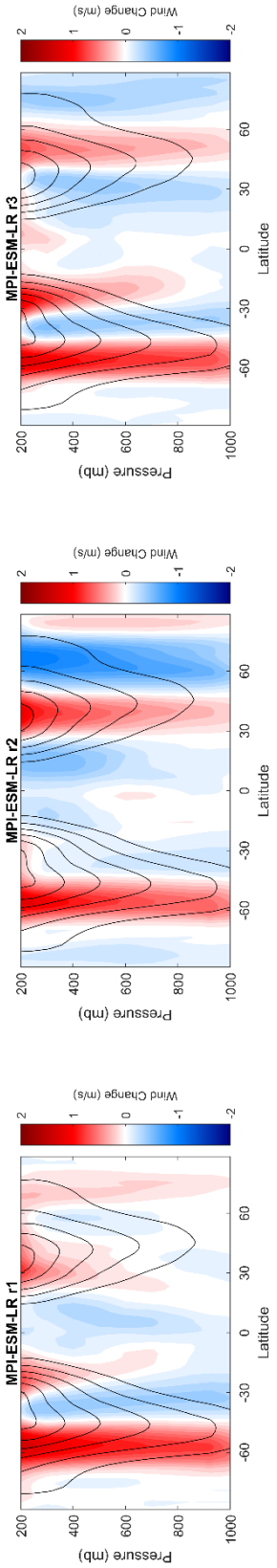

Figure B34 –As in Figure B2 but for all the ensemble members of MPI-ESM-LR.